Impact of Parkinson's Disease- linked- *Lrrk2* mutation (*Lrrk2*^{G2019S}) on the innate immune response during infection with *Listeria monocytogenes*.

Leila Sam

Thesis submitted to the University of Ottawa
in partial Fulfillment of the requirements for the Master of Science Microbiology
and Immunology, Pathology and Experimental medicine.

Department of Biochemistry, Microbiology and Immunology
Faculty of Medicine
University of Ottawa

© Leila Sam, Ottawa, Canada, 2020

PREFACE

Contribution of collaborators

Lrrk2^{G2019S} knock-in mice were provided by Dr. Schlossmacher (University of Ottawa) for the experiments.

Approvals

The experimental protocols used were approved by the University of Ottawa Animal Care Committee and include the protocols BMI1638 and BMI1639. A Biohazardous Materials Use Certificate was obtained from the University of Ottawa Office of Risk Management Environmental Health and Safety.

Abstract

Mutations in the *Leucine-rich repeat kinase 2* (*Lrrk2*) gene are associated with familial and sporadic cases of Parkinson's disease but are also found in inflammatory-related disorders such as Crohn's disease, systemic lupus erythematosus, tuberculosis and leprosy. There is also evidence that LRRK2 is highly expressed in immune cells, particularly in macrophages, and has been functionally linked to pathways pertinent to immune cell function such as modulating the course of infections, cytokine release, autophagy and phagocytosis. Indeed, *G2019S* mutation in *Lrrk2* is the most common mutation in Parkinson's disease. Accordingly, we hypothesized that *G2019S* mutation in *Lrrk2* might enhance the activation of the innate immune system. We tested our hypothesis by performing challenge experiments in a mouse model of *Listeria monocytogenes*, and by measuring the activation of bone marrow derived macrophages (BMDMs) following *in vitro* infection with the bacterium.

We found that $Lrrk2^{G2019S}$ mutant mice controlled *L. monocytogenes* better than WT mice. The mechanism behind the better control of *L. monocytogenes* by the *G2019S* mutation of *Lrrk2* was investigated in BMDMs following *in vitro* infection with *L. monocytogenes*. Interestingly, we found that $Lrrk2^{G2019S}$ mutation enhances the production of TNF-α, IL-1β and IL-10 by infected BMDMs. The impact on TNF-α and IL-1β was specifically due to the *G2019S* mutation of *Lrrk2* since there was no impact on the expression of these cytokines in *Lrrk2* knockout macrophages. Western blotting experiments revealed that the *G2019S* mutation of *Lrrk2* enhances MAPK signaling (TAK1, p38 and ERK). Modulation of the expression of the pro-inflammatory cytokines, TNF-α and IL-1β by *G2019S* mutation of *Lrrk2* occurred via p38 MAPK activation. The impact on IL-10 expression occurred through increased ERK activation by the *G2019S* mutation of *Lrrk2*.

We did not observe any impact of *G2019S* mutation of *Lrrk2* on the activation of NF-κB and JNK MAPK pathways.

Increased expression of IL-1β by *G2019S* mutation of *Lrrk2* revealed increased inflammasome signaling. Inflammasome signaling in response to *L. monocytogenes* was mainly mediated by the AIM2- and partly by NLRP3- inflammasome and was dependent on activation of caspase-1. We found that $Lrrk2^{G2019S}$ mutation enhanced the expression of NLRP3 and caspase-1.

Finally, we found that the expression of reactive oxygen species (ROS) following infection with *L. monocytogenes* was augmented by *G2019S* mutation of *Lrrk2*, and this can be an important mechanism that promotes the enhanced clearance of the bacterium *in vivo*.

Overall, these results present new insights into the signaling mechanisms through which the *G2019S* mutation of *Lrrk2* augments innate immune response which leads to better control of infection.

Acknowledgements

Having worked in the medical laboratory as a medical doctor and pathologist, my ultimate wish has always been to study science to explore the mechanisms behind the diseases. In this journey, first and foremost, I would like to express my sincere thanks to my supervisor, Professor Dr. Subash Sad, for providing me with this opportunity. His invaluable advice, insight, knowledge and patience during these two years are very appreciated. Words cannot express my gratitude for your continuous encouragement and support. I would like to extend my gratitude to the members of my thesis advisory committee: Dr. Michael Schlossmacher, Dr. Ashok Kumar and Dr. Jonathan Angel for their precious advice and contribution. I would like to thank our collaborating lab, Dr. Schlossmacher lab, and particularly Professor Dr. Schlossmacher, Dr. Bojan Shutinuski and Dr. Julianna Tomlinson for their pivotal role and precious guidance in this project.

I am extremely grateful to Stephanie Hajjar, one of my best friends and colleagues in the lab, for being my technical mentor in performing experiments and particularly in writing my thesis. Her immeasurable assistance will be unforgettable for me. I would also like to thank Dr. Ardeshir Ariana for his special technical help, advice and support during this project. My special thanks to Pallavi Saxena, one of my best friends and colleagues, for always being there for me, helping me with the experiments and assisting me in writing my thesis. I also appreciate the support which my colleagues Melissa Sen Phuong, David Cai and Parva Thakker have given me throughout this journey.

Lastly and most importantly, I thank my husband and my son, my close friends, for their continuous love and encouragement. This would not have been possible without your support.

Table of contents

PREFACE……...….i

Abstract……..ii

Acknowledgements…….…..iv

Table of contents……..…..v

List of figures……..x

List of abbreviations……..…..xii

1.Introduction…… .1

1.1. LRRK2 structure and function…….……. ..….1

1.1.1. *Lrrk2* gene and LRRK2 protein……1

1.1.2. LRRK2 and Parkinson's Disease…….... 2

1.1.3. Tissue distribution of LRRK2……..…3

1.1.4. LRRK2 and other diseases……...3

1.1.5. LRRK2 and infections ……..……..…4

1.1.6. LRRK2 and signaling pathways……..5

1.2. The innate immune system……..…….…7

1.2.1. The innate immune components…….……7

1.2.2. Cytokines…… …...8

1.2.3. Innate inflammatory signaling pathways……..10

1.2.3.1. NF-κB signaling pathway…….….10

1.2.3.2. MAPK signaling pathway……...……12

1.2.3.3. Inflammasome signaling pathway……..…..……13

1.2.3.3.1. NLRP3 inflammasome signaling pathway……14

1.2.3.3.2. NLRC4 inflammasome signaling pathway……..…..……16

1.2.3.3.3. AIM2 inflammasome signaling pathway……..……..…16

1.2.3.3.4. Canonical and non-canonical inflammasome pathways……...…...…...…17

1.3. *Listeria monocytogenes* (*L. monocytogenes*)…….….19

1.3.1. The innate immune response to *L. monocytogenes*……20

1.3.2. *L. monocytogenes* and innate inflammatory signaling pathways……...21

1.3.2.1. *L. monocytogenes* and the NF-kB and the MAPK signaling pathways……..21

1.3.2.2. *L. monocytogenes* and the inflammasome signaling pathways…….…..22

2. Rational……...…24

3. Hypothesis…….….25

4. Objectives…….……..25

5. Materials and methods……...…26

5.1. Experimental mice models……..…26

5.2. Preparing *Lm-EGD* for the experiments……...……27

5.2.1. Preparing the *Lm-EGD* growth curve……27

5.2.2. Preparing *Lm-EGD* vials for the experiments…….……..……30

5.2.3. Preparing *Lm-EGD* for intravenous (IV) injection…….…..30

5.2.4. Preparing *Lm-EGD* for oral gavage ……30

5.3. Measurement of the spleen and the brain bacterial burden……...….31

5.4. Generation of bone marrow derived macrophages (BMDMs)……34

5.5. Seeding BMDM for *in vitro* experiments……...……34

5.6. *In vitro* infection……...…35

5.7. Cytokine analysis…….…...……...…35

5.8. Western Blotting…….……..……37

5.8.1. Lysate preparation from cell culture…….…38

5.8.2. Loading and running the gel……...…..38

5.8.3. Transferring the samples…….…….39

5.8.4. Immunoblotting and detection……...…..……..39

5.9. Measurement of cell death……..…….……...…41

5.9.1. Zombie Yellow staining…….……..……..…41

5.10. Statistical analysis…….…….…..…….42

6. Results…….…43

6.1. The first objective……...……43

6.1.1. The *Lrrk2* ^{G2019S} mutant mice and WT mice show the same bacterial burden in the spleen and the brain tissues upon oral gavage. ……...……..45

6.1.2. Female WT mice display a trend towards higher bacterial burden in the spleen and the brain via intravenous (IV) route compared to male WT mice…….…47

6.1.3. *Lrrk2*^{G2019S} mutant-mice show significantly lower bacterial burden in the spleen than WT mice……...……..51

6.2. The second objective……...55

6.2.1. *Lrrk2*^{G2019S} mutation enhances inflammasome activity in macrophages…….....55

6.2.2. *Lrrk2*^{G2019S} mutation does not modulate inflammasome activity in macrophages in response to the combined treatment with LPS and ATP……..….58

6.2.3. *G2019S* mutation in *Lrrk2* promoted increased expression of pro-inflammatory cytokines (IL-1β and TNF-α) and the anti-inflammatory cytokine (IL-10) in response to *Lm-EGD*……...62

6.2.4. Exploring the inflammasome signaling modulated by *Lrrk2*^{G2019S} mutation during infection with *Listeria monocytogenes-EGD*……68

6.2.4.1. Inflammasome signaling in BMDMs in response to *Lm-EGD* infection is partially dependent on the NLRP3 inflammasome……....69

6.2.4.2. Inflammasome signaling in response to *Lm-EGD* is independent of the NLRC4 pathway……75

6.2.4.3. Inflammasome signaling in response to *Lm-EGD* is mainly dependent on caspase-1 for IL-1β expression and caspase-11 for cell death induction……...80

6.2.4.4. AIM2 promotes inflammasome signaling in response to *Lm-EGD*……...87

6.2.4.5. *Lrrk2*^{G2019S} mutation promotes the expression of NLRP3 and the activation of caspase-1 and caspase-11……...91

6.2.5. *Lrrk2*^{G2019S} mutation does not modulate NF-κB pathway in response to *Lm-EGD* infection…….……95

6.2.6 *Lrrk2*^{G2019S} mutation enhances the activation of the MAPK pathway in macrophages in response to *Lm-EGD* infection…….99

6.2.7. *Lrrk2*^{G2019S} mutation enhances the activation of TAK1 in macrophages in response to *Lm-EGD* infection…….....…....108

6.2.8. *Lrrk2*^{G2019S} mutation enhances the activation of RIPK1 in macrophages in response to *Lm-EGD* infection……....112

6.2.9. Infected *Lrrk2*^{G2019S} mutant mice produced more Reactive Oxygen Species (ROS) in response to *L. monocytogenes* infection…….……117

7. Discussion……123

7.1. The role of *Lrrk2* mutations in controlling microbial infections……123

7.2. *Lrrk2* modulates IL-1β expression in macrophages in response to *Lm-EGD*……...125

7.2.1. The role of the inflammasome signaling pathways through which BMDMs respond to *Lm-EGD*……125

7.2.2. The role of the inflammasome mediators in the context of $Lrrk2^{G2019S}$ macrophages in response to *Lm-EGD*……128

7.3. The profile of the inflammatory cytokines in the context of *Lrrk2* mutations……130

7.3.1. The role of LRRK2 in NF-κB and MAPK inflammatory signaling pathways in response to *Lm-EGD*……...……..…131

8.Conclusion……..…136

9.REFERENCES……138

Curriculum Vitae……151

List of figures

Figure 1. Growth curve of *Listeria monocytogenes, EGD* strain (*Lm-EGD*)……..….29

Figure 2. Intracardiac perfusion and brain dissection…….…….33

Figure 3. The infection of WT and *Lrrk2*^{G2019S} mutant mice through the oral route results in a similar bacterial burden in the spleen and the brain…….….46

Figure 4. Female WT mice display a trend towards higher bacterial burden in the spleen and the brain compared to male WT mice…….….50

Figure 5. *Lrrk2* ^{G2019S} mutant mice showed significantly reduced *Lm-EGD* burden in the spleen…….54

Figure 6. *Lrrk2*^{G2019S} mutation results in increased expression of IL-1β by macrophages……..57

Figure 7. Expression of IL-1β is similar in WT and *Lrrk2*^{G2019S} mutant bone marrow derived macrophages (BMDMs) in response to the combined LPS and ATP treatment……..….61

Figure 8. Expression of IL-1β, TNF-α, IL-10 and IL-12 by WT and *Lrrk2* ^{G2019S} macrophages in response to *Lm-EGD*…….….65

Figure 9. Expression of IL-1β, TNF-α, IL-10 and IL-12 by WT and *Lrrk2* deficient BMDMs in response to *Lm-EGD*…….…..…67

Figure 10. *Nlrp3* deficiency results in reduced expression of IL-1β and cell death……..…72

Figure 11. *Nlrp3* deficiency modulates the expression of inflammatory cytokines by BMDMs in response to infection……..….74

Figure 12. *Nlrc4* deficiency results in a similar expression of IL-1β and cell death, compared to WT cells…….77

Figure 13. *Nlrc4* deficiency does not impact the expression of cytokines in response to *Lm-EGD*. ……...…79

Figure 14. Inflammasome signaling in BMDMs, in response to *Lm-EGD*, is mainly dependent on caspase-1 for IL-1β expression and caspase-11 for cell death……...84

Figure 15. *Caspase 1/11* deficiency modulates the expression of inflammatory cytokines by BMDMs in response to *Lm-EGD* infection……...86

Figure 16. *Aim2* deficiency results in a striking abolishment of IL-1β and a partial reduction in cell death..……....90

Figure 17. High expression of NLRP3, active caspase-11 and active caspase-1 in the *Lrrk2*^{G2019S} mutant macrophages versus WT cells in response to *Lm-EGD*……...….94

Figure 18. Activated IKKα/β and activated p65 expression were similar in *Lrrk2*^{G2019S} mutant and WT BMDMs in response to *Lm-EGD* infection……...98

Figure 19. Enhanced expression of activated p38 and ERK 1/2 in the *Lrrk2*^{G2019S} mutant macrophages versus WT cells in response to *Lm-EGD* infection……103

Figure 20. Inhibition of p38 reduced the levels of TNF-α and IL-1β in *Lrrk2*^{G2019S} macrophages to WT levels……..…105

Figure 21. Inhibition of ERK1/2 reduced the levels of IL-10 in *Lrrk2*^{G2019S} macrophages to WT levels……107

Figure 22. Increased activation of TAK1 and similar expression of MK2 in the *Lrrk2*^{G2019S} mutant macrophages versus WT cells in response to *Lm-EGD* infection…….....…111

Figure 23. Increased activation of RIPK1 (P (Ser166) RIPK1) in the *Lrrk2*^{G2019S} mutant macrophages versus WT cells in response to *Lm-EGD* infection……...116

Figure 24. *G2019S* mutation of *Lrrk2* modulates reactive oxygen species (ROS) production by macrophages in response to *Lm-EGD* infection ……...…120

Figure 25. *Lrrk2*^{G2019S} mutant and WT mice of various ages produced reactive oxygen species (ROS) similarly…….…...…….122

List of abbreviations

AIM-2	Absent in Melanoma
ALR	Aim-2 Like Receptors
ASC	Apoptosis-Associated Speck-Like Protein Containing CARD
BHI	Brain Heart Infusion
BMDM	Bone Marrow Derived Macrophages
BSA	Bovine Serum Albumin
CARD	Caspase Activating Recruitment Domain
CFU	Colony Forming Unit
ELISA	Enzyme-Linked Immunosorbent Assay
ERK	Extracellular Signal Regulated Kinases
FBS	Fetal Bovine Serum
GSDMD	Gasdermin D
IKK	Inhibitor of Nuclear Factor Kappa-B Kinase
IL	Interleukin
JNK	c-Jun-N-Terminal-Kinases
LLO	Listeriolysin O
Lm-EGD	*Listeria monocytogenes-EGD*
LPS	Lipopolysaccharide
LRR	Leucine-Rich Repeat
LRRK2	Leucine-Rich-Repeat Kinase 2
MAPK	Mitogen Activated Protein Kinase

MCSF	Macrophage Colony Stimulating Factor
MOI	Multiplicity of Infection
MK2	MAPK-activated protein kinase 2
NF-kB	Nuclear Factor Kappa-Light-Chain-Enhancer of Activated B cells
NLR	NOD-Like Receptors
NLRC4	NOD, LRR family CARD Domain-containing Protein 4
NLRP3	NOD, LRR family Pyrin Domain-Containing Protein 3
OD	Optical Density
PAMP	Pathogen Associated Molecular Pattern
PBS	Phosphate buffer Saline
PCR	Polymerase Chain Reaction
PD	Parkinson's Disease
PFA	Paraformaldehyde
RIPK	Receptor-Interacting Protein Kinase
RNA	Ribonucleic Acid
ROC	Ras of Complex
ROS	Reactive Oxygen Species
RPMI	Roswell Park Memorial Institute Medium
SAPK	Stress-Activated Protein Kinases
T3SS	Type Three Secretion System
TAK1	TGFβ-activating kinase1
TBST	Tris Buffered Saline with Tween
TMB	Tetramethylbenzidine

TNF-a	Tumor Necrosis Factor Alpha
TNFR1	TNF-α receptor 1
TLR	Toll-Like Receptor
WT	Wild type mice

1. Introduction

1.1. LRRK2 structure and function

1.1.1. *Lrrk2* gene and LRRK2 protein

The *leucine-rich repeat kinase 2 (Lrrk2)* gene is emerging as a genetic hotspot for disease associations. The gene locus for *Lrrk2* or *Park8* is on human chromosome 12 and mouse chromosome 15 (Funayama et al., 2002; Tong et al., 2009). The mouse and human LRRK2 proteins share 86.7% amino acid identity (www.ncbi.nlm.nih.gov/homologene). The *Lrrk2* gene contains 51 exons that encode a very large (286 kDa) protein, termed LRRK2 or Dardarin, which consists of 2527 amino acids constituting several domains with different functions (Klein and Schlossmacher, 2006).

LRRK2 is a multi-domain protein and belongs to ROCO protein family that includes a central region of Ras-of-complex protein (Roc) domain, which encodes a GTPase and a serine/threonine kinase domain surrounded by several protein-protein interaction domains (Mills et al., 2014; Rudenko and Cookson, 2014; Wallings and Tansey, 2019). The N terminal harbors the armadillo, the ankyrin and the leucine-rich repeat region (Wallings and Tansey, 2019). At the C-terminal, there is the WD40 domain, which has been demonstrated to be crucial for protein folding (Kang and Marto, 2017; Rudenko et al., 2012).

In mammals, LRRK2 and its closest homolog, LRRK1, are the only known members of the ROCO protein family that combine a GTPase and a kinase domain within the same protein, perhaps suggesting an intricate regulatory mechanism for LRRK2 protein (Biskup et al., 2007) Furthermore, structural studies, along with in vitro and cell-based assays, suggest that the biochemical activity of LRRK2 is orchestrated through a complex interplay between the protein's

scaffolding and enzymatic domains (Kang and Marto, 2017). Given the multiple, highly diverse, enzymatic and protein-interacting domains, it is likely that LRRK2 may have different binding partners in different cell types and be instrumental in many different cellular pathways (Wallings and Tansey, 2019).

1.1.2. LRRK2 and Parkinson's Disease

In 2002, *Lrrk2* was mapped to 12p11.2-q13.1 in a Japanese family with late-onset autosomal dominant Parkinson's Disease (ADP) by using genome-wide linkage analysis (Funayama et al., 2002). Additionally, *Lrrk2* mutations were also found in some patients with sporadic PD in the following years (Kluss et al., 2019). In families, mutations in LRRK2 can cause PD with age-dependent but variable penetrance (Kluss et al., 2019).

Lrrk2 mutations are considered as the most commonly known genetic cause of PD worldwide (Martin et al., 2014). Over 80 variants in *Lrrk2* have been reported so far, but only six mutations including *p.G2019S, p.N1437H, p.R1441G, p.R1441C, p.Y1699C* and *p.I2020T* provide further evidence that *Lrrk2* mutations can cause PD phenotype (Singleton et al., 2013). Of these mutations, the *G2019S* (glycine to serine substitution at amino acid 2019) is the most common genetic determinant of PD and results in increased kinase activity in LRRK2 (Kang and Marto, 2017). The $Lrrk2^{G2019S}$ mutation accounts for 1–3% of apparently sporadic and 4-8% of familial PD cases with an uneven penetrance worldwide (Kang and Marto, 2017). It is worthy to note that PD patients with the $Lrrk2^{G2019S}$ mutation display similar clinical characteristics to patients with sporadic PD (Thaler et al., 2009).

1.1.3. Tissue distribution of LRRK2

LRRK2 is highly expressed throughout the brain in the cortex, striatum, hippocampus, midbrain, cerebellum and olfactory bulb (Kang and Marto, 2017). Furthermore, LRRK2 is expressed in peripheral organs such as kidney, lung, spleen and peripheral blood mononuclear cells (Hakimi et al., 2011; Herzig et al., 2011). Interestingly, both the kidney and the lung appear to harbor higher LRRK2 expression compared to brain tissues (Herzig et al., 2011).

In addition to the brain and peripheral tissues, recent studies point out a high expression of LRRK2 in immune cells, such as monocytes, macrophages, microglia (resident macrophages in the CNS), neutrophils and B lymphocytes in tissue culture models (Hakimi et al., 2011; Moehle et al., 2012). LRRK2 protein expression was confirmed in murine bone marrow derived macrophages, dendritic cells, macrophage cell line RAW264.7 and the human monocytic cell line THP-1 (Hakimi et al., 2011). Hakimi *et al*. (2011) also observed a significant up-regulation of *Lrrk2* mRNA in bone marrow-derived macrophages after exposure to microbial structures including bacterial LPS and lentiviral particles.

1.1.4. LRRK2 and other diseases

Polymorphisms in the *Lrrk2* gene have been linked to several immune-mediated inflammatory diseases such as inflammatory bowel disease (IBD), systemic lupus erythematosus (SLE) and leprosy (Hui et al., 2018; Wang et al., 2015; Zhang et al., 2019).

Genome-wide association studies have identified *Lrrk2* as being encoded by a major susceptibility gene for Crohn's disease (Liu et al., 2011). Of note, the $Lrrk2^{G2019S}$ mutation, which increases the kinase activity of LRRK2, was increased in Crohn’s disease (CD) patients in the Ashkenazi Jewish population (Rivas et al., 2018).

The systemic lupus erythematosus (SLE) is a prototypic autoimmune disease characterized by the presence of pathogenic autoantibodies associated with polyclonal B cell hyperreactivity. LRRK2 expression is upregulated in B cells from SLE patients with strong correlations to disease severity (Zhang et al., 2019). It also has been shown that LRRK2 deficiency largely attenuates the pathogenic progress of lupus-like features in pristane-induced mice (Zhang et al., 2019).

Leprosy is a chronic dermato-neurological infectious disease caused by *Mycobacterium leprae (M. leprae*). Wang *et al.* (2015) demonstrated that *Lrrk2* variants are significantly associated with Leprosy via eighteen single nucleotide polymorphisms (SNPs) in *Lrrk2* which have been shown to preferentially associate with type 1 inflammatory reactions (excessive inflammation) (Wang et al., 2015).

The mechanisms by which distinct *Lrrk2* alleles modulate the risk of developing different types of inflammatory diseases in various organs, i.e., the gut (IBD), the brain (PD), the kidney (SLE) and the peripheral nervous system (leprosy), are still unclear and require further investigations.

1.1.5. LRRK2 and infections

LRRK2 has been implicated in several infections. Interestingly, there are contrasting reports between the effects of LRRK2 in various bacterial infections.

Mycobacterium tuberculosis (Mtb) is an intracellular pathogen that causes an infectious disease called Tuberculosis (TB). LRRK2 deficiency in mice resulted in a significant decrease in *M. tuberculosis* burden early during the infection (Härtlova et al., 2018). A molecular mechanism was proposed wherein LRRK2 regulates phagosome maturation which control *Mycobacterium tuberculosis* replication (Härtlova et al., 2018).

Salmonella Typhimurium is a facultative, Gram-negative and intracellular bacterium, which causes a systemic inflammatory disease and an enlargement of the spleen in mice (splenomegaly) that mimics the typhoid disease caused by S. enterica serovar Typhimurium in humans. It was recently reported that a high burden of *Salmonella Typhimurium* was observed in the spleens of infected *Lrrk2*-deficient mice resulting in their reduced survival compared to WT littermates (Liu et al., 2017b). Conversely, mice expressing *Lrrk2*^{G2019S} mutation, which increases the kinase activity of LRRK2, controlled the infection better and displayed improved survival (Liu et al., 2017b; Shutinoski et al., 2019).

Listeria monocytogenes (Lm) is a facultative, Gram-positive and intracellular bacterium, which causes systemic inflammatory disease (septicemia) and meningoencephalitis in mice and immunocompromised humans. *Lrrk2*- deficient mice showed increased susceptibility to *Lm* upon oral infection (Zhang et al., 2015).

Reovirus is a double-stranded RNA virus used as a tractable experimental system for studies of viral pathogenesis in new-born mice. Mouse pups with reovirus-induced encephalitis that expressed the *Lrrk2*^{G2019S} mutation showed an increased mortality rate despite having lower viral titers in the brain and the lung (Shutinoski et al., 2019).

Collectively, these data point towards the importance of *Lrrk2* mutations in exerting pleiotropic effects on bacterial control and inflammation depending on the type of bacterial infection and host susceptibility.

1.1.6. LRRK2 and signaling pathways

The specific domains and structure of LRRK2 implicate that it regulates various cellular signal transduction events. Determination of the signaling pathway of LRRK2 is somewhat complicated

by the extensive list of protein binding partners and cellular processes to which LRRK2 has been linked (Manzoni et al., 2015). Determining which of these processes and interactors are physiologically relevant to various diseases is a significant challenge**.**

There is mounting evidence that LRRK2 exhibits autophosphorylation and external substrates phosphorylation activity (Webber et al., 2011). Indeed, several LRRK2 variants result in increasing kinase activity such as *Lrrk2*^{G2019S} mutation (Greggio, 2012). Recent studies suggest a functional link between LRRK2 kinase and GTPase activity, and mutation in either kinase or GTPase enzymatic activity of LRRK2 can induce PD (Webber et al., 2011).

Of note, several studies also highlight the interplay of LRRK2 with major innate immune signaling pathways, such as MAPK and NF-κB signaling pathways (Harvey and Outeiro, 2019). The MAPK signaling pathway has received attention in the PD field based on recent studies suggesting that neuroinflammation may contribute to the degeneration of dopaminergic neurons (Chen et al., 2012). The evidence supports the hypothesis that LRRK2 intersects endogenous cellular pathways to mediate neuroinflammation, disrupt endocytosis vesicle trafficking as well as mitochondrial homeostasis and promote cell death (Singh et al., 2019). It has also been shown that LRRK2 is abundantly expressed in immune cells and enhances NF-κB dependent transcription, thereby suggesting its important role within the immune signaling pathways (Dzamko et al., 2012). Thus, by impacting major signaling pathways, LRRK2 can regulate multiple inflammatory pathways via different mechanisms.

1.2. The innate immune system

1.2.1. The innate immune components

The immune system consists of the innate (non-specific) and the adaptive (specific) components. The first line of defense against pathogens is mediated by the innate immune system. The innate immune response consists of physical, cellular and chemical defenses against pathogens. Physical barriers, such as the skin and the mucous membranes, prevent the invasion of microbes into potential sites of infection. Cellular defenses constitute the non-specific effector immune cells, such as macrophages, neutrophils, dendritic cells, natural killer cells, mast cells, and microglia (resident macrophages in the CNS), that produce cytokines, chemokines and reactive oxygen species (ROS) (Lacy and Stow, 2011). The main purpose of the innate immune response is to rapidly prevent the spread and movement of pathogens throughout the body.

Macrophages and neutrophils, which are critical innate immune cell types, are essential in controlling common bacterial infections (Silva, 2010). After invading host epithelial surfaces, microorganisms are immediately encountered by the innate immune cells.

The early detection of pathogens leads to the prompt activation of macrophages, neutrophils and other innate immune populations required to contain the initial infection. Phagocytic macrophages conduct the defense against bacteria by means of pattern recognition receptors (PRRs) that can recognize and bind pathogen-associated molecular patterns (PAMPs) (Mogensen, 2009). Pattern recognition receptors (PRRs), which are expressed on most cells of the innate immune system including macrophages, were initially characterized by their capacity to recognize conserved molecular patterns common to various microbes (PAMPs) (Takeuchi and Akira, 2010). Microbial nucleic acids, bacterial secretion systems and components of the microbial cell wall such as Lipopolysaccharide (LPS) are examples of the conserved microbial factors that are sensed by

PRRs (Newman et al., 2013). They share several different general "patterns" or structures that alert immune cells to destroy invading pathogens. Damaged host cells can also trigger PRRs by releasing danger-associated molecular patterns (DAMPs), such as uric acid crystals, ATP and the heat-shock proteins hsp70 and hsp90 (Lamkanfi and Dixit, 2014).

Currently, four different classes of PRR families have been identified. These families include transmembrane proteins such as the Toll-like receptors (TLRs) and C-type lectin receptors (CLRs), as well as cytoplasmic proteins such as the Retinoic acid-inducible gene (RIG)-I-like receptors (RLRs) and nucleotide-binding and oligomerization domain-like receptors (NLRs) (Takeuchi and Akira, 2010). Sensing of PAMPs or DAMPs by PRRs upregulates the transcription of genes involved in inflammatory responses (Takeuchi and Akira, 2010). These genes encode proinflammatory cytokines, type I interferons (IFNs), chemokines and antimicrobial peptides (Takeuchi and Akira, 2010).

Eventually, innate immune cells subsequently express an appropriate array of cytokines that activate the adaptive immune response leading to full pathogen clearance.

1.2.2. Cytokines

Cytokines are considered as intercellular messengers released from a broad range of cells. They relay soluble regulatory signals that modulate inflammatory responses required for constraining infections. This array of soluble mediators secreted by different innate immune cells particularly macrophages, includes Tumor Necrosis Factors (TNFs), Interferons (IFNs), Interleukins (ILs) and a wide variety of cytokines and chemokines.

IL-1β is a member of the interleukin family of cytokines. This cytokine is produced by activated macrophages as a pro-protein (pro-IL-1β), which is proteolytically processed to its active form IL-

1β (Duque and Descoteaux, 2014). This cytokine is an important pro-inflammatory mediator involved in a variety of cellular activities, including cell proliferation, differentiation and apoptosis (Duque and Descoteaux, 2014). It is also considered as a possible candidate for enhancing neurodegeneration in the brain (Stojakovic et al., 2017). Inflammasome signaling pathways are the main signaling pathways that contribute to IL-1β expression (Schroder and Tschopp, 2010).

TNF-α is a powerful pro-inflammatory cytokine, which is rapidly released after infection or danger signals and is one of the most abundant early mediators in inflamed tissues (Duque and Descoteaux, 2014). It is also considered as a "master regulator" of pro-inflammatory cytokine production (Maini et al., 1995). TNF-α induces at least five different types of signals that include the activation of NF-κB signaling pathway, initiation of apoptosis and activation of extracellular signal-regulated kinase (ERK), p38 mitogen-activated protein kinase (p38MAPK) and c-Jun N-terminal kinase (JNK) (Muhammad, 2019). Of note, TNF-α is also considered as one of the major cytokines that possibly plays an important role in neuroinflammation (Muhammad, 2019).

IL-12 is a heterodimeric cytokine comprised of the p35 and p40 subunits, which come together after their synthesis and make the bioactive form of IL-12 (P70) (Duque and Descoteaux, 2014). Whereas IL-12 is considered as a proinflammatory cytokine, some other families of this group such as IL-27 and IL-35 are inhibitory cytokines (Duque and Descoteaux, 2014). Accordingly, it is suggested that the IL-12 family of cytokines epitomizes the central role of immunoregulation (Vignali and Kuchroo, 2012). This raises the possibility that there is an unappreciated spectrum of immune balance that is established by the IL-12 family of cytokines (Vignali and Kuchroo, 2012). This is affected by multiple positive and negative feedback loops and interactions that modulate many aspects of immune function. One of their signaling pathways is the JAK- STAT signaling pathway, which is not discussed in this thesis (Vignali and Kuchroo, 2012).

IL-10 is an anti-inflammatory cytokine that plays a critical role in the control of immune responses. IL-10 regulates the production of pro-inflammatory cytokines by distinct mechanisms in different cells and tissues. Shin *et al*.(1999) showed that IL-10 inhibits monocyte TNF-α production by about half, and its effect is independent of IL-12 and IL-1β (Shin et al., 1999). IL-10 also is known to repress IL-12 cytokine production in RAW cells (Rahim et al., 2005a). However, the mechanisms of action remain poorly understood and some believe that IL-10 inhibits many proinflammatory cytokines. One of the several mechanistic pathways through which IL-10 operates is the JAK-STAT3 pathway, which is not discussed in this thesis (Mosser and Zhang, 2008).

Although numerous studies describe cytokine signaling and its effect on various signaling pathways, the interplay between such pathways and mechanisms of cytokine release remains unclear.

1.2.3. Innate inflammatory signaling pathways

Recognition of pathogen-associated molecular patterns (PAMPs) by pattern recognition receptors (PRRs) leads to the activation of three main inflammatory pathways in macrophages including the NF-kB signaling pathway, the MAPK signaling pathway and the inflammasome signaling pathway. Eventually, activation of these pathways leads to the expression of cytokines, inflammation and various mechanisms of cell death to clear out the pathogen.

1.2.3.1. NF-kB signaling pathway

NF-kB (nuclear factor kappa-light-chain-enhancer of activated B cells) is a protein complex that serves as an inducible transcription factor, which regulates a network of genes involved in immune cell responses, cellular differentiation and cellular proliferation (Oeckinghaus and Ghosh, 2009). Indeed, NF-kB is a central mediator of pro- and anti-inflammatory gene induction in the immune

response to infection in both innate and adaptive immune cells (Oeckinghaus and Ghosh, 2009). In response to diverse PAMPs and DAMPs, innate immune cells become rapidly activated and secrete a large array of cytokines, chemokines and additional inflammatory mediators via NF-kB signaling pathway (Liu et al., 2017a).

In mammals, the NF-kB/Rel family comprises five members: p50, p52, p65 (Rel-A), c-Rel, and Rel-B proteins (Oeckinghaus and Ghosh, 2009). Among them, p65: p50 is the most abundant form, which is activated by pathologic stimuli via the IKK complex (Oeckinghaus and Ghosh, 2009).

There is a strong biochemical and genetic evidence that the IKK complex, which consists of two catalytic subunits IKKα and IKKβ and the regulatory subunit IKKγ (NEMO), is bound to the P65: P50 to make a resting complex in the cytoplasm (Solt and May, 2008). IKKβ proteins play an important inhibitory role to keep this complex inactivated (Solt and May, 2008). Phosphorylation of IKKβ proteins results in the degradation of the IKK complex leading to the release of the p65: p50 dimers from the inhibitory complex (Solt and May, 2008). This exposes the arginine- and lysine-rich parts of the p65 for interaction with the importin α/β heterodimers (Giridharan and Srinivasan, 2018). However, importin β has been shown to directly bind p65 and promote its nuclear translocation (Giridharan and Srinivasan, 2018). Within the nucleus, the Ran-GTP protein binds and dissociates the importin-β from the complex with p65 (Giridharan and Srinivasan, 2018). The free p65 then binds specific nucleotide sequence of the target genes and mediates tightly controlled transcriptional programs that exhibit a wide degree of cytokine expression (Giridharan and Srinivasan, 2018).

Nevertheless, the diversity of NF-kB function still raises questions about how a limited set of signaling mediators can integrate diverse stimuli to achieve a stimulus-specific response. However, NF-kB does not exist in isolation, and studies have begun to elucidate how crosstalk with parallel

signaling networks such as inflammasomes or MAPKs can shape the inflammatory response to infections.

1.2.3.2. MAPK signaling pathway

MAPKs (Mitogen-activated protein kinases) are serine-threonine protein kinases that regulate a variety of cellular processes, including innate immune responses, metabolism, apoptosis and proliferation (Keshet and Seger, 2010). MAPKs consist of at least three sequentially acting serine/threonine kinases, a MAP kinase kinase kinase (MAPKKK), a MAP kinase kinase (MAPKK) and finally the MAP kinase (MAPK) itself, with each phosphorylating and hence activating the next kinase in the cascade (Keshet and Seger, 2010). MAPK can regulate effector proteins or transcription factors to positively or negatively regulate suites of genes (Horton et al., 2011).

The MAPKs can be grouped into three main families including p38/SAPKs (stress-activated protein kinases), ERKs (extracellular-signal-regulated kinases) and JNKs (Jun amino-terminal kinases) (Horton et al., 2011).

P38 family members contain a TGY motif in the activation segment and include p38α, p38β, p38γ and p38δ modules (Zarubin and Han, 2005). The p38 module is strongly activated by pathogens, environmental stresses and inflammatory cytokines particularly proinflammatory cytokines (Cuenda and Rousseau, 2007). Evidence indicates that p38MAPK activity is critical for normal immune and inflammatory response. The p38MAPK pathway is a key regulator of pro-inflammatory cytokines biosynthesis at the transcriptional and translational levels (Zarubin and Han, 2005). The upstream cascade for the p38MAPK pathway includes MLK2, MLK3, MEKKs, ASKs, TAK1, TAO1 and TAO2 (Keshet and Seger, 2010). Furthermore, important substrates in

p38 modules include the downstream kinases MK2/3, PRAK, MSK1 and MSK2, as well as various transcription factors (Morrison, 2012).

ERK family members possess a TEY motif in the activation segment and can be subdivided into two groups: the classic ERKs that consist mainly of a kinase domain (ERK1 and ERK2) and the larger ERKs (such as ERK5) that contain a much more extended sequence carboxy-terminal to their kinase domain (Zhang and Dong, 2007). MAPKKs for the classic ERK1/2 module are MEK1 and MEK2, and the MAPKKKs include members of the Raf family, TAK1, and Tpl2 (Morrison, 2012). MEK/ERK signaling is likely to enhance macrophage activity against intracellular pathogens (Través et al., 2012).

JNK family members contain a TPY motif in the activation segment and include JNK1, JNK2 and JNK3. The JNK module is activated by pathogens, environmental stresses and inflammatory cytokines. JNK module plays an important role in cytokine production, apoptosis, inflammation, and metabolism. Upstream cascades for the JNK modules are MKK4, MKK7, MEKK1, MEKK4, MLK2, MLK3, ASK1, TAK1, and Tpl2 (Huang et al., 2009; Qi and Elion, 2005).

While pathogen recognition begins at the receptor level, the signaling components downstream of each receptor and the way they interact with each other ultimately determine the specific transcriptional response and immunological outcome through these modules.

1.2.3.3. Inflammasome signaling pathway

The inflammasome is an essential component of the innate immune response, which plays an important role in the clearance of pathogens or damaged cells. Traditionally, inflammasomes have mainly been studied in professional innate immune cells such as macrophages. Inflammasomes are large multiprotein complexes, which are intracellular PRRs that are localized within the

cytoplasm (Broz and Dixit, 2016). They are mainly formed of a cytosolic pattern recognition receptor (specifically, a nucleotide-binding domain and leucine-rich-repeat [NLR] or absence in melanoma 2 [AIM2]-like receptor [ALR] family member), an adaptor protein (ASC) and an effector pro-caspase-1 (Takeuchi and Akira, 2010). Assembly of the various components of the inflammasomes occurs following the detection of virulence factors or other structural entities of pathogens.

The inflammasomes recruit pro-caspase-1 via ASC (the adaptor molecule apoptosis-associated speck-like protein), which harbors PYD (pyrin domain) or CARD (caspase activation recruitment domain) (Broz and Dixit, 2016). Eventually, assembly and activation of this cascade lead to cleavage of pro-caspase-1 to its active form caspase-1 (Casson and Shin, 2013). Active caspase-1 cleaves the precursors of pro-IL-1β and pro-IL-18 into mature IL-1β and IL-18 (Shi et al., 2014).

Upon activation, the inflammasomes also promote an inflammatory form of cell death named pyroptosis, which is regulated by the inflammatory caspases and gasdermin D (GSDMD) by forming pores in the plasma membrane (Ramos-Junior and Morandini, 2017).

Several inflammasomes have been described so far including NLRP3, NLRP6, NLRP7, NLRP12, NLRC4 and Aim2 (Broz and Dixit, 2016).

1.2.3.3.1. NLRP3 inflammasome signaling pathway

The NLRP3 (NOD-like receptor family with pyrin domain containing receptor 3) inflammasome is the best studied and most characterized inflammasome by far among the other inflammasomes. Activation of NLRP3 inflammasome in macrophages requires two steps: priming and activation. The priming step (signal 1) is provided by inflammatory stimuli such as PAMP-PRR interactions, which result in the activation of NF-kB pathway and the expressions of NLRP3 and pro-IL-1β

(Yang et al., 2019). The second activation step (signal 2) is not that clear (Bauernfeind et al., 2009). It has been reported that a decrease in intracellular K^+ concentration is a common trigger of NLRP3 inflammasome activation among other triggers such as Ca^{2+} signaling, Na^+ influx and chloride efflux. Indeed, numerous NLRP3 inflammasome activators are known to induce K^+ efflux such as bacterial toxins, nigericin and ATP (Yang et al., 2019). Additionally, reactive oxygen species (ROS) generation, especially from the mitochondria, is considered as the other identified trigger of NLRP3 inflammasome activation (Yang et al., 2019).

The NLRP3 inflammasome contains a nucleotide-binding domain (NOD domain), a leucine rich-repeat (LRR) domain and a pyrin domain (Malik and Kanneganti, 2017). The NOD domain has an ATPase activity that is required for NLRP3 oligomerization following activation (Yang et al., 2019). This ATPase activity has recently been implicated as the target of MCC950, which is commonly used as an NLRP3 inhibitor (Coll et al., 2015). MCC950 is a compound that specifically inhibits NLRP3 inflammasome activation, but its molecular mechanism has not been fully elucidated (Yang et al., 2019).

Upon activation, the NLRP3 interacts with ASC via their pyrin domains. The pyrin domain of NLRP3 interacts with the pyrin domain of ASC to initiate inflammasome assembly (Yang et al., 2019). It was speculated that MCC950 directly binds to NLRP3 to inhibit NLRP3–NLRP3 interaction and the subsequent ASC oligomerization (Yang et al., 2019). Thus, it may regulate a key step in NLRP3 activation, such as post-translational modifications (Coll et al., 2015).

Next, the CARD domain of ASC interacts with the CARD domain of pro-caspase-1 to form NLRP3–ASC–pro-caspase-1 complex (Yang et al., 2019). The close proximity of pro-caspase-1 results in self-cleavage and activation of caspase-1 that cleaves pro IL-1β to mature IL-1β, which is secreted out of the cell (Malik and Kanneganti, 2017). Caspase-1 cleaves the cytosolic protein

gasdermin-D, which migrates to the cell membrane and disrupts membrane integrity, resulting in pyroptosis or inflammatory cell death (Shi et al., 2015).

1.2.3.3.2. NLRC4 inflammasome signaling pathway

The other innate immune response against infection is the activation of the NLRC4 inflammasome, which is one of the important inflammasomes, particularly against pathogens. Unlike NLRP3, NLRC4 does not contain a pyrin domain but contains a CARD domain through which it can directly interact with the pro-caspase-1 without the requirement for ASC (Duncan and Canna, 2018). The NLRC4 uses the NAIPs (NLR family apoptosis inhibitory proteins) as the cytosolic detectors to recognize PAMPs as well as the virulence factors secreted by the bacterial type 3 secretion system (T3SS) as well as flagellin, the molecular building block of flagella (Lage et al., 2014; Scholarlycommons and Reyes Ruiz, 2019). Following ligand binding, NAIPs interact with NLRC4 to initiate the assembly of the NAIP/NLRC4 inflammasome, which then recruits and activates pro-caspase-1 via its CARD domain (Lage et al., 2014).

Like NLRP3, NLRC4 activation results in the activation of caspase-1 and IL-1β as well as gasdermin-D leading ultimately to pyroptosis (Duncan and Canna, 2018).

1.2.3.3.3. AIM2 inflammasome signaling pathway

AIM2 (Absent in Melanoma 2) was identified as a gene that was differentially expressed in a model of melanoma (DeYoung et al., 1997). While the function of this protein was unknown at the time, hints on its function emerged from studies that characterized its localization and pattern of expression. AIM2 is localized mostly within the cytoplasm of cells, suggesting that it was likely not involved in directly regulating transcriptional processes (Choubey et al., 2000). AIM2 is a 343 amino acid protein with an N-terminal pyrin domain (amino acids 1-87) and a C-terminal HIN-

200 domain (amino acids 138-337), which is known to have two oligonucleotide-binding folds (Fernandes-Alnemri et al., 2009). AIM2 binds cytosolic DNA via its HIN domain and initiates inflammasome formation via its pyrin domain (Fernandes-Alnemri et al., 2009). The C-terminal HIN domain binds double-stranded DNA (either viral, bacterial, or even host) and acts as a cytosolic dsDNA sensor (Tsuchiya et al., 2010). This leads to the oligomerization of the inflammasome complex. Like NLRP3, the N-terminal pyrin domain of AIM2 interacts with the pyrin domain of ASC protein containing a CARD domain (caspase activation and recruitment domain) that recruits pro-caspase-1 to the complex (Fernandes-Alnemri et al., 2009). Like other inflammasome mediators, this leads to the activation of caspase-1, an enzyme that processes pro-inflammatory cytokines IL-1β and IL-18 and inflammatory cell death (Schroder and Tschopp, 2010). Several inflammasomes such as NLRP3 and AIM2 require an initial pro-inflammatory signal to promote the expression of inflammasome platforms and substrates. This priming phase also referred to as “signal 1”, is mostly mediated by NF-kB transcriptional activation for NLRP3 and type I IFN induction for AIM2 (Lugrin and Martinon, 2018).

1.2.3.3.4. Canonical and non-canonical inflammasome pathways

Inflammasomes are also classified into canonical and non-canonical inflammasomes. Both the canonical and non-canonical inflammasome activation modes eventually lead to cell lysis and the release of proinflammatory cytokines, but their mechanisms of induction differ significantly.

Canonical inflammasomes include members of the NLR family, such as NLRP1, NLRP3, NLRC4 and AIM2, which interact with pro-caspase-1, with or without ASC (Casson and Shin, 2013). Eventually, the activation of this cascade leads to cleavage of pro-caspase-1 to its active form which cleaves the precursors of pro- IL-1β and pro- IL-18 into mature IL-1β and IL-18 (Casson and Shin, 2013). Caspase-1 activation promotes pyroptosis, independently of IL-1β

maturation (Malik and Kanneganti, 2017). Recent evidence has shown that caspase-1 cleaves the linker between the amino-terminal gasdermin-N and carboxy-terminal gasdermin-C domains in gasdermin D, which plays a critical role in the process of pyroptosis (Ramos-Junior and Morandini, 2017).

Pyroptosis (inflammatory cell death) is a key defense mechanism against microbial infections that blocks the replication of intracellular pathogens via cytoplasmic swelling and promotes phagocytosis of released bacteria by neutrophils and macrophages (Casson and Shin, 2013). Pyroptosis can control pathogen replication, stimulate adaptive immune responses and enhance host survival (Bergsbaken et al., 2009).

Non-canonical inflammasome signaling does not involve caspase-1. In mice, the non-canonical inflammasome signaling is dependent on caspase-11, whereas human non-canonical inflammasomes rely on caspase-4 and caspase-5 (Broz and Dixit, 2016). All these caspases can directly bind intracellular LPS in Gram-negative bacteria and Lipoteichoic acid (LTA) in Gram-positive bacteria to form the macromolecular complexes, which mediate gasdermin-D cleavage and induction of inflammatory cell death (Hara et al., 2018; Ming Man et al., 2017). In addition, non-canonical inflammasomes may also indirectly activate the NLRP3 inflammasome by triggering potassium efflux through membrane pores formed by gasdermin-D (Yang et al., 2019). The NLRP3 inflammasome can then mediate the processing of pro-inflammatory cytokines and result in the release of IL-1β and IL-18 in response to non-canonical inflammasome activation and cell death (Yi, 2018).

1.3. *Listeria monocytogenes* (*L. monocytogenes*)

L. monocytogenes is a facultative intracellular and Gram-positive rod-shaped bacterium that lives in a variety of environments, such as soil and decaying vegetation. It can infect animals and humans through ingestion of contaminated food and cause significant disease in neonates, the elderly and immunocompromised individuals (Swaminathan and Gerner-Smidt, 2007).

The pathogenic properties of *L. monocytogenes* rely on its ability to cross three host barriers (the intestinal, placental, and blood-brain barriers) alongside its ability to enter, replicate and survive in a wide range of human cell types, such as macrophages, epithelial cells, and endothelial cells (Swaminathan and Gerner-Smidt, 2007). Following ingestion, *L. monocytogenes* can invade intestinal epithelial cells, enter the host's phagocytic cells including monocytes, macrophages or polymorphonuclear leukocytes and cause a systemic infection (Swaminathan and Gerner-Smidt, 2007).

Its presence intracellularly in phagocytic cells ultimately results in its dissemination to the liver, the spleen and the central nervous system. Infection causes symptoms ranging from mild gastroenteritis to more severe meningitis and encephalitis (Swaminathan and Gerner-Smidt, 2007). Of note, the brain infection is directly linked to the extent of bacteria in the systemic compartments; hence, the brain can be monitored for CNS infection in the context of sepsis (Drevets and Bronze, 2008).

Additionally, *L. monocytogenes* elicits a strong innate immune response and is considered a well-characterized and widely used model organism to study innate immune functions as well as the mechanisms and pathways associated with host infections (Eitel et al., 2011; Pamer, 2004a). *L. monocytogenes* infection also impacts a variety of different host cell death pathways including

inflammasome-mediated pyroptosis (inflammatory cell death), apoptosis (programmed cell death), necrosis (unprogrammed cell death) and necroptosis (programmed necrosis) (McDougal and Sauer, 2018).

EGD and *10403S* strains of *L. monocytogenes* have been widely used in research labs, and while both the strains are genetically close, *EGD* has a point mutation in the transcriptional regulator PrfA leading to constitutive expression of several major virulence genes with higher invasiveness in cultured cells and enhanced virulence in animal models. (Bécavin et al., 2014).

1.3.1. The innate immune response to *L. monocytogenes*

Innate immunity to *L. monocytogenes* is mediated via toll like receptors (TLRs) signaling, particularly TLR2, or the nucleotide-binding oligomerization domain (NOD)-like receptors (NLRs) (Eitel et al., 2011; Torres et al., 2004). They have been shown to play an important role in the host's innate immune responses to *L. monocytogenes* infections through the induction of pro-inflammatory cytokines, chemokines and type I interferons by macrophages and dendritic cells (Torres et al., 2004).

L. monocytogenes has evolved to live within the harsh environment of the host cytosol, and this is critical for both causing disease and inducing an immune response. Upon entry into the host cell, *L. monocytogenes* is initially contained within a phagocytic vacuole (phagosome) (Eitel et al., 2011). Expression of the lytic enzymes, such as the pore-forming toxin listeriolysin O (LLO), allows it to escape from the phagosome into the cytosol (Dramsi and Cossart, 2002). Once *L. monocytogenes* accesses the cytosol, it is rarely exposed to extracellular host defenses. Therefore, activation of the cytosolic innate inflammatory pathways is critical for combating *L. monocytogenes.*

1.3.2. *L. monocytogenes* and innate inflammatory signaling pathways

L. monocytogenes can activate various inflammatory signaling pathways mediated by the phagocytes. Among them, three signaling pathways including the NF-kB signaling pathway, the MAPK signaling pathway, and the inflammasome signaling pathway are considered as important innate signaling pathways to combat with *L. monocytogen* (Dinner et al., 2017; Pamer, 2004b; Tsuchiya et al., 2010). Eventually, this activation leads to the expression of cytokines, inflammation and various mechanisms of cell death to clear *L. monocytogenes*.

1.3.2.1. *L. monocytogenes* and the NF-kB and the MAPK signaling pathways

Multiple cytosolic recognition molecules of the innate immune system have been demonstrated to detect *L. monocytogenes.* As in many other Gram-positive bacteria, lipoteichoic acids in the *L. monocytogenes* cell wall stimulate the NF-κB pathway and the production of proinflammatory cytokines (Hauf et al., 1997). It has been shown also that LLO secreted by *L. monocytogenes* can induce phosphorylation of the IKKα/β, which subsequently promotes the translocation of NF-kB to the nucleus (Kaya et al., 2002). Furthermore, infection with *L. monocytogenes* in the macrophage-like cell lines results in the rapid formation of p65/p50 heterodimeric NF-kB complexes, which might be involved in the subsequent induction of *TNF-α* and *IL-1* genes (Hauf et al., 1994).

Alternate signaling mechanisms, including MAPK pathways (consisting of p38, JNK and ERK), also contribute to the expression of inflammatory cytokines in HeLa epithelial cell lines following recognition of *L. monocytogenes* (Tang et al., 1998). *L. monocytogenes* can also activate the ERK-1 and ERK-2 MAPK through the action of LLO in the host cells (Tang et al., 1998). It has been found that the two other MAPK pathways, including p38 MAPK and c-Jun N-terminal kinase, are also activated by wild-type *L. monocytogenes* (Tang et al., 1998).

1.3.2.2. *L. monocytogenes* and the inflammasome signaling pathways

L. monocytogenes has been reported to activate a variety of inflammasomes via its expression of LLO, flagellin or DNA released through bacteriolysis (Tsuchiya et al., 2010). In the canonical inflammasome pathway, activation of caspase-1 leads to inflammatory cell death by pyroptosis, as well as the processing of the pro-inflammatory cytokines IL-1β and IL-18 into mature (secreted) forms.

The NLRP3 inflammasome can be activated by *L. monocytogenes* infection in different ways. There is evidence that LLO secreted by *L. monocytogenes* can form pores and damage cell membranes, which results in leakage of intracellular K+ and activation of the NLRP3 inflammasome (Kim et al., 2010).

The NLRC4 inflammasome, like other NLRC4 agonists, can be activated by the flagellin of *L. monocytogenes* in addition to components of the type III secretion system (T3SS) (Zhao et al., 2011). As *L. monocytogenes* is a Gram-positive pathogen and lacks the T3SS, its flagellin is likely the key activator of the NLRC4 inflammasome (Valeria et al., 2017).

The AIM2 is another member of the inflammasome pathway that detects the presence of altered or mis-localized DNA molecules within the cell (Tsuchiya et al., 2010). Sauer *et al.* (2010) demonstrated that AIM2 can be triggered by bacterial DNA released during cytosolic lysis of *L. monocytogenes* (Sauer et al., 2010). Indeed, Warren *et al.* in 2010 observed that a component of lysed *L. monocytogenes* as well as transfected *L. monocytogenes'* genomic DNA can activate the AIM2 inflammasome and subsequently caspase-1.

The non-canonical inflammasome is usually triggered by the binding of cytosolic lipopolysaccharide (LPS) of Gram- negative bacteria to caspase-11. Although, *L. monocytogenes*

is a Gram-positive bacterium and does not have LPS in its cell wall, it has been shown that transfection of *L. monocytogenes* extracts into the cytosol of macrophages induced the activation of caspase-11 (Hara et al., 2018). It has been demonstrated that the transfection of lipoteichoic acid (LTA), which is present on the cell wall of *L. monocytogenes* can trigger caspase-11 via NLRP6 inflammasome to induce pyroptosis (Hara et al., 2018).

Rational

Various *Lrrk2* mutations are associated with different inflammatory diseases such as PD, Crohn's disease and Leprosy, diseases with inflammation as their important component (Hui et al., 2018; Kluss et al., 2019; Wang et al., 2015). Hakimi *et al.* (2011) demonstrated that LRRK2 was highly expressed in murine BMDMs and is upregulated in response to infection (Hakimi et al., 2011). Therefore, LRRK2 might have a function in the innate immune system. Subsequently, Liu *et al*. (2017) revealed that while *Lrrk2* deficiency in peritoneal macrophages resulted in reduced activation of caspase-1 and secretion of IL-1β in response to *Salmonella Typhimurium*, hyperactive $Lrrk2^{G2019S}$ mutation enhanced the inflammasome activity revealed by increased caspase-1 activation and IL-1β production (Liu et al., 2017b).

Indeed, prior collaborative works in the labs of Dr. Schlossmacher and Dr. Sad (2019) showed that upon infection with *Salmonella Typhimurium***,** *Lrrk2* deficiency in female mice resulted in a high burden of *Salmonella Typhimurium* in the spleen leading to reduced survival of mice compared to WT littermates (Shutinoski et al., 2019). Conversely, female mice expressing $Lrrk2^{G2019S}$ mutation controlled *Salmonella Typhimurium* better, and infected mice displayed enhanced survival suggesting that the $Lrrk2^{G2019S}$ gain of function mutation results in an enhanced inflammatory response (Shutinoski et al., 2019). Interestingly, this mutation of *Lrrk2* resulted in a reduced viral load in pups infected with reovirus; however, the mice succumbed earlier than WT mice perhaps due to an enhanced cytokine storm (Shutinoski et al., 2019). Shutinoski *et al*. (2019) also demonstrated that this gain-of-function effect conferred by the *G2019S* mutation and loss of function effect conferred by $Lrrk2^{-/-}$ mutation were mediated by myelogenous cells, which are considered as critical cells in the innate immune system.

Collectively, all these results show that *Lrrk2* mutations may alter the course of microbial infections by modulating inflammation due to innate immune response, and this may be dependent on the genotype of the host as well as the type of pathogen (Shutinoski et al., 2019).

Of note, *L. monocytogenes*, which is an intracellular bacterium elicits a strong innate immune response and is a well-characterized and widely used model organism to study innate immune functions as well as the mechanisms and pathways associated with host infections (Pamer, 2004a). Furthermore, following systemic infection with some strains of *Listeria*, the brain can be monitored for CNS infection, which is directly linked to the extent of bacteremia (Drevets and Bronze, 2008). Additionally, *Lm-EGD* has a point mutation in the transcriptional regulator factor leading to the constitutive expression of several major virulence genes with higher invasiveness in human cells and animal models (Bécavin et al., 2014). Hence, *Listeria monocytogenes-EGD* (*Lm-EGD*) seems to be an appropriate model for monitoring systemic infection and innate immune responses via various mechanisms.

3. Hypothesis

Lrrk2^{G2019S} mutation in myelogenous cells enhances the inflammatory response which promotes better control of *L. monocytogenes* in a mouse model.

4. Objectives

Aim 1. Evaluate the impact of *Lrrk2*^{G2019S} mutation in controlling *L. monocytogenes-EGD* infection.

Aim 2. Evaluate the impact of *Lrrk2* ^{G2019S} mutation on specific innate immune mechanisms induced by *L. monocytogenes-EGD* infection.

5. Materials and Methods

5.1. Experimental mice models

All mice used in the experiments were housed at the University of Ottawa's animal facility and maintained in accordance with the guidelines of the Canadian Council on Animal Care (CCAC).

In evaluating the physiological role of *Lrrk2* in the immune system, we have utilized WT and *Lrrk2*^{G2019S} mutant mouse models in most of our experiments, for both *in vivo* and *in vitro* studies. The *Lrrk2*^{G2019S} mutant mice were originally generated by Novartis Pharma company and maintained in Dr. Schlossmacher lab at the University of Ottawa. We obtained homozygous mice from his lab and maintained them in our facility. They were bred by mating male homozygous knock-in with female homozygous knock-in mice. To confirm the genotype of mice, polymerase chain reaction (PCR) was performed on the ear samples collected from the mice in the breeding cages. Of note, *Lrrk2*^{G2019S} mutant mice do not show any specific phenotype. Herzig *et al*. (2011) reported that this group of mice also displayed normal locomotor activity (Herzig et al., 2011).

Ripk1^{K45A} mutant mice were maintained in our facility by adopting heterozygous breeding strategy. *Lrrk2*$^{G2019S/G2019S}$ *-Ripk1*$^{K45A/K45A}$ double knock-in mice, were generated by crossing corresponding heterozygote mouse lines. Polymerase chain reaction (PCR) was performed on the ear samples collected from the pups to determine the genotype.

Most knock-out mice used for the experiments were purchased from the Jackson Laboratory. These include *Nlrp3*$^{-/-}$, *Aim2*$^{-/-}$, *Caspase 11*$^{-/-}$ mice. *Lrrk2*$^{-/-}$ mice were obtained from Dr. Schlossmacher lab and bone marrow from *Nlrc4*$^{-/-}$ mice were obtained from Dr. Jenny P. Ting (University of North Carolina). *Caspase1/11*$^{-/-}$ mice were obtained from Jackson Laboratory and bred in our facility.

Wild type (WT) C57BL/6J mice were obtained from the Jackson Laboratory (Bar Harbor, Maine, USA) and bred in our facility.

All mice used in the experiments were age (6weeks-12 weeks) and sex-matched (mostly females) for experiments. All protocols and procedures were approved by the University of Ottawa Animal Care Committee and Ethics Board**.**

5.2. Preparing *Listeria monocytogenes-EGD* (*Lm-EGD*) for the experiments

5.*2.1.* Preparing the *Listeria monocytogenes-EGD (Lm-EGD)* growth curve

Listeria monocytogenes, EGD strain (*Lm-EGD*) was used for all the experiments. The original stock of *Lm-EGD* was obtained from Dr. Dana Philpott (Immunology Department, University of Toronto). To prepare standard vials for experiments, the growth curve of *Lm-EGD* was required. *Lm-EGD* from the original stock (stored in -80^{o}C) was cultured overnight on Brain Heart Infusion (BHI) agar plates. The next day, a single colony was selected and added to the liquid BHI media and left overnight in a shaker incubator. On the following day, a 1/20 dilution of the culture was performed, the Optical Density (OD) of cultures was measured at different intervals and a growth curve was constructed (Figure1).

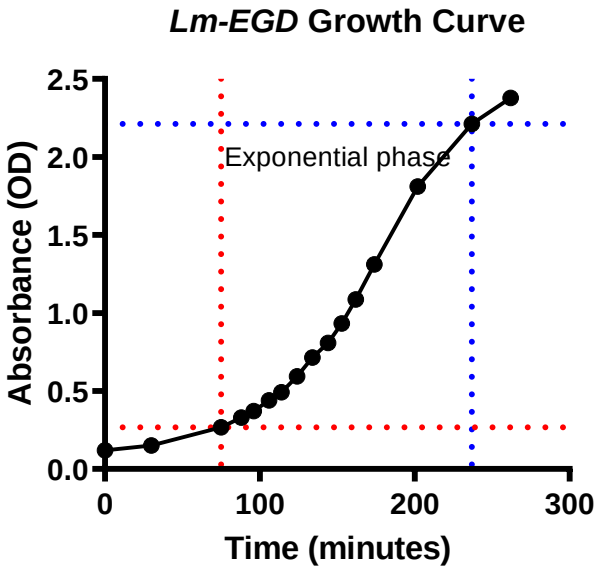
Lm-EGD Growth Curve
Exponential phase
Absorbance (OD)
2.5
2.0
1.5
1.0
0.5
0.0
0
100
200
300
Time (minutes)

Figure 1. Growth curve of *Listeria monocytogenes, EGD* strain *(Lm-EGD)*.

Growth of *Lm-EGD* in liquid BHI media and measurement of optical density (OD) at different time points to determine the exponential growth phase of bacteria. Accordingly, *Lm-EGD* exponentially proliferates between OD=0.268 and OD=2.211.

5.2.2. Preparing *Lm-EGD* vials for the experiments

To prepare standard vials for all the experiments, bacterial growth was halted at the early phase, when OD reached around 0.5 (Figure 1). At this phase, the bacterial concentration would be around 4-5x10e8 CFU/ml. Glycerol was added as a preservative to the bacterial culture, and the aliquots were then distributed in 1 ml vials and stored in -80^{o}C. After one week, 3 random frozen vials were re-suspended in phosphate-buffered saline (PBS) and serial dilutions were plated on BHI agar plates. Plates were incubated at 37^{o}C overnight and colony forming units (CFU) were counted the next day to determine the average of CFU per millilitre (CFU/ml) in each vial. Of note, the colonies of *EGD* strain are smaller in size than other types of *Listeria* such as 10403S strain (Bécavin et al., 2014).

5.2.3. Preparing *Listeria monocytogenes-EGD* (*Lm-EGD*) for intravenous (IV) injection

Lm-EGD obtained from the frozen vial, were resuspended in cold PBS to prepare different concentrations of either 10e5 or 5x10e5 CFU/ml.100 µL (10e4 or 5x10e4 CFU per mice) from this prepared stock was injected into each mouse, intravenously. It is worthy to note that the appropriate concentrations should be prepared just before injecting the mice.

5.2.4. Preparing *Listeria monocytogenes-EGD* (*Lm-EGD*) for oral gavage

Orally acquired *L. monocytogenes* must pass through multiple barriers as well as compete with the gut microbiota to reach the blood and subsequently the spleen and the brain. Hence, a high dose of the active form of *Listeria* is required for infecting mice orally.

To prepare the bacteria in high concentrations, bacterial growth was stopped at the mid-point of the exponential phase, where OD reached around 1.0 (Figure 1) and the bacterial concentration

was estimated to be around 10e9 CFU/ml. Bacteria were resuspended in PBS and immediately used to infect mice by using a thin, flexible catheter for orogastric inoculation.

5.3. Measurement of the spleen and the brain bacterial burden

After infecting mice either intravenously or orally, mice were euthanized by using CO_2 inhalation followed by cervical dislocation on a specific day to measure bacterial burden in the spleen. Spleens were removed, homogenized using frosted glass slides (Fisher Scientific #12-550-343) and resuspended in 5 ml of R8 media. R8 consists of Roswell Park Memorial Institute (RPMI) medium (Thermo Fisher Scientific #31800089), with 8% heat-inactivated Fetal Bovine Serum (FBS) (North Bio #NBSF-701) and 50μM 2-mercaptoethanol (Thermo Fisher Scientific #21985-023) without any antibiotics.

Ten-fold serial dilutions of the spleen suspensions were made and 100 ul aliquots were plated onto BHI agar plates. Plates were incubated at 37^{o}C overnight and colony forming units (CFU) were counted the next day (Bécavin et al., 2014).

To measure specifically brain parenchymal CFU, intracardiac perfusion was adopted to remove the blood from the brain capillaries (Gage et al., 2012). Mice were euthanized with CO2 instead of cervical dislocation, and then the chest cavity was opened to expose the heart. A blunt needle was inserted up from the left ventricle, to initiate the flow of PBS solution with pressure. The right atrium was then excised to allow the incoming blood out until the color of the liver or blood became white (Figure 2 A). The scalp was then opened, and the brain removed for the measurement of the bacterial burden (Figure 2 B). The next steps are similar to the measurement of the spleen bacterial burden.

A

B

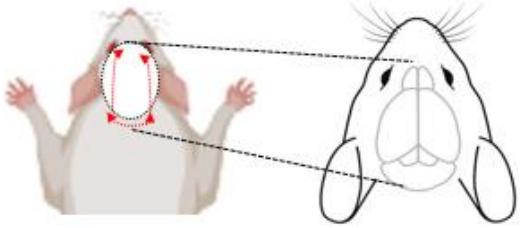

Figure 2. Intracardiac perfusion and brain dissection.

Infected mice were euthanized with CO2 instead of cervical dislocation.

A. The chest wall was opened. The sternum was lifted in order to expose the heart. A small incision was made to the posterior end of the left ventricle. A perfusion needle was inserted up from the left ventricle, to initiate the flow of PBS solution with pressure. The right atrium was then excised to allow the incoming blood out until the color of the liver or blood became white.

B. An incision was made in the skin along the midline from the neck to the nose to expose the skull. The scalp was then carefully opened, and the brain removed for the measurement of the bacterial burden.

5.4. Generation of bone marrow derived macrophages (BMDMs)

Bone marrow derived macrophages (BMDMs) are considered as primary macrophages, derived from bone marrow hematopoietic stem cells *in vitro*, in the presence of growth factors such as macrophage colony-stimulating factor (M-CSF). M-CSF is a recombinant secreted cytokine, which allows myeloid precursors to differentiate specifically into macrophages.

To generate BMDMs, mice were euthanized by using CO_2 inhalation followed by cervical dislocation. Then, femur and tibia bones were removed, and bones were flushed to collect the bone marrow cells. Bone marrow cells were washed with PBS and then re-suspended in R8 medium containing 2-Mercaptoethanol (55μM) and Gentamycin (50μg/mL) to prevent contamination. 100 mm plastic petri dishes were evenly coated with M-CSF (R&D Systems #416-ML-010) at 5 ng/ml and around 15x10e6 cells were added in each petri dish. R8 media with gentamicin was also added on top of the cells, in order to provide nutrients to the growing cells. The final volume in each petri dish was 10mL. These cells were then incubated at 37°C with 5% CO2 for 6 to 9 days.

5.5. Seeding BMDMs for *in vitro* experiments

The resulting differentiated bone marrow derived macrophages (BMDMs) can be harvested from day 6 to day 9. Since these cells stick to the bottom of the petri dishes, supernatants can be aspirated. Cells were then washed with PBS and gently collected by using cell scrapers. Next, cells were washed again and re-suspended in R8 media. Of note, R8 media must be free of antibiotics to allow the cells to be infected by bacteria on the following day

Around 10e5 cells per well were added in 96 well plates or 3-4x10e5 cells per well were added in 24 well plates. The seeded macrophages were incubated overnight at 37°C and 5% CO2. The

following day, they would be ready to be treated with inhibitors/agonists as well as for bacterial infection.

5.6. *In vitro* infection

The following day, cells were infected with *Lm-EGD*. The frozen vial of *Lm-EGD* was thawed, washed and re-suspended in R8 media without any antibiotics. For infecting the cells, various multiplicities of infection (MOIs) are required. MOI defines the ratio of the number of bacteria to the cells. While lower MOI including 0, 1,10 and 25 MOI of *Lm-EGD* were used to infect the cells for measuring cytokines, 10, 25 and 50 MOI were used for the measurement of cell death. Upon addition of the bacteria, the plates were centrifuged at 1500 RPM for 7 minutes, followed by a 30-minute incubation at 37°C to allow bacteria to penetrate the cells. Since *Lm-EGD* is an intracellular bacterium, cells were washed with R8 containing Gentamicin (10μg/mL) to eliminate extracellular bacteria. Next, cells were incubated at 37°C for different time points such as 1, 3, 6 and 24 hours. In some experiments, cells were also treated with various inhibitors at different time points while being infected with *Lm-EGD*. Eventually, supernatants were collected and stored in the freezer (-80°C) for future experiments. Of note, after 18-24 hours incubation, cells were also used for cell death assays.

5.7. Cytokine analysis

There are several methods that detect and analyze cytokines in a sample, of which Enzyme-linked immunosorbent assay (ELISA) is the most commonly used. It is an immunoassay method that detects the presence and measures the concentration of specific analytes (e.g. cytokines) in a sample. There are several types of ELISAs including direct, indirect, sandwich and competitive ELISA (Sakamoto et al., 2018). Among them, sandwich ELISA is the most common method

which has been used in research labs, due to its high sensitivity and specificity (Sakamoto et al., 2018). Sandwich ELISA is named so as the antigen is sandwiched between two antibodies, capture antibody and detection antibody (Sakamoto et al., 2018). All murine ELISA experiments in our lab were performed by using the sandwich ELISA method. Additionally, all ELISAs were performed using commercial kits purchased from BD Biosciences and R&D systems. Among cytokines, TNF-α, IL-10, IL-1β and IL-12 were measured in our experiments.

(Mouse TNF-α (BD) #555268, Mouse IL-10 (BD)#555252, Mouse IL-12 (BD)#555256 and Mouse IL-1β (R&D) #DY401)

The steps involved in an ELISA are almost the same for all our experiments. ELISAs were run in 96-well microplates coated with a capture antibody specific for the analyte of interest. These plates were sealed and left at 4^{o}C or room temperature overnight. On the next day, after washing the plate with PBS-T (1X PBS and Tween 20 in H_2O) blocking buffer or assay diluent was added to the wells. Blocking buffer passively binds to all remaining binding surfaces of the plate that are not occupied by the capture antibody. It reduces the background signal and improves the sensitivity of the assay. 10% FBS in PBS for TNF-α, IL-10 and IL-12 and 1% BSA in PBS for IL-1β were used as blocking buffers.

In the next step, after incubation, the plates were washed again with PBST and, the standards and the samples were added to the wells. Of note, the ELISA standard curve is prepared by making serial dilutions of standards with known concentrations. It is one of the essential parts of the ELISA because cytokines can be quantified by using the standard curve. The samples then were supernatants of the infected/treated macrophages.

Upon incubation and washing again, the detection antibody along with an enzyme Streptavidin-HRP (horseradish peroxidase) (HRP) was added to the wells, leading to the formation of an antigen-antibody complex. Of note, the plate should be washed several times in every step of ELISA to remove the unbound antibody or enzyme conjugates.

Finally, after incubation and last washing, the substrate, tetramethylbenzidine (TMB), was added to the wells. The substrate is the chemical which is converted by the enzyme to generate color. After developing the color thoroughly, stop solution (diluted sulphuric acid 2 N) was added to the wells to stop the reaction.

Of note, the amounts of reagents, the incubation time and the number of washes for each specific cytokine have been explained in the kits in detail.

Eventually, absorbance was measured at 450 nm in a microplate reader. Data were analyzed and quantified using SoftMax Pro software.

5.8. Western Blotting

Western blotting is commonly used to separate and identify proteins among a mixture of proteins. In this technique, proteins are separated based on their molecular weight through gel electrophoresis (Mahmood and Yang, 2012). The proteins are then transferred to a membrane producing a band for each protein**,** following which the membrane is incubated with labelled antibodies specific to the protein of interest. The bound antibodies are then detected by developing the film. The thickness of the band corresponds to the amount of protein present (Mahmood and Yang, 2012). While this method is considered to be highly sensitive and specific which has been used by research and clinical laboratories, there are some disadvantages such as high cost, high

technical demand as well as false-positive results (Ghosh et al., 2014). It means that an antibody can react with a non-intended protein, which sometimes happens. There are several steps involved in the western blot method.

5.8.1. Lysate preparation from cell culture

The BMDMs which were infected with 10 MOI of *Lm-EGD*, as described in section 5.6., were used as samples for cell lysate collection. The cells were lysed at 0, 1, 3, and 6 hours post-infection for measurement of the desired proteins by western blot. Of note, 4x10e5 cells were seeded in a 24 well plate to have more amount of proteins present in the lysates. The lysis breaks down the cell membrane to separate proteins from the non-soluble parts of the cells. 1% Sodium dodecyl sulfate (SDS) lysis buffer with β -Mercaptoethanol was used to lyse the cells. 120 µL of lysis buffer was used to lyse 4x10e5 cells. Immediately following cell lysis, proteolysis, dephosphorylation, and denaturation begin to occur (Ghosh et al., 2014). This activity should be kept to a minimum by preparing samples on ice. The lysates were boiled at 96^{o}C for 5 minutes, to reduce disulfide bridges in the proteins and denature (unfold) the proteins, so that they can get better access to the antibody. They were then stored in the freezer (-20^{o}C) for future experiments.

5.8.2. Loading and running the gel

The cell lysates were loaded on different percentages of polyacrylamide gels, depending on the size of the protein of interest. As a rule, the higher the size of the protein, the lower percentage of the gel should be used.

A protein marker or ladder was used to estimate the size of proteins resolved by gel electrophoresis. Western blot ladders were obtained from Bio-Rad company (lot number#161-0375) which showed sizes from 10 kDa to 250 kDa. The protein ladder was added to the gel

followed by the addition of 12-15 μL of lysates to the wells. Electrophoresis of the gel was then run at 100-130 V for 1-2 hours.

Electrophoresis is performed with a negative pole on one end of the gel and a positive pole on the opposite end of the gel. The negatively charged SDS, which is present in the gel, bound to proteins causes migration of protein complexes towards the positive pole during electrophoresis, allowing proteins to be separated by size (Ghosh et al., 2014)

5.8.3. Transferring the samples

Once electrophoresis is completed, proteins must be transferred from the gel onto a suitable membrane for antibody staining and detection. Polyvinylidene fluoride (PVDF) membranes were used in all of my experiments, as they offer better protein retention and physical strength compared to other membranes. To transfer the proteins from the gel onto the PVDF membrane, a sandwich of layers including filter sponge, filter paper, membrane and gel is made. The transferring time and voltage are around 100 v for 1-2 hours, depending on the protein of interest.

5.8.4. Immunoblotting and detection

The first step in immunoblotting is to rinse and block the membrane with non-specific protein, such as 5% bovine serum albumin (BSA) in TBST. Tris Buffered Saline Solution (TBS) with 0.5% Tween- 20 (TBST) was used as a washing buffer in every step of my western blot experiments to wash unbound proteins. BSA as a non- specific protein, binds to the surface of the membrane where proteins are not already present to avoid binding of antibody non-specifically to the membrane.

After blocking, the membrane was incubated with a primary antibody diluted in buffer containing BSA. The primary antibody detects and binds to the specific amino-acid sequence of the protein

of interest. Incubation time for the membrane soaked in the primary antibody can be from some hours in room temperature to overnight at 4^{o}C, depending on the protein of interest.

Upon washing to remove unbound primary antibody, secondary antibody diluted with blocking buffer was added. Secondary antibody, which detects the primary antibody, can be anti-mouse, rabbit or rat, depending on the type of primary antibody used. Secondary antibodies used for western blotting are typically conjugated with an enzyme; the most commonly used enzymes are Horse Radish Peroxidase (HRP). Once the substrate is added, it reacts with HRP and emits light. The membrane is then exposed to a radiography film in a dark room or can be imaged with a chemiluminescent imaging system, to detect the light emitted which appears in the form of protein bands on the film. Eventually, the protein ladder was marked on the radiography film to provide a reference for various molecular weights of proteins in order to compare with the proteins of interest.

Eventually, the membrane can be stripped to remove previous primary and secondary antibody and used for the detection of another protein of interest.

-Primary and secondary antibodies used for western blot analysis purchased from Cell signaling company:

Rabbit anti-IKKα/β (#2370), Rabbit anti-phospho- IKKα/β (#2697), Rabbit anti-p65 (#8242), Rabbit anti-phospho P65(3033), Rabbit anti-P38MAPK (#8690), Rabbit anti-phospho-p38MAPK(#4511), Rabbit anti-MK2 (#3042), Rabbit anti-phospho-MK2(#3007), Rabbit anti-ERK1/2(#4695), Rabbit anti-phospho ERK1/2 (#4370), Rabbit anti-NLRP3(#15101), Rabbit anti-TAK1 (#5206s), Rabbit anti- phospho TAK1 (#9339s), Rabbit anti-total JNK(#9252), Rabbit anti-phospho JNK (#9251), Rabbit anti-P-RIPK1(Ser 166)(#65746), Rabbit anti- RIPK1(#3493)

Mouse anti-B actin (33700), Goat anti- rabbit, HRP-linked antibody (#7074), Horse anti-mouse, HRP-linked antibody (#7076), Goat anti-rat, HRP-linked antibody (#7077).

Mouse anti caspase-1 (Santa cruz#SC-56036), Rat anti-caspase-11 (Novus biologicals#10454)

5.9. Measurement of cell death

Cell death experiments determine the proportion of dead cells within a population of cells, which have been treated with a chemical or infected with bacteria. There are various methods for measuring cell death. When the cells die, the cell membrane losses its integrity. Cell death can also be assessed by using a dye which penetrates the cell and stains the dead cells. Evaluating the percentage of cells stained represents the proportion of dead cells in the population. Staining cells with a dye, zombie yellow is one such method for the measurement of cell death that we used in all of our experiments.

5.9.1. Zombie Yellow staining

The BMDMs which were infected with *Lm-EGD* at 0, 10, 25 and 50 MOI, as explained in section 5.6., were used as samples. Zombie Yellow™ (BioLegend, San Diego, CA) is an amine-reactive fluorescent dye, which is detectable by flow cytometry. Although it can pass through the cells with permeable membranes (dead cells), it cannot penetrate the cells with the intact membrane (live cells).

The cells were washed with PBS and stained with diluted Zombie Yellow dye (1:100 in PBS). Since Zombie Yellow dye is light sensitive, the plates were incubated in dark at least for 30 minutes. After washing with PBS again, the dead and live cells were fixed in order to prevent deterioration. 1% paraformaldehyde (PFA) was used to fix the cells. Finally, the fixed-stained cells were transferred to FACS tubes and acquired on LSR Fortessa flow cytometer. Of note, one group

of cells was not stained with Zombie to detect the background fluorescence of cells. Acquired data were analyzed by FlowJo software.

5.10. Statistical analysis

All statistical analyses were carried out using SoftMax Pro software and graphs were made using GraphPad Prism 8 software. The error bars indicate standard error of the mean ± S.E.M. All values were compared using one-way ANOVA or unpaired t-test depending on the number of variables involved and the factors to be compared. The statistical test used for analysis has been indicated in the individual figure legends, where *$p<0.05$; **$p<0.01$; ***$p<0.001$; ****$p<0.001$.

6. Results

6.1. The first objective is evaluating the impact of *Lrrk2* ^{G2019S} mutation in controlling *Listeria monocytogenes-EGD* (*Lm-EGD*) infection.

6.1.1. The *Lrrk2* ^{G2019S} mutant mice and WT mice show the same bacterial burden in the spleen and the brain tissues upon oral gavage.

Lm-EGD is one of several enteric microbes that is acquired orally through the ingestion of contaminated food, invades the gastric mucosa and then disseminates to peripheral tissues causing systemic disease (Swaminathan and Gerner-Smidt, 2007). Orally acquired *Lm-EGD* must pass through multiple barriers as well as compete with the gut microbiota to reach the spleen and the brain. It has been estimated that only 1 in 10^6 bacteria reach the underlying lamina propria (Pitts and D'Orazio, 2018). Hence, a large dose ($\geq 10^9$ CFU) of bacteria is required for infecting mice orally. Preparing bacteria for oral gavage and the method of oral gavage have been described thoroughly in the materials and methods section 5.2.4.

To begin with, we infected only WT mice orally with *Lm-EGD* (10e9 CFU), euthanized mice at 3- and 5- days post-infection and finally quantified the bacterial burden (CFU) in the spleens and brains of infected mice as described in the materials and methods section 5.3. While one mouse displayed the spleen involvement at day 3, every other mouse showed the spleen bacterial burden at day 5 (Figure 3 A, B).

In this regard, *Lrrk2*^{G2019S} mutant mice and WT mice were infected orally with 10e9 CFU *Lm-EGD* and then were euthanized at day 5 post-infection, at which the bacterial burdens (CFU) in the spleens and the brains were evaluated. The bacterial burden in the spleen and the brain was comparable between two groups (Figure 3 C, D). It should be noted that infection through the oral

route did not achieve a high bacterial burden in the spleen as most of the mice had approximately 10e4 CFU/spleen. Furthermore, we did not want to evaluate the gut immune system in response to *Listeria monocytogenes*; thus, we did not continue this method.

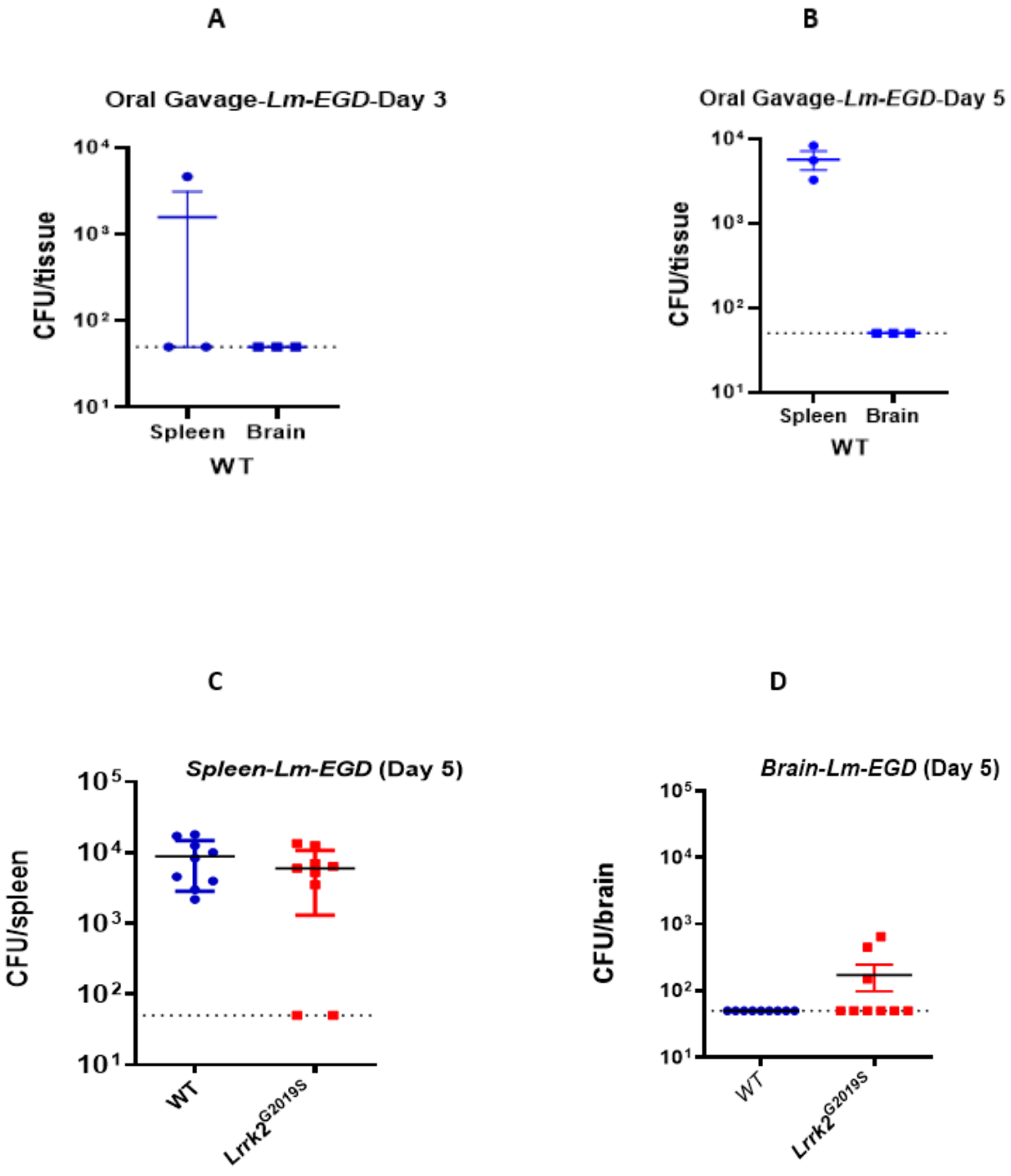
A
Oral Gavage-*Lm-EGD*-Day 3
CFU/tissue
10^4
10^3
10^2
10^1
Spleen
Brain
WT
B
Oral Gavage-*Lm-EGD*-Day 5
CFU/tissue
10^4
10^3
10^2
10^1
Spleen
Brain
WT
C
Spleen-Lm-EGD (Day 5)
CFU/spleen
10^5
10^4
10^3
10^2
10^1
WT
$Lrrk2^{G2019S}$
D
Brain-Lm-EGD (Day 5)
CFU/brain
10^5
10^4
10^3
10^2
10^1
WT
$Lrrk2^{G2019S}$

Figure 3. The infection of WT and *Lrrk2*^{G2019S} mutant mice through the oral route results in a similar bacterial burden in the spleen and the brain.

Graphs display bacterial colony forming unit (CFU) in adult mice following oral infection with *Lm-EGD*.

A, B. WT mice were infected orally with *Lm-EGD* (10e9 CFU) and (A) at day 3 and (B) at day 5 post-infection, spleens and brains were collected, and the bacterial burden was evaluated after plating serial dilutions on BHI agar plates. Every dot corresponds to a single mouse (n=3 in each group).

C, D. *Lrrk2*^{G2019S} mutant and WT mice were infected orally with *Lm-EGD* (10e9 CFU) and at day 5 post-infection, (C) spleens and (D) brains were collected, and the bacterial burden was evaluated after plating serial dilutions on BHI agar plates. Data are pooled from 3 independent experiments, and each experiment has 3 replicates (n=9 in each group), presented as mean ± SEM. Every dot corresponds to a single mouse. Statistical significance was calculated by unpaired two-tailed Student's t-test, where *p<0.05; **p<0.01; ***p<0.001; ****p<0.001 using GraphPad Prism 8 software.

6.1.2. Female WT mice display a trend towards higher bacterial burden in the spleen and the brain via intravenous (IV) route compared to male WT mice.

Intravenous (IV) infection model is widely used in research laboratories because it is highly reproducible (Pitts and D'Orazio, 2018). Mice given a lethal dose of *Listeria monocytogenes* by the IV route generally succumb to the infection within four days, and sub-lethal infection results in CFU in the spleen and the liver that show little mouse-to-mouse variation (Pitts and D'Orazio, 2018). Therefore, we continued our experiments by injecting mice with *Lm-EGD* in the tail vein instead of oral gavage, which we performed previously.

To determine the appropriate gender and the optimal doses for injection, male and female adult WT mice (8-12 weeks old) were injected with various doses of *Lm-EGD*. Bacteria were prepared from the frozen stock for injection as described in the materials and methods section 5.2.3.

To begin with, only WT male mice were injected with 10e4 CFU of *Lm-EGD* (Bécavin et al., 2014). Since day 3 is considered as the peak of bacterial burden following infection of mice with *Lm-EGD*, we euthanized mice at day 3 post-infection and quantified the bacterial burden (CFU) in the spleens and the brains of infected mice as described in the materials and methods section 5.3. Although all spleens showed bacterial burden, brains did not show any infection (Figure 4 A). Then, only female WT mice were injected with a higher bacterial dose of 10e5 CFU. All spleens and brains displayed *Lm-EGD* infection (Figure 4 B). Eventually, both female and male WT mice were injected with a bacterial dose of 5x10e4 CFU (a bacterial dose between 10e4 and 10e5 CFU). Interestingly, female WT mice showed a trend towards higher CFU in both brains and spleens compared to male WT mice (Figure 4 C).

Therefore, we continued our experiments by injecting female *Lrrk2*^{G2019S} and WT mice with either 10e4 or 5x10e4 CFU for most experiments.

A

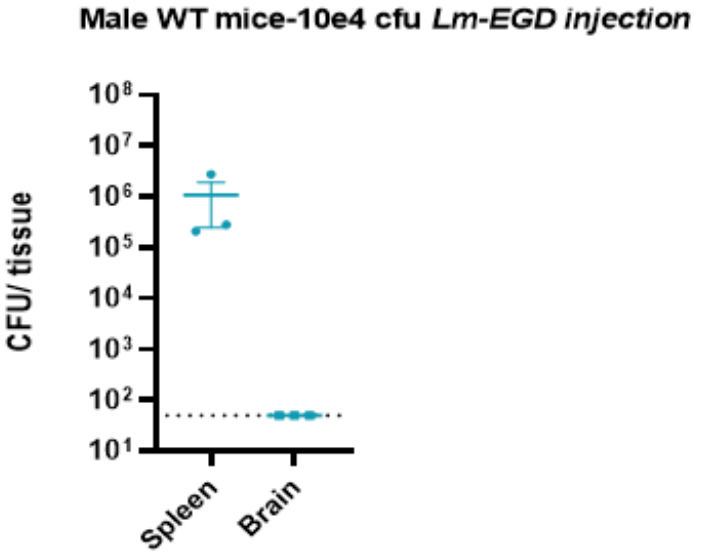
Male WT mice-10e4 cfu *Lm-EGD injection*
CFU/ tissue
10^8
10^7
10^6
10^5
10^4
10^3
10^2
10^1
Spleen
Brain

B

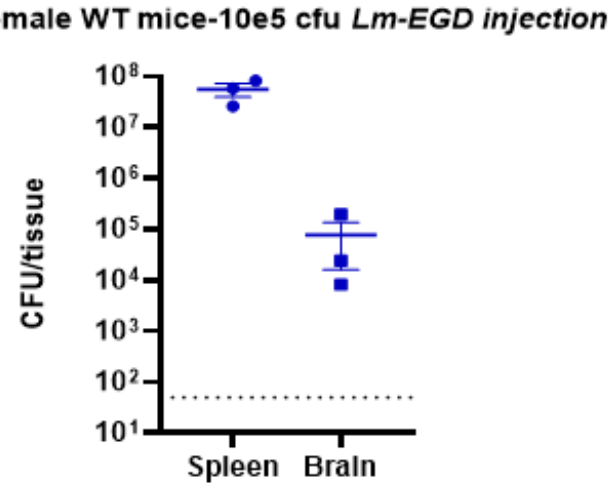
Female WT mice-10e5 cfu *Lm-EGD injection*
CFU/tissue
10^8
10^7
10^6
10^5
10^4
10^3
10^2
10^1
Spleen
Brain

C

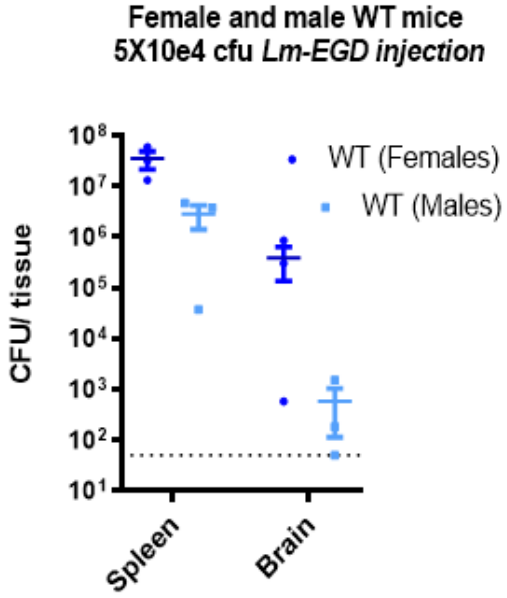
Female and male WT mice
5X10e4 cfu *Lm-EGD injection*
CFU/ tissue
10^8
10^7
10^6
10^5
10^4
10^3
10^2
10^1
WT (Females)
WT (Males)
Spleen
Brain

Figure 4. Female WT mice display a trend towards higher bacterial burden in the spleen and the brain compared to male WT mice.

Graphs show bacterial colony forming units (CFU) of the spleen and the brain from adult male and female WT mice (8 weeks-12 weeks) inoculated with *Lm-EGD* via tail vein injection. Spleens and brains were collected, and the bacterial burden was evaluated after plating serial dilutions on BHI agar plates.

A. Spleens and brains were collected from male WT mice (n=3) injected with 10e4 CFU at day 3 post-infection.

B. Spleens and brains were collected from female WT mice (n=3) injected with 10e5 CFU at day 3 post-infection.

C. Spleens and brains were collected from male and female WT mice (n=3) injected with 5x10e4 CFU at day 3 post-infection.

Every dot corresponds to a single mouse.

6.1.3. *Lrrk2*^{G2019S} mutant-mice show significantly lower bacterial burden in the spleen than WT mice.

It has been shown that *G2019S* mutation in *Lrrk2* enhances microbial control in response to *Salmonella* infection (Shutinoski et al., 2019). Therefore, we aimed to investigate the impact of *Lrrk2*^{G2019S} mutation on controlling *Listeria monocytogenes*. Both *Lrrk2*^{G2019S} and WT mice were injected with 10e4 and 5x10e4 CFU of *Lm-EGD* via the tail vein. Bacteria were prepared from the frozen stock for injection as described in the materials and methods section 5.2.3.

Mice were sacrificed at day 3 following infection, and the bacterial burdens in spleens were quantified as described in the materials and methods section 5.3. *Lrrk2* ^{G2019S} mutant mice injected with 5x10e4 CFU had significantly lower bacterial CFU in the spleens in comparison to WT mice (Figure 5 A). A similar trend was observed in the spleens of mice injected with a reduced dose of *Lm-EGD* (10e4 CFU) intravenously (Figure 5 B).

It should be noted that infection through the IV route resulted in a very high bacterial burden in WT mice that was significantly reduced in the *Lrrk2* ^{G2019S} mutant mice (Figure 5 A, B). In contrast, the oral route did not achieve a high bacterial burden in the spleen as most of the mice had approximately 10e4 CFU/spleen (Figure 3).

Since infection in the brain is directly linked to the extent of bacteria in the systemic compartment, the brain was monitored for CNS infection in the context of sepsis (Drevets and Bronze, 2008). Accordingly, we decided also to evaluate bacterial burden in the brains of infected mice. It should be noted that blood was perfused from the brains to determine the bacterial burden specifically in the brain parenchyma. The brains were perfused via intracardiac perfusion method which has been described in the materials and methods section 5.3. The bacterial burden was

assessed in the perfused brains of WT and *Lrrk2* ^{G2019S} mutant mice. Brains of infected *Lrrk2*^{G2019S} mice showed a trend towards lower bacterial burden compared to infected WT brain tissues (Figure 5 C).

A

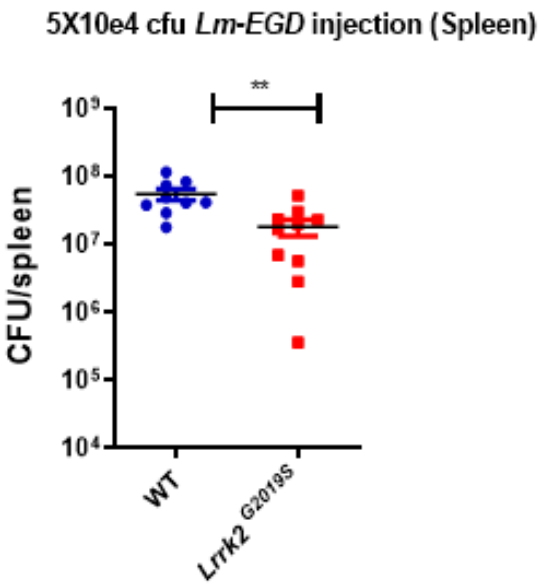
5X10e4 cfu Lm-EGD injection (Spleen)
**
CFU/spleen
10⁹
10⁸
10⁷
10⁶
10⁵
10⁴
WT
Lrrk2 G2019S

B

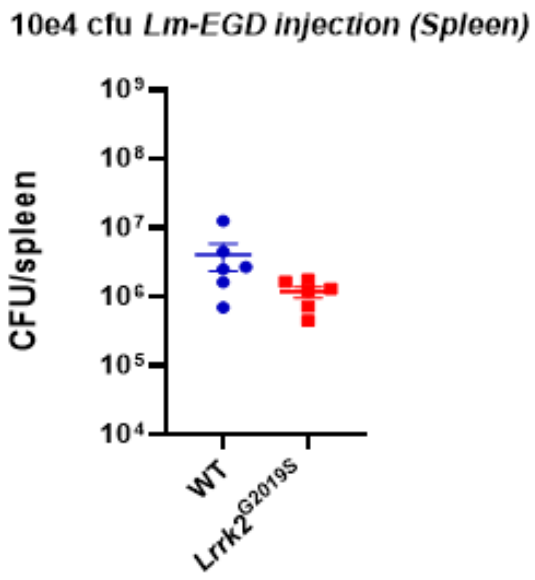
10e4 cfu Lm-EGD injection (Spleen)
CFU/spleen
10⁹
10⁸
10⁷
10⁶
10⁵
10⁴
WT
Lrrk2G2019S

C

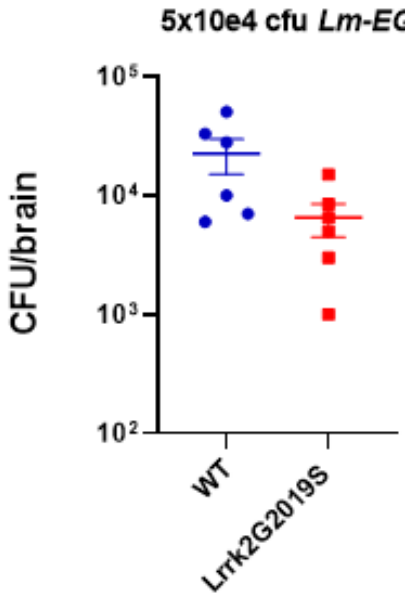
5x10e4 cfu Lm-EGD injection (Brain)
CFU/brain
10⁵
10⁴
10³
10²
WT
Lrrk2G2019S

Figure 5. *Lrrk2* ^{G2019S} mutant mice showed significantly reduced *Lm-EGD* burden in the spleen.

Graphs display bacterial colony forming unit (CFU) of spleens and brains from adult *Lrrk2*^{G2019S} and WT mice inoculated with *Lm-EGD* via tail vein injection.

A, B. Spleens were collected from *Lrrk2*^{G2019S} mutant and WT mice infected with 5x10e4 or 10e4 CFU *Lm-EGD*

C. Brains were perfused with PBS and collected from *Lrrk2*^{G2019S} mutant and WT mice infected with 5x10e4 CFU *Lm-EGD*.

At day 3 post-infection, the bacterial burden was evaluated in the collected spleens and perfused brains upon plating serial dilutions on BHI agar plates. Data are pooled from 2-3 independent experiments, and each experiment has at least 3 replicates and presented as mean ± SEM.

Every dot corresponds to a single mouse. Statistical significance was calculated with unpaired two-tailed Student's t-test, where *p<0.05; **p<0.01; ***p<0.001; ****p<0.001 using GraphPad Prism 8 software.

6.2. The second objective is evaluating the impact of *Lrrk2* ^{G2019S} mutation on specific innate immune mechanisms induced by *L. monocytogenes-EGD* infection.

6.2.1. *Lrrk2*^{G2019S} mutation enhances inflammasome activity in macrophages.

Our *in vivo* results have so far indicated that *Lrrk2* ^{G2019S} mutant mice displayed a lower bacterial burden in the spleen in response to *Lm-EGD.* Since the second aim of this thesis was to determine the innate immune mechanism through which *Lrrk2* ^{G2019S} mediates better control of *Lm-EGD*, we decided to perform in vitro experiments on BMDMs, representative cells of the innate immune system.

Liu *et al*. (2017) showed that the *Lrrk2*^{G2019S} mutation modulates the innate immune system by enhancing the inflammasome activity via promoting caspase-1 activation and IL-1β production in peritoneal macrophages infected with *Salmonella* (Liu et al., 2017b). In this regard, we were interested in evaluating whether *Lrrk2*^{G2019S} modulates inflammasome signaling in response to *Lm-EGD.*

To this end, *Lrrk2*^{G2019S} and WT bone marrow derived macrophages (BMDMs) were prepared and infected with *Lm-EGD* as described in the materials and methods sections 5.4,5.5 and 5.6. We used lower MOI including 0, 1, 10, 25 MOI for measuring IL-1β secretion and 0, 10, 25 and 50 MOI for measuring cell death.

We observed that IL-1β expression was significantly increased in *Lrrk2* ^{G2019S} mutant macrophages compared to WT cells (Figure 6 A). Interestingly, the impact on cell death was less pronounced as *Lrrk2* ^{G2019S} mutant macrophages displayed slightly increased cell death in comparison to WT cells (Figure 6 B). These results indicate that *Lrrk2* ^{G2019S} mutation enhances inflammasome activity by promoting IL-1β expression without a significant impact on cell death.

A

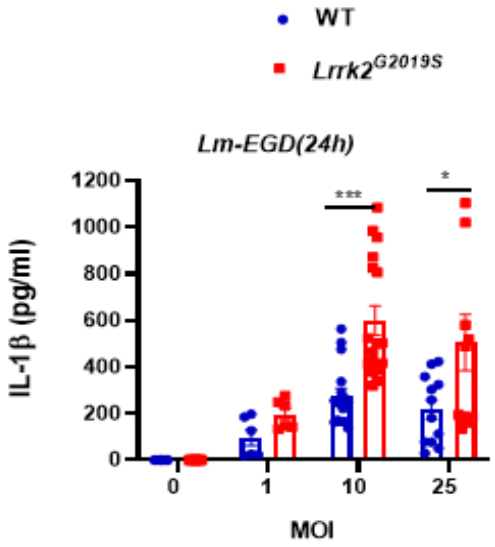
WT
Lrrk2G2019S
Lm-EGD(24h)
IL-1β (pg/ml)
1200
1000
800
600
400
200
0
***
*
0
1
10
25
MOI

B

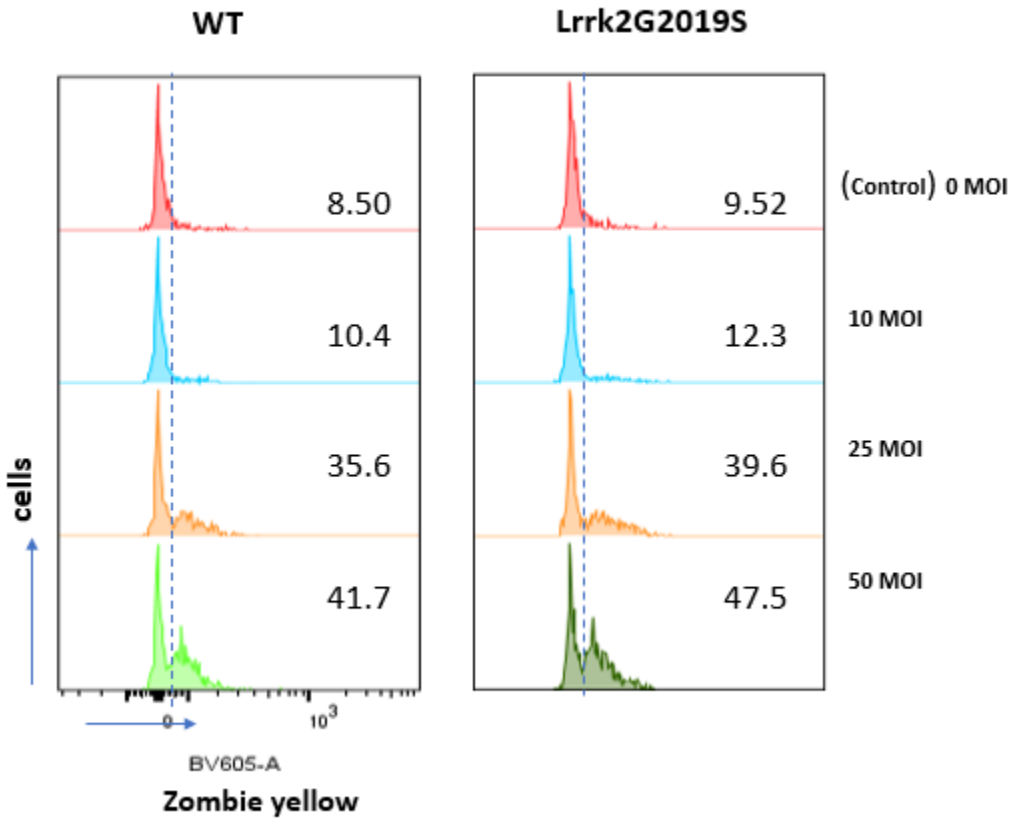
WT
Lrrk2G2019S
8.50
10.4
35.6
41.7
9.52
12.3
39.6
47.5
(Control) 0 MOI
10 MOI
25 MOI
50 MOI
cells
0
10^3
BV605-A
Zombie yellow

Figure 6. *Lrrk2*^{G2019S} mutation results in increased expression of IL-1β by macrophages.

Lrrk2^{G2019S} and WT BMDMs were generated, and at day 6 to 9 of differentiation, they were infected with *Lm-EGD* for 24 hours.

A. Expression of IL-1β in the supernatants of infected WT and *Lrrk2*^{G2019S} mutant BMDMs was evaluated by ELISA. Macrophages were infected with various MOIs of *Lm-EGD* (0,1,10,25), and IL-1β expression was evaluated at 24 hours post-infection. Data were pooled at least from 3 biological replicates, each performed in triplicates. Graphs depict mean ±S.E.M. Statistics were done using unpaired t-tests, where *p<0.05; **p<0.01; ***p<0.001; ****p<0.001 using GraphPad Prism 8 software.

B. WT and mutant BMDMs were infected with various MOIs (0,10,25 and 50) and cell death evaluated in control and infected cells at 24 hours post-infection by Zombie Yellow staining via flow cytometric analysis. The graph displays the percentages of cell death. The data shown is representative of three similar experiments, and each experiment was performed in triplicates.

6.2.2. *Lrrk2*^{G2019S} mutation does not modulate inflammasome activity in macrophages in response to the combined treatment with LPS and ATP.

Having shown that the inflammasome activity was enhanced in *Lrrk2*^{G2019S} mutant macrophages in response to *Lm-EGD* infection, we aimed to investigate whether this also occurs following other triggers. While *Lm-EGD* is a Gram-positive bacterium, we used LPS, which is the major component of the Gram-negative bacteria and is considered as a potent activator of the inflammasome signaling pathway when used in conjunction with ATP (Zha et al., 2016). Among the various inflammasomes, NLRP3 inflammasome is considered as the most studied inflammasome platform. Two-signal model has been proposed for NLRP3 inflammasome activation in macrophages. The first signal (priming) is provided by LPS that enhances the expression of NLRP3 and pro-IL-1β through the activation of the NF-kB pathway (Lu et al., 2008). The second signal (activation) is triggered by ATP, which results in the efflux of potassium ions that triggers the assembly of the NLRP3 inflammasome and consequent processing of pro-IL-1β and pro-caspase-1 to IL-1β and caspase-1 respectively (Zha et al., 2016).

In this regard, WT and *Lrrk2*^{G2019S} mutant macrophages were generated as described in the materials and methods sections 5.4 and 5.5. Instead of using *Lm-EGD*, we stimulated cells with LPS and ATP.

We observed that WT and *Lrrk2*^{G2019S} mutant macrophages express similar levels of IL-1β in response to LPS+ATP treatment (Figure 7A). However, there was more cell death in *Lrrk2*^{G2019S} mutant macrophages (Figure 7B). This indicates that *Lrrk2*^{G2019S} might be regulating cell death via different pathways from the IL-1β expression in response to LPS and ATP.

To determine the role of NLRP3 signaling further, we treated macrophages with an NLRP3-inhibitor (MCC 950). MCC950 is a potent and selective inhibitor of the NLRP3 inflammasome, which blocks the release of IL-1β. It inhibits NLRP3 inflammasome by preventing oligomerization of the inflammasome adaptor protein ASC (apoptosis-associated speck-like protein containing the CARD) (Coll et al., 2015). Upon the addition MCC950, the expression of IL-1β was completely abrogated (Figure.7A). This indicates that IL-1β expressed by BMDMs in response to the combined LPS and ATP treatment is mainly dependent on the NLRP3 inflammasome.

A

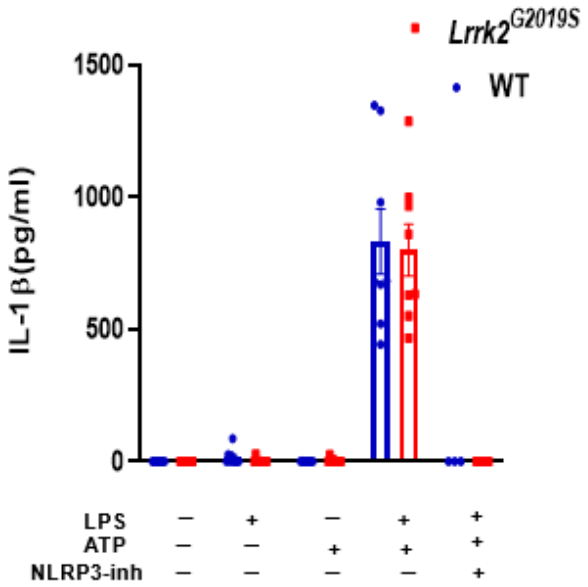
Lrrk2G2019S
WT
IL-1β(pg/ml)
1500
1000
500
0
LPS
ATP
NLRP3-inh

B

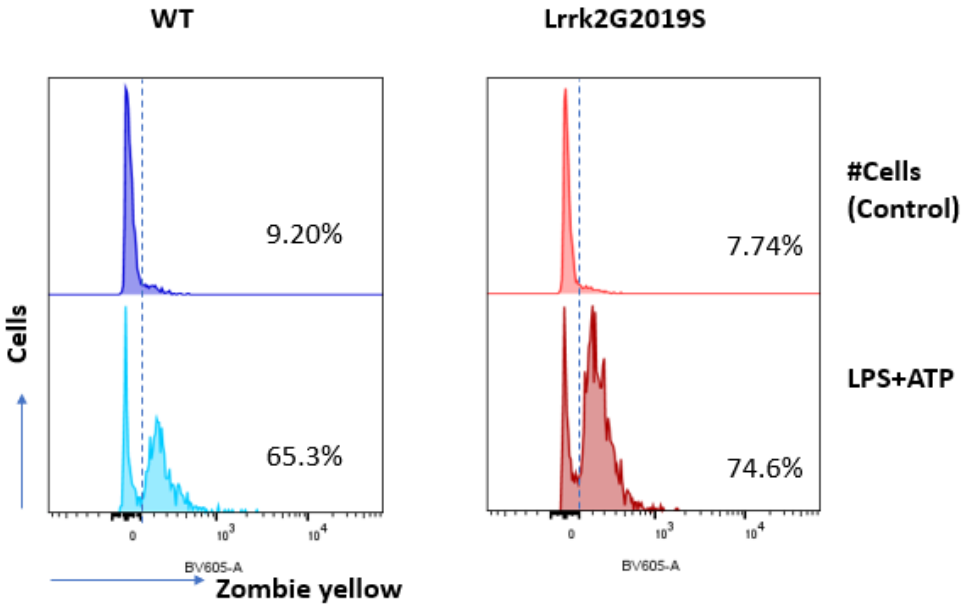
WT
Lrrk2G2019S
Cells
9.20%
65.3%
7.74%
74.6%
BV605-A
Zombie yellow
#Cells
(Control)
LPS+ATP

Figure 7. Expression of IL-1β is similar in WT and *Lrrk2*^{G2019S} mutant bone marrow derived macrophages (BMDMs) in response to the combined LPS and ATP treatment.

WT and *Lrrk2* ^{G2019S} mutant BMDMs were generated and treated with LPS (100 ng/ml) and ATP(2.5mM) *in vitro*.

A. WT and mutant BMDMs were treated with 100 ng/mL of LPS for 3.5 hours followed by the addition of ATP (2.5mM) for 30 minutes. Expression of IL-1β in the supernatants of treated WT and *Lrrk2*^{G2019S} mutant BMDMs was evaluated by ELISA. To inhibit NLRP3, the cells were pre-treated with 10μM of the NLRP3 inhibitor (MCC 950) for 30 minutes (where indicated). Data were pooled from three biological replicates, and each experiment was performed in triplicates. Graphs depict mean ± SEM. Statistical analysis was done by unpaired student's t-test using GraphPad Prism 8 software.

B. WT and mutant BMDMs were treated with LPS (100ng/ml) and ATP (2.5 mM) at the same time. Cell death was evaluated in control and treated cells by Zombie Yellow staining via flow cytometric analysis at 4 hours post-incubation. The graph displays the percentages of cell death. The data shown is the representative data from three experiments, and each experiment was performed in triplicates.

6.2.3. *G2019S* mutation in *Lrrk2* increases the expression of pro-inflammatory cytokines (IL-1β and TNF-α) and the anti-inflammatory cytokine (IL-10) in response to *Lm-EGD*.

Since *Lrrk2*^{G2019S} promoted the expression of IL-1β in our experiments, we decided to measure the expression of additional cytokines by macrophages (BMDMs) in response to *Lm-EGD*. To this end, *Lrrk2*^{G2019S} and WT macrophages were generated and infected *in vitro* as described in the materials and methods section 5.4,5.5 and 5.6.

While the expression of IL-1β, TNF-α and IL-10 was increased in *Lrrk2*^{G2019S} mutant macrophages compared to WT, the expression of IL-12 was almost the same (Figure 8). IL-10 is a potent anti-inflammatory cytokine, whereas TNF-α, IL-1β and IL-12 are pro-inflammatory cytokines. Since the expression of several cytokines was modulated by *Lrrk2* ^{G2019S} mutation, these results indicate that *Lrrk2*^{G2019S} mutation brings about an imbalance between pro-inflammatory and anti-inflammatory cytokines in response to *Lm-EGD.*

Moehle *et al*. (2012) demonstrated that *Lrrk2* knockdown or kinase inhibition in primary microglia reduced the production of the pro-inflammatory cytokines TNF-α and IL-1β (Moehle et al., 2012).

Meanwhile, we measured cytokines in the context of *Lrrk2*- deficient macrophages in response to *Lm-EGD* (Figure 9). We observed that while the expression of IL-10 was high in *Lrrk2*^{G2019S} cells (Figure 8C), *Lrrk2*- deficient macrophages reduced its production (Figure 9C). In addition, there was no difference in the expressions of IL-1β and TNF-α produced by *Lrrk2*- deficient versus WT macrophages (Figure 9 A, B). Furthermore, the expression of IL-12 was enhanced in *Lrrk2*-deficient macrophages, presumably due to the reduction in the inhibitory effect of IL-10 (Figure 9 D).

These results indicate that the impact on TNF-α and IL-1β was specifically due to the *G2019S* mutation of *Lrrk2* since there was no impact on the expression of these cytokines in *Lrrk2* knockout macrophages.

Indeed, various mutations in the *Lrrk2* gene reveal various effects on the expression of cytokines. Thus, we proceeded with further investigations to delineate how the effects of $Lrrk2^{G2019S}$ mutation on the production of cytokines can be interpreted mechanistically.

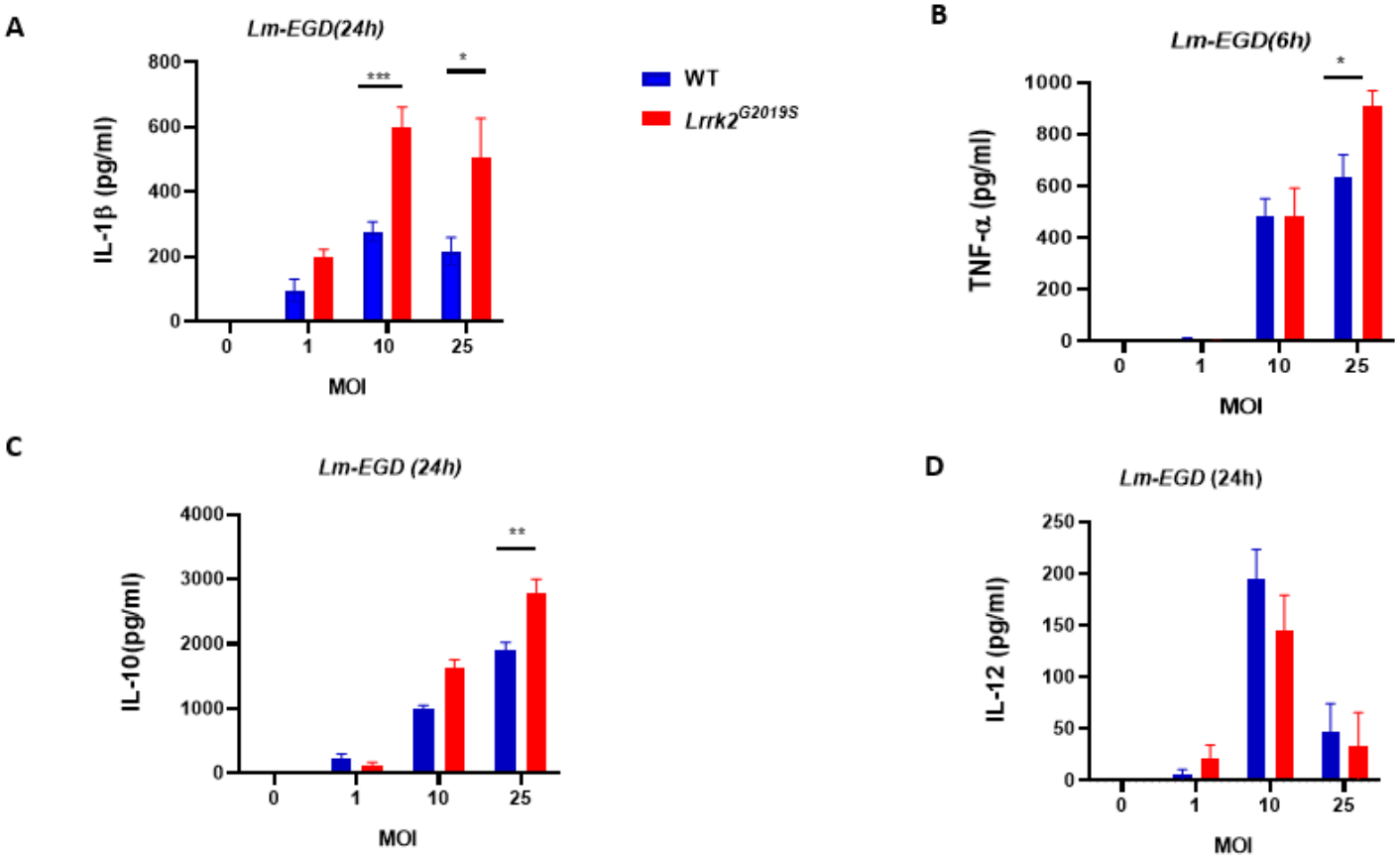
A
Lm-EGD(24h)
IL-1β (pg/ml)
800
600
400
200
0
***
*
0
1
10
25
MOI
WT
Lrrk2G2019S
B
Lm-EGD(6h)
TNF-α (pg/ml)
1000
800
600
400
200
0
*
0
1
10
25
MOI
C
Lm-EGD (24h)
IL-10(pg/ml)
4000
3000
2000
1000
0
**
0
1
10
25
MOI
D
Lm-EGD (24h)
IL-12 (pg/ml)
250
200
150
100
50
0
0
1
10
25
MOI

Figure 8. Expression of IL-1β, TNF-α, IL-10 and IL-12 by WT and *Lrrk2* ^{G2019S} macrophages in response to *Lm-EGD*.

WT and *Lrrk2* ^{G2019S} BMDMs were generated and infected with *Lm-EGD* (0, 1, 10 and 25 MOI) *in vitro*. The expression level of IL-1β, TNF-α, IL-10 and IL-12 in the supernatants of infected WT and mutant BMDMs was quantified by ELISA.

(A) IL-1β expression at 24-h post-infection.

(B) TNF-α expression at 6-h post-infection,

(C) IL-10 expression at 24-h post-infection,

(D) IL-12 expression at 24-h post-infection.

Results are pooled from at least 3 biological replicates with each being an average of 3 experimental replicates. Graphs depict mean ±S.E.M. Statistics were done using unpaired t-tests, where *p<0.05; **p<0.01; ***p<0.001; ****p<0.001 using GraphPad Prism 8 software.

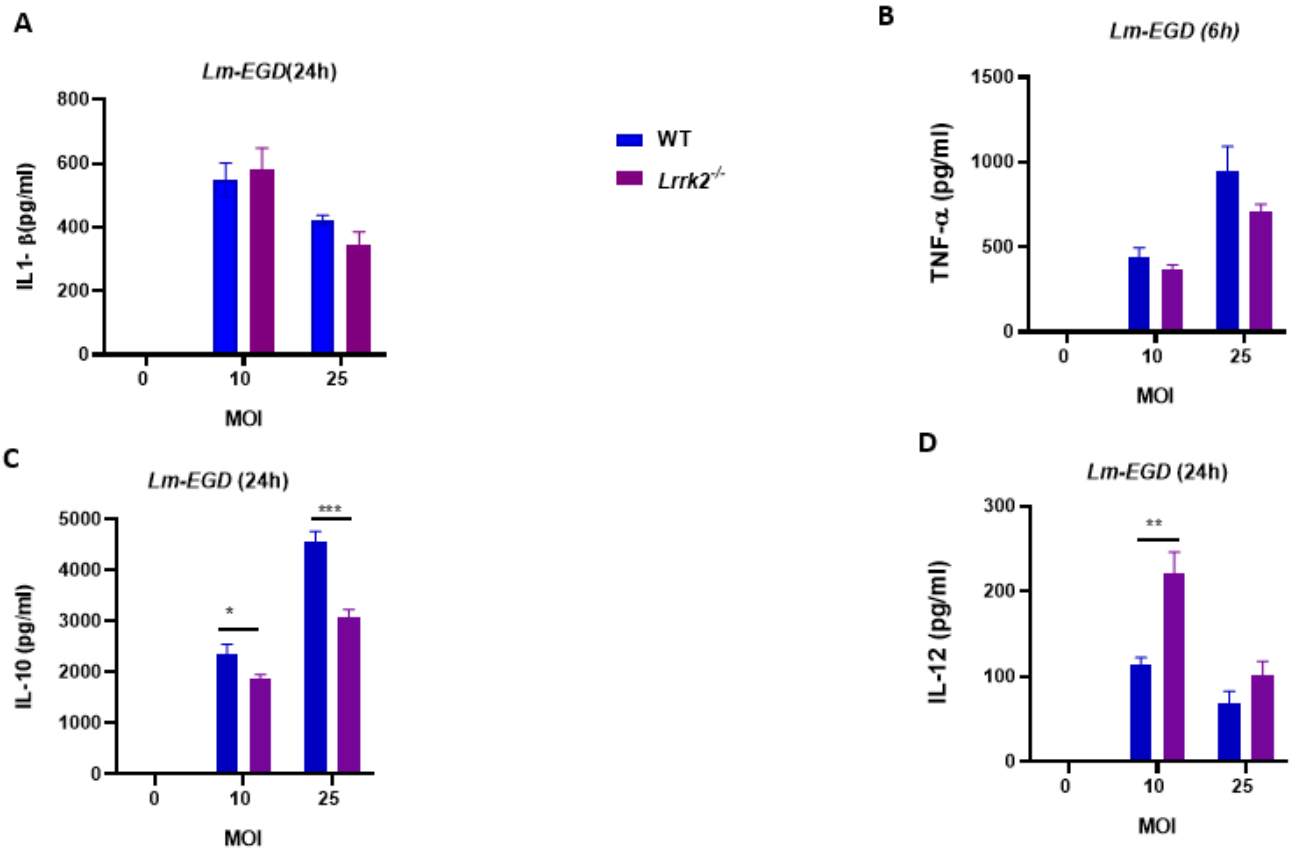
A
Lm-EGD(24h)
IL 1- β(pg/ml)
800
600
400
200
0
0
10
25
MOI
WT
Lrrk2-/-
B
Lm-EGD (6h)
TNF-α (pg/ml)
1500
1000
500
0
0
10
25
MOI
C
Lm-EGD (24h)
IL-10 (pg/ml)
5000
4000
3000
2000
1000
0
*
***
0
10
25
MOI
D
Lm-EGD (24h)
IL-12 (pg/ml)
300
200
100
0
**
0
10
25
MOI

Figure 9. Expression of IL-1β, TNF-α, IL-10 and IL-12 by WT and *Lrrk2*- deficient BMDMs in response to *Lm-EGD*.

WT and *Lrrk2*- deficient BMDMs were generated and infected with *Lm-EGD* (0, 10 and 25 MOI) *in vitro*. The expression level of IL-1β, TNF-α, IL-10 and IL-12 in the supernatants of infected WT and mutant BMDMs was quantified by ELISA.

(A) IL-1β expression at 24-h post-infection.

(B) TNF-α expression at 6-h post-infection,

(C) IL-10 expression at 24-h post-infection,

(D) IL-12 expression at 24-h post-infection.

Results are pooled from 2-3 biological replicates with each being an average of 3 experimental replicates. Graphs depict mean ±S.E.M. Statistics were done using unpaired t-tests, where *p<0.05; **p<0.01; ***p<0.001; ****p<0.001 using GraphPad Prism 8 software.

6.2.4. Exploring the inflammasome signaling modulated by *Lrrk2*^{G2019S} mutation during infection with *Listeria monocytogenes-EGD.*

Inflammasomes are multiprotein complexes, which constitute an essential component of the cytosolic innate immune response. They are mainly composed of a cytosolic pattern recognition receptor (PRR) such as NLRP3, NLRC4 and AIM2.

Assembly of the various components of the inflammasomes occurs following PAMP-PRR interactions, which result in the activation of canonical or/and non-canonical inflammasome cascades. While activation of the canonical cascade leads to the cleavage of pro-caspase-1 to active caspase-1, activation of the non-canonical cascade leads to the cleavage of pro-caspase-11 to caspase-11(Shi et al., 2015). Active caspase-1 also called interleukin-1β (IL-1β)-converting enzyme (ICE) cleaves pro-IL-1β into mature IL-1β, which is then secreted out of the cell (Ming Man et al., 2017). Additionally, active caspase-1 along with active caspase-11 leads to an inflammatory form of cell death called pyroptosis (Ming Man et al., 2017). Having shown that *Lrrk2*^{G2019S} mutant macrophages displayed high IL-1β expression in response to infection with *Lm-EGD*, we aimed to understand the mechanisms by which the inflammasome signaling pathways are modulated in response to *Lm-EGD*.

L. monocytogenes has evolved to live within the harsh environment of the host cytosol. Access to the cytosol is critical for both causing disease and inducing an immune response. Upon entry into the host cell, *L. monocytogenes* is initially contained within a phagocytic vacuole. Secretion of the virulence factor, listeriolysin O (LLO) pokes hols in the phagosomal membrane, which facilitates the escape of *L. monocytogenes* into the cytosol (Nguyen et al., 2019).

Of note, understanding how *Lm-EGD* activates or avoids the inflammasomes is critical to interpret results obtained in the context of *Lrrk2*^{G2019S} mutant macrophages. Therefore, we grew bone marrow derived macrophages from various mutant mice, carrying a mutation in different components of inflammasomes, and then infected the cells with various MOIs (0,10,25 and 50) of *Lm-EGD* to measure the impact on cytokine expression and cell death as described in the materials and methods sections 5.4,5.5 and 5.6.

6.2.4.1. Inflammasome signaling in BMDMs in response to *Lm-EGD* infection is partially dependent on the NLRP3 inflammasome.

Listeriolysin O (LLO), which is a pore-forming toxin, is a member of a large family of cholesterol-dependent cytolysins that are secreted by *L. monocytogenes* inside the host cell (Meixenberger et al., 2010; Nguyen et al., 2019). Mariathasan and colleagues have demonstrated that LLO acts like many other NLRP3 triggers and results in intracellular K+ disruption to activate the NLRP3 inflammasome (Mariathasan et al., 2006). While their original interpretation was that the role of LLO was to facilitate access of *L. monocytogenes* to the cytosol, it is also possible that pore formation was the critical function of LLO in NLRP3 activation (Mariathasan et al., 2006). Hamon *et al*. (2011) also demonstrated that extracellular LLO induces NLRP3 dependent caspase-1 processing and IL-1β released by stimulating K^+ efflux (Hamon and Cossart, 2011).

We observed that *Nlrp3* knock out macrophages infected with *Lm-EGD* showed a slightly lower expression of IL-1β (Figure 10A). Interestingly, *Nlrp3* knock out cells remarkably displayed less cell death compared to WT cells (Figure 10B). These results indicate that modulation of inflammasome signaling in response to *Lm-EGD* infection as a result of host mutation may occur through perturbation of NLRP3. It is, therefore, possible that *Lrrk2*^{G2019S} mutation modulates inflammasome signaling through the activation of NLRP3.

We also observed that the expression of TNF-α and IL-10 was slightly higher in *Nlrp3*-knockout macrophages compared to WT cells (Figure 11 A, B). One possible explanation of increased expression of TNF-α and IL-10 by *Nlrp3*$^{-/-}$ macrophages may be related to their reduced cell death which may allow cells more time to express cytokines. Interestingly, the expression of IL-12 by *Nlrp3*$^{-/-}$ macrophages was profoundly reduced when compared to WT cells (Figure 11 C). This occurred even at low MOI of *L. monocytogenes* which does not induce cell death, indicating that NLRP3 promotes IL-12 expression by macrophages independently of cell death. The expression of IL-10 was similar in WT versus *Nlrp3*$^{-/-}$ macrophages infected with 10 MOI of *L. monocytogenes*, indicating that the impact of NLRP3 on IL-12 may not be related to IL-10 levels. It is likely that NLRP3 interacts with another signaling pathway to promote IL-12 expression.

Overall, it is interesting that *Nlrp3*-deficient cells show not only a reduction in IL-1β but also an imbalance in the expression of other cytokines.

A

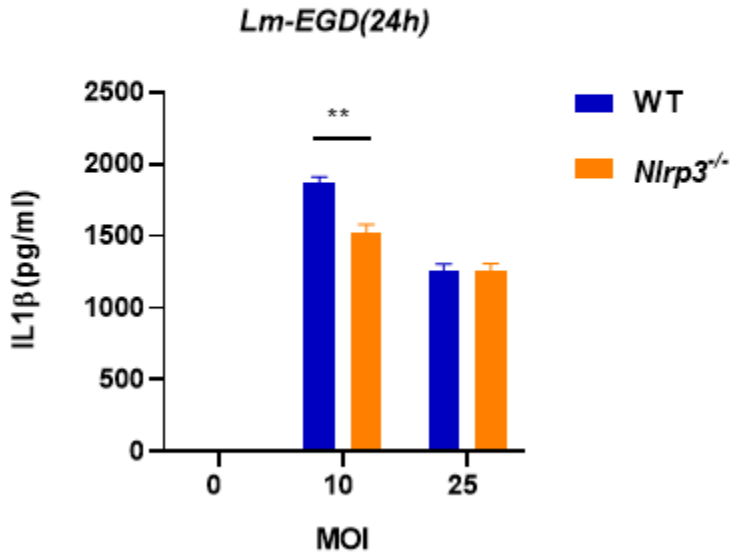
Lm-EGD(24h)
2500
2000
1500
1000
500
0
IL1β(pg/ml)
**
WT
Nlrp3-/-
0
10
25
MOI

B

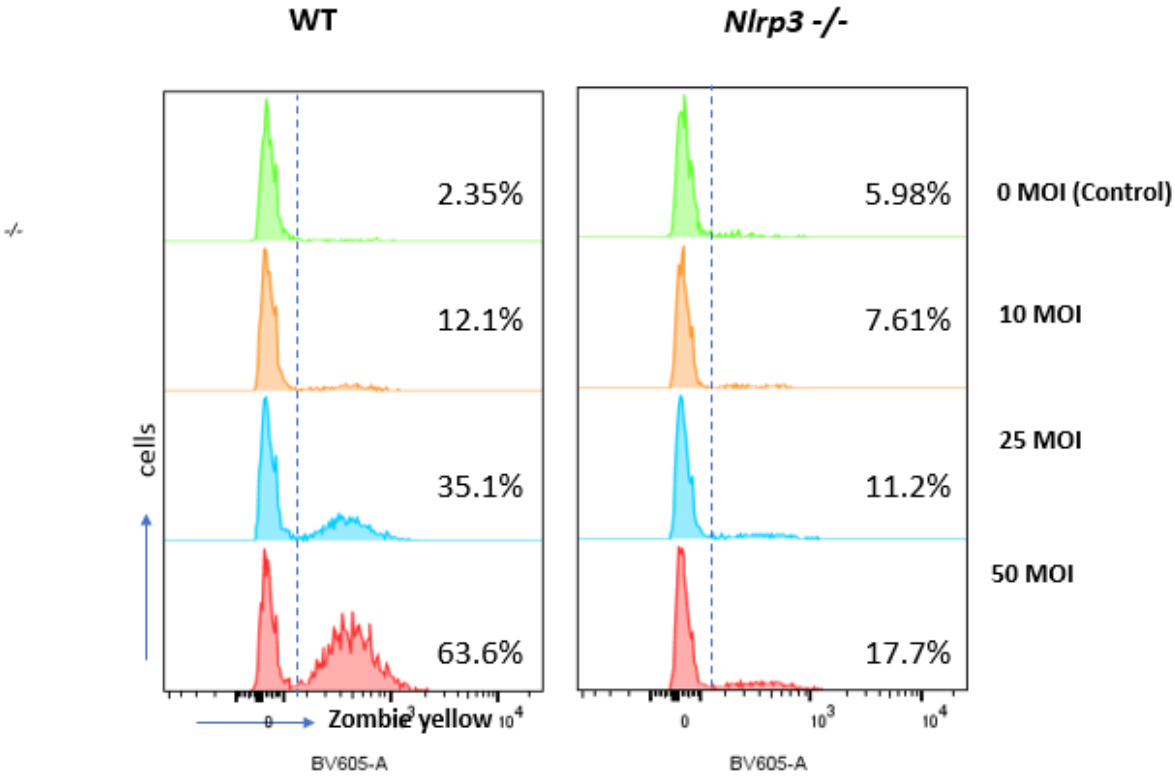
WT
Nlrp3 -/-
cells
2.35%
12.1%
35.1%
63.6%
5.98%
7.61%
11.2%
17.7%
0 MOI (Control)
10 MOI
25 MOI
50 MOI
Zombie yellow
BV605-A
BV605-A

Figure 10. *Nlrp3* deficiency results in reduced expression of IL-1β and cell death.

WT and *Nlrp3* knock out bone marrow derived macrophages were infected with *Lm-EGD* and supernatants were collected at 24 h post-infection.

A. The expression of IL-1β was evaluated in the supernatants of infected WT and *Nlrp3* $^{-/-}$ BMDMs by ELISA. Macrophages were infected with various MOIs of *Lm-EGD* (0,10,25), and IL-1β expression was quantified at 24-hours post-infection. Data shown is the representative of 3 biological replicates, each performed in triplicates. Graphs depict mean ±S.E.M. Statistics were done using unpaired t-tests, where *p<0.05; **p<0.01; ***p<0.001; ****p<0.001 using GraphPad Prism 8 software.

B. WT and *Nlrp3* $^{-/-}$ BMDMs were infected with various MOIs (0,10,25 and 50) and cell death was evaluated in control and infected cells at 24 hours post-infection by Zombie Yellow staining via flow cytometric analysis. The graph displays the percentages of cell death. Data shown is the representative data of three similar biological replicates, and each experiment was performed in triplicates.

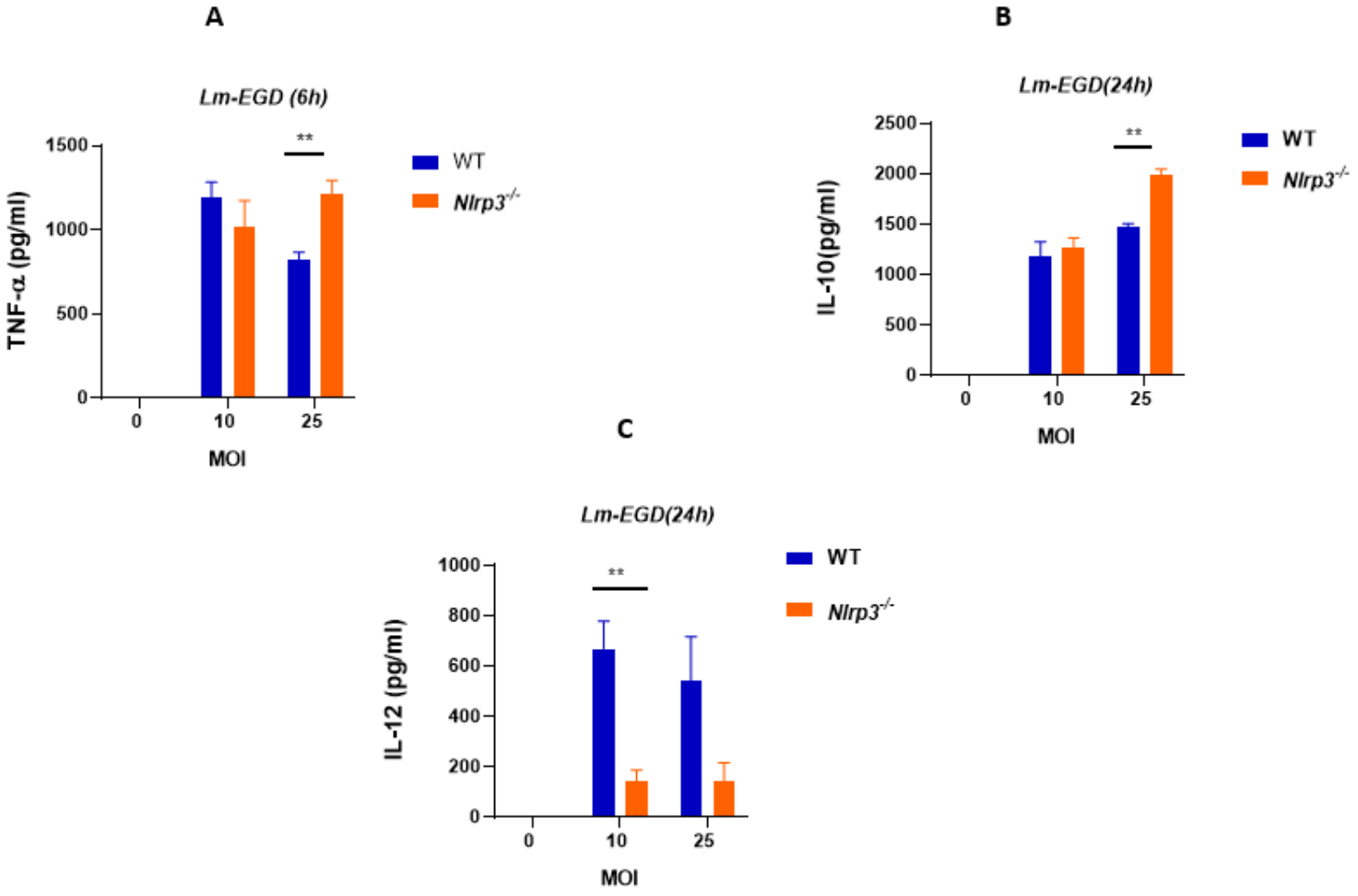
A
Lm-EGD (6h)
TNF-α (pg/ml)
1500
1000
500
0
**
0
10
25
MOI
WT
Nlrp3-/-
B
Lm-EGD(24h)
IL-10(pg/ml)
2500
2000
1500
1000
500
0
**
0
10
25
MOI
WT
Nlrp3-/-
C
Lm-EGD(24h)
IL-12 (pg/ml)
1000
800
600
400
200
0
**
0
10
25
MOI
WT
Nlrp3-/-

Figure 11. *Nlrp3* deficiency modulates the expression of inflammatory cytokines by BMDMs in response to infection

WT and *Nlrp3* $^{-/-}$ BMDMs were generated and infected with *Lm-EGD* (0, 10 and 25 MOI) *in vitro*. The expression of various cytokines was quantified by ELISA in the supernatants of control and infected cells at different time points.

(A) TNF-α expression levels at 6-h post-infection,

(B) IL-10 expression levels at 24-h post-infection,

(C) IL-12 expression levels at 24-h post-infection.

Results are pooled from 2 biological replicates with each being an average of 3 experimental replicates. Graphs depict mean ±S.E.M. Statistics were done using unpaired t-tests, where *p<0.05; **p<0.01; ***p<0.001; ****p<0.001, using GraphPad Prism 8.

6.2.4.2. Inflammasome signaling in response to *Lm-EGD* is independent of the NLRC4 pathway.

The NLRC4 inflammasome is another member of the Nod-like receptor (NLR) family of pattern recognition receptors that detect various pathogens and danger signals. The NLRC4 inflammasome detects flagellin and the components of the type III secretion system (T3SS) (Zhao et al., 2011). Since *Lm-EGD* is a Gram-positive pathogen and lacks T3SS, its flagellin is likely the key activator of the NLRC4 inflammasome (Sauer et al., 2011). However, it has been suggested that *Lm-EGD* avoids activation of the NLRC4 inflammasome by shutting off flagellin expression in mammalian hosts (Way et al., 2004). As such, *L. monocytogenes* inflammasome activation was shown to be independent of NLRC4 (Sauer et al., 2010). Additionally, our results did not show any significant difference in the expression of IL-1β and cell death in WT and *Nlrc4*-deficient macrophages in response to *Lm-EGD* (Figure.12 A, B).

Moreover, the levels of TNF-α , IL-10 and IL-12 were comparable in *Nlrc4*$^{-/-}$ and WT cells post *Lm-EGD* infection (Figure 13 A, B, C).

Consequently, since the NLRC4 inflammasome does not seem to contribute to the cytokine expression and cell death resulting from *Lm-EGD* infection, we decided not to proceed with further experiments to evaluate this inflammasome signaling pathway in the context of infected *Lrrk2*^{G2019S} macrophages.

A

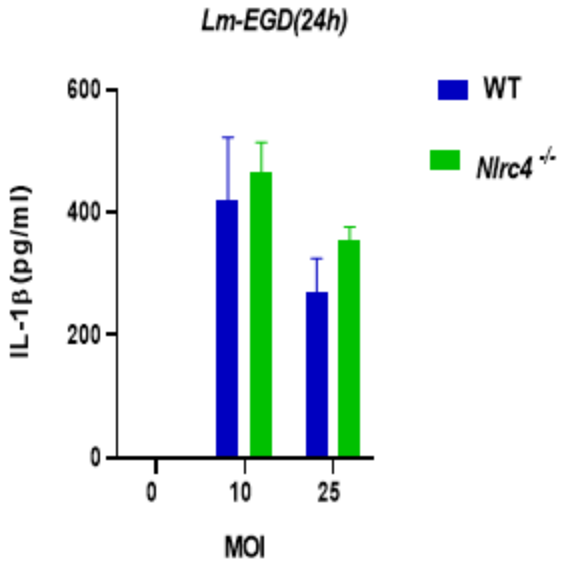
Lm-EGD(24h)
WT
Nlrc4 -/-
IL-1β (pg/ml)
600
400
200
0
0
10
25
MOI

B

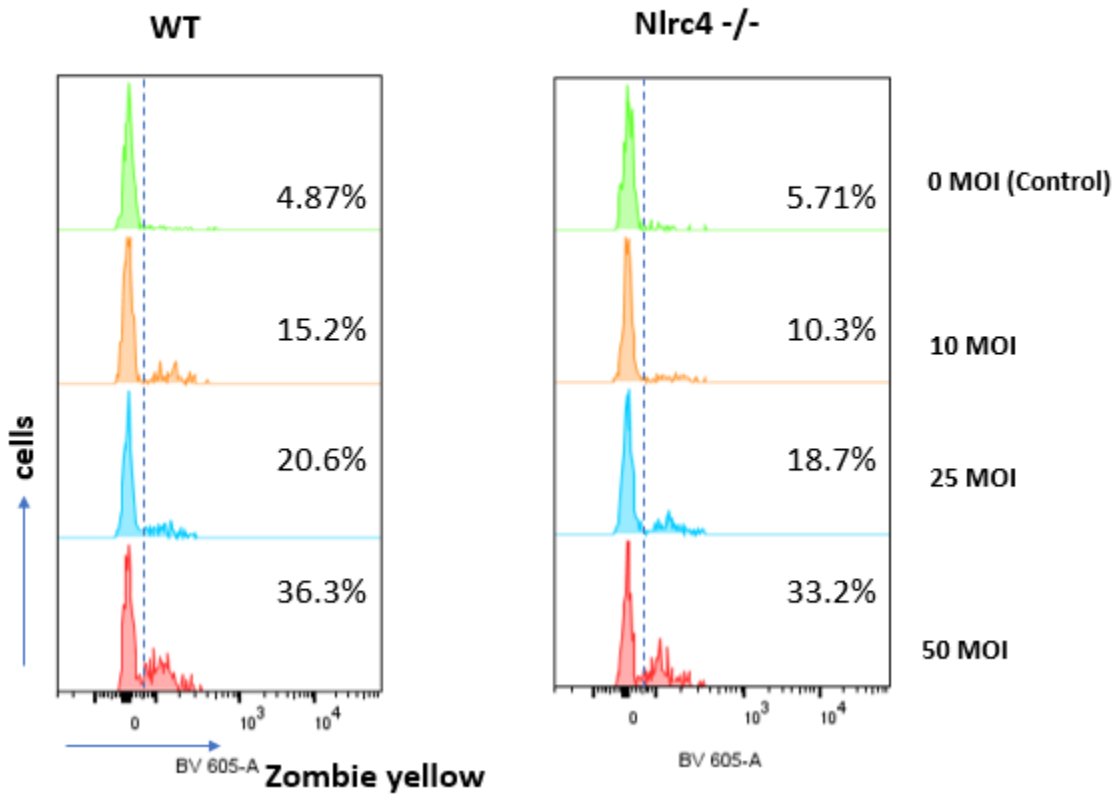
WT
Nlrc4 -/-
4.87%
15.2%
20.6%
36.3%
5.71%
10.3%
18.7%
33.2%
0 MOI (Control)
10 MOI
25 MOI
50 MOI
cells
BV 605-A
Zombie yellow

Figure 12. *Nlrc4* deficiency results in a similar expression of IL-1β and cell death, compared to WT cells.

WT and *Nlrc4* knock out bone marrow derived macrophages were infected with *Lm-EGD* and supernatants were collected at 24 h post-infection.

A. The expression of IL-1β was quantified in the supernatants of infected WT and *Nlrc4*$^{-/-}$ BMDMs by ELISA. Macrophages were infected with various MOIs of *Lm-EGD* (0,10,25), and IL-1β expression was evaluated at 24-hours post-infection. Data is representative of two biological replicates, each performed in triplicates. Graphs depict mean ±S.E.M. Statistics were done using unpaired t-tests, where *p<0.05; **p<0.01; ***p<0.001; ****p<0.001 using GraphPad Prism 8 software.

B. WT and *Nlrc4* knock out BMDMs were infected with various MOIs (0,10,25 and 50) of *Lm-EGD* and cell death was evaluated in control and infected cells at 24 hours post-infection by Zombie Yellow staining via flow cytometric analysis. The graph displays the percentages of cell death. The data shown is representative of two similar experiments, and each experiment was performed in triplicates.

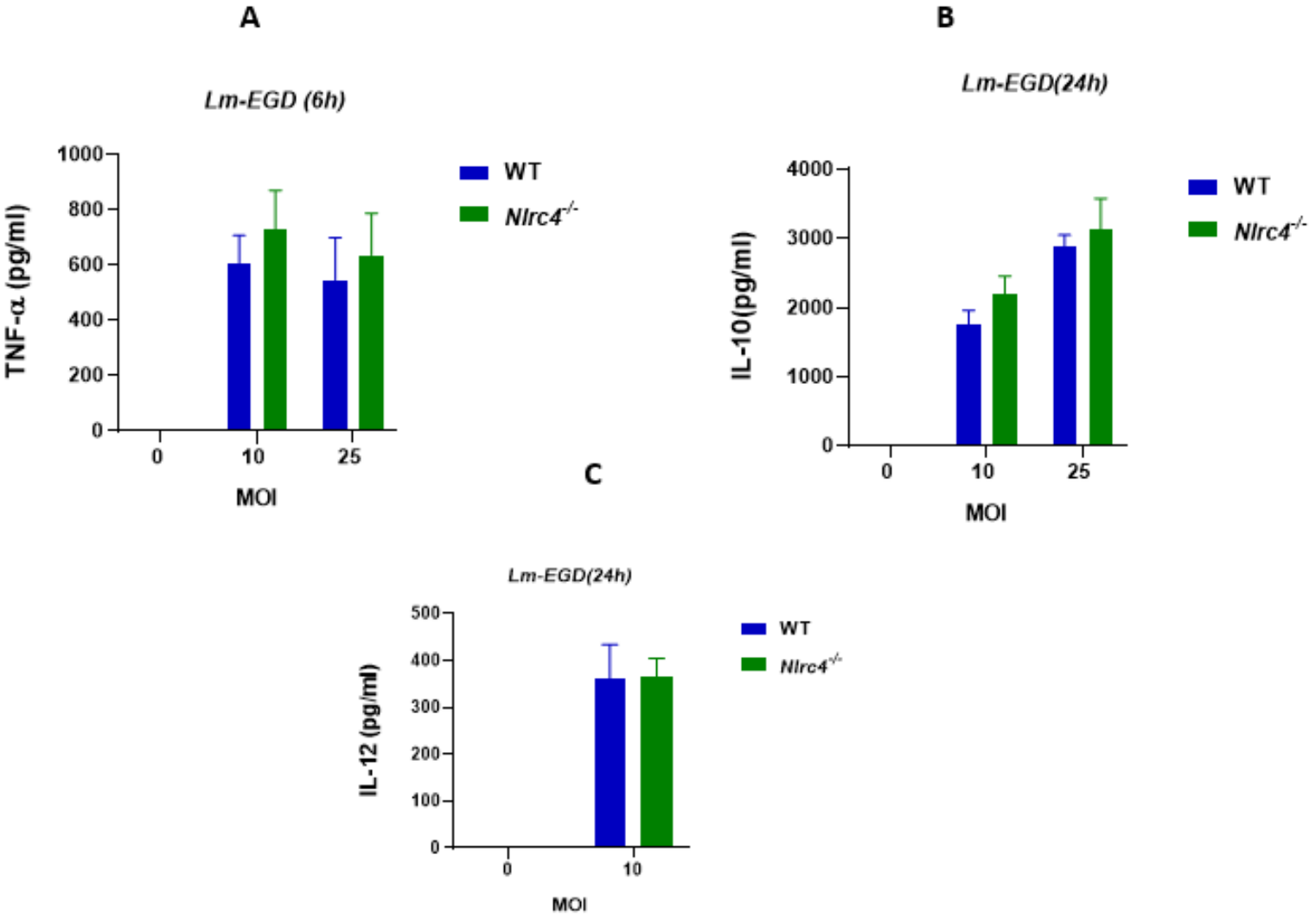
A
Lm-EGD (6h)
TNF-α (pg/ml)
1000
800
600
400
200
0
0
10
25
MOI
WT
Nlrc4-/-
B
Lm-EGD(24h)
IL-10(pg/ml)
4000
3000
2000
1000
0
0
10
25
MOI
WT
Nlrc4-/-
C
Lm-EGD(24h)
IL-12 (pg/ml)
500
400
300
200
100
0
0
10
MOI
WT
Nlrc4-/-

Figure 13. *Nlrc4* deficiency does not impact the expression of cytokines in response to *Lm-EGD*.

WT and *Nlrc4* $^{-/-}$ BMDMs were generated and infected with *Lm-EGD* (0, 10 and 25 MOI) *in vitro*. Expression of various cytokines was quantified by ELISA in the supernatants of control and infected cells at different time points.

(A) TNF-α expression levels at 6-h post-infection,

(B) IL-10 expression levels at 24-h post-infection,

(C) IL-12 expression levels at 24-h post-infection.

Results are pooled from 2 biological replicates with each being an average of 3 experimental replicates. Graphs depict mean ±S.E.M. Statistics were done using unpaired t-tests, where *p<0.05; **p<0.01; ***p<0.001; ****p<0.001, using GraphPad Prism 8

6.2.4.3. Inflammasome signaling in response to *Lm-EGD* is mainly dependent on caspase-1 for IL-1β expression and caspase-11 for cell death induction.

Assembly of the various components of the inflammasomes occurs following PAMP-PRR interactions, which result in the activation of inflammatory caspases. Inflammatory caspases are a family of cysteine proteases that play essential roles in inducing inflammatory cell death and proteolytic activation of cytokines (Ming Man and Kanneganti, 2015). Inflammasomes are also classified into canonical and non-canonical inflammasome signaling pathways. Both canonical and non-canonical inflammasome activation eventually leads to cell lysis and the release of proinflammatory cytokines, but their mechanisms of activation are different (Casson and Shin, 2013).

Canonical inflammasomes include members of the NLR family, such as NLRP1, NLRP3, NLRC4 and AIM2, which interact with pro-caspase-1 (Franchi et al., 2009; Tsuchiya et al., 2010). This interaction leads to the consequent of pro-caspase-1 cleavage and the expression of the effector (active form) caspase-1. Caspase-1, which is the most characterized inflammatory caspase in humans and mice, was originally identified as IL-1β converting enzyme (ICE) (Thornberry et al., 1992). Studies with caspase-1 also demonstrated that caspase-1 can also induce cell death (Bergsbaken et al., 2009). However, *caspase-1*-deficient mice, while deficient in the processing of proinflammatory cytokines, show no overt defect in cell death (Li et al., 1995).

Non-canonical inflammasome signaling does not involve caspase-1. Murine caspase-11 is a partially characterized member of the non-canonical inflammasome signaling family. Murine caspase-11 can be activated by intracellular LPS in Gram-negative bacteria and/or Lipoteichoic acid (LTA) in Gram-positive bacteria (Hara et al., 2018; Kayagaki et al., 2013).

We harvested BMDMs from *caspase 1/11* and *caspase 11* knock out mice and infected them as described in the materials and methods section 5.4, 5.5, 5.6.

Although *caspase 1/11*- deficient BMDMs do not produce IL-1β at all, cell death was partially reduced (Figure 14 A, B). This indicates that there are other pathways which are independent of inflammasome-mediated pathways that induce cell death in macrophages infected with *L. monocytogenes* (Mcdougal and Sauer, 2018)

Interestingly, *caspase-11* deficient BMDMs express remarkably high levels of IL-1β while significantly reducing cell death compared to WT macrophages (Figure14 A, B). These results suggest that the expression of IL-1β in BMDMs is mainly dependent on caspase-1, but cell death is mainly dependent on caspase-11 in response to *Lm-EGD*.

Consequently, modulation of inflammasome signaling in response to *Lm-EGD* infection, as a result of host mutation, may occur through caspase-1 or caspase-11. It is, therefore, possible that *Lrrk2*^{G2019S} mutation modulates inflammasome signaling through the activation of either of these two inflammatory caspases.

We further evaluated other cytokines secreted by the infected *caspase 1/11*-deficient macrophages. Although TNF-α expression level was comparable between *caspase 1/11*$^{-/-}$ macrophages and WT cells, the level of IL-10 was increased in *caspase 1/11*$^{-/-}$ cells (Figure 15 A, B). Conversely, the level of IL-12 was significantly reduced (Figure 15 C). This pattern of cytokines is somehow similar to the pattern of infected *Nlrp3*$^{-/-}$ BMDMs as already discussed (Figure 11 B, C). Like *Nlrp3*$^{-/-}$, one possible explanation of increased expression of IL-10 produced by *caspase 1/11*$^{-/-}$ macrophages may be related to their reduced cell death. Meanwhile, IL-10 is considered as a potent inhibitor of IL-12; thus, it can reduce the expression of IL-12 (Rahim et

al., 2005b). However, this occurred even at low MOI of *L. monocytogenes* which does not induce much more cell death significantly, indicating that IL-10 and IL-12 expression can be regulated by another pathway independently of cell death.

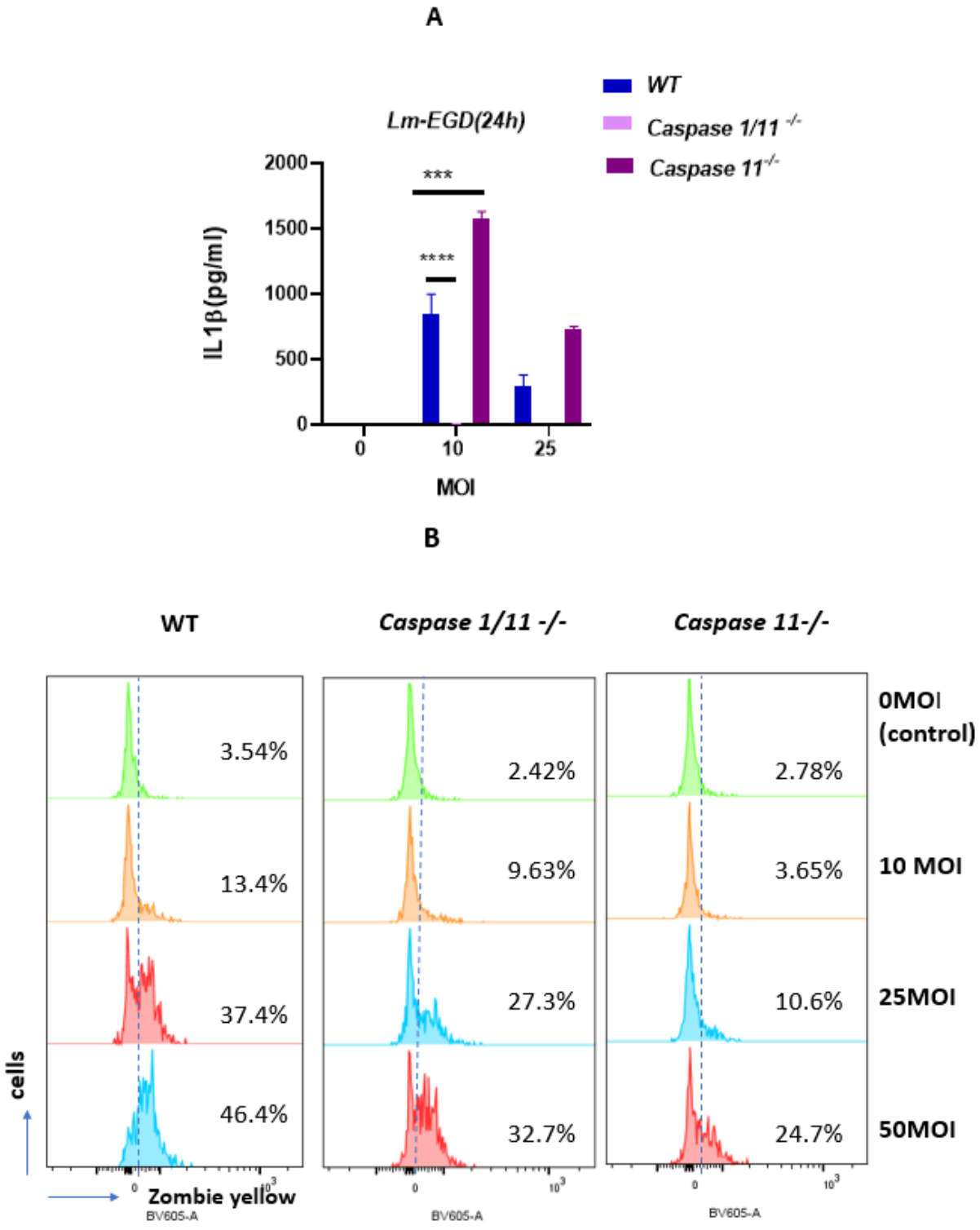
A
WT
Caspase 1/11 -/-
Caspase 11-/-
Lm-EGD(24h)
IL1β(pg/ml)
2000
1500
1000
500
0
***
****
0
10
25
MOI
B
WT
Caspase 1/11 -/-
Caspase 11-/-
0MOI (control)
10 MOI
25MOI
50MOI
3.54%
13.4%
37.4%
46.4%
2.42%
9.63%
27.3%
32.7%
2.78%
3.65%
10.6%
24.7%
cells
Zombie yellow
BV605-A

Figure 14. Inflammasome signaling in BMDMs, in response to *Lm-EGD*, is mainly dependent on caspase-1 for IL-1β expression and caspase-11 for cell death.

A. Expression of IL-1β was quantified in the supernatants of infected WT and *caspase1/11 and caspase 11* knock out BMDMs by ELISA. Macrophages were infected with various MOIs of *Lm-EGD* (0,10,25), and IL-1β expression was evaluated at 24-hours post-infection. Pooled data of 2-3 biological replicates, each performed in triplicates. Graphs depict mean ±S.E.M. Statistics were done using one way ANOVA, where *p<0.05; **p<0.01; ***p<0.001; ****p<0.001 using GraphPad Prism 8 software.

B. WT, *caspase 1/11*- and *caspase 11*- deficient BMDMs were infected with various MOIs (0,10,25 and 50), and cell death was evaluated in control and infected cells at 18-24 hours post-infection by Zombie Yellow staining via flow cytometric analysis. The graph displays the percentages of cell death. Data shown is the representative data of 2-3 similar experiments, and each experiment was performed in triplicates.

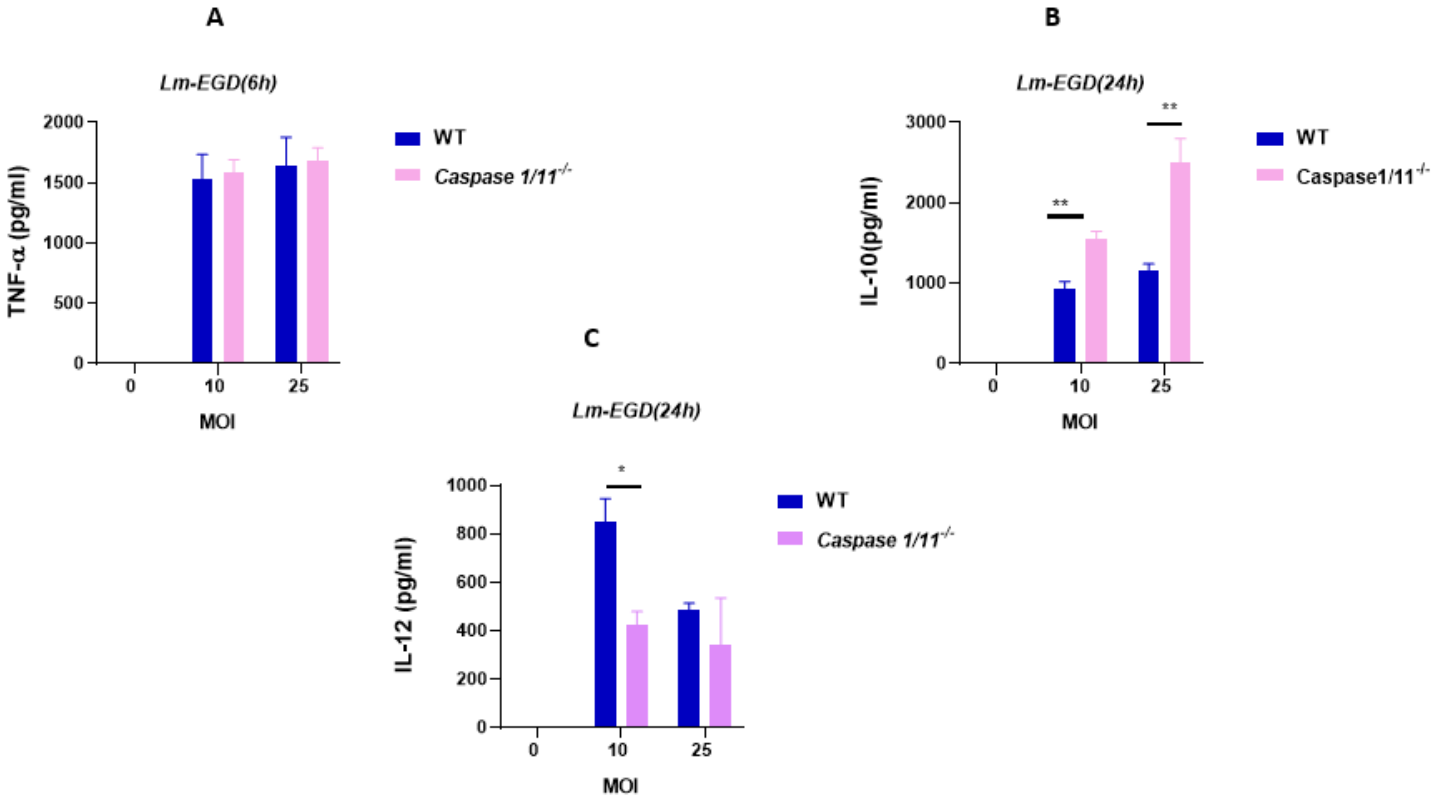
A
Lm-EGD(6h)
TNF-α (pg/ml)
2000
1500
1000
500
0
0
10
25
MOI
WT
Caspase 1/11-/-
B
Lm-EGD(24h)
IL-10(pg/ml)
3000
2000
1000
0
**
**
0
10
25
MOI
WT
Caspase1/11-/-
C
Lm-EGD(24h)
IL-12 (pg/ml)
1000
800
600
400
200
0
*
0
10
25
MOI
WT
Caspase 1/11-/-

Figure 15. *Caspase 1/11* deficiency modulates the expression of inflammatory cytokines by BMDMs in response to *Lm-EGD* infection.

WT and *caspase 1/11*- deficient BMDMs were infected with *Lm-EGD* (0, 10 and 25 MOI) *in vitro*. The expression of various cytokines was quantified by ELISA in the supernatants of control and infected cells at different time points.

(A) TNF-α expression levels at 6-h post-infection,

(B) IL-10 expression levels at 24-h post-infection,

(C) IL-12 expression levels at 24-h post-infection.

Results are pooled from 2 biological replicates with each being an average of 3 experimental replicates. Graphs depict mean ±S.E.M. Statistics were done using unpaired t-tests, where *p<0.05; **p<0.01; ***p<0.001; ****p<0.001, using GraphPad Prism 8.

6.2.4.4. AIM2 promotes inflammasome signaling in response to *Lm-EGD*.

Our results have so far indicated that the inflammasome signaling resulting from *Lm-EGD* infection is mainly dependent on caspase-1 for IL-1β expression. Additionally, we have already investigated the contribution of NLRP3 and NLRC4 inflammasome signaling for IL-1β expression in response to *Lm-EGD.* We found that while NLRC4 played no role in inducing IL-1β expression, NLRP3 deficiency led to a slight reduction compared to WT, thereby suggesting that receptors other than NLRP3 and NLRC4 could be activated in response to *Lm-EGD* to induce IL-1β expression.

The AIM2 inflammasome detects the presence of altered or mis-localized DNA molecules, such as genomic DNA released into the cytosol upon loss of nuclear envelope integrity or foreign DNA accumulating in the cytosol during the life cycle of intracellular pathogens including viruses, bacteria, and parasites (Theisen and Sauer, 2016). Warren *et al*. in 2010 observed that transfected *L. monocytogenes'* genomic DNA could activate the AIM2 inflammasome (Warren et al., 2010). Additionally, it has been demonstrated that AIM2 is an intracellular DNA receptor that plays an important role in the activation of caspase-1 upon infection with *L. monocytogenes* (Tsuchiya et al., 2010). Accordingly, we were interested in exploring AIM2, another inflammasome signaling pathway, which may significantly modulate IL-1β expression through caspase-1 in response to *Lm-EGD*.

In this regard, we generated bone marrow-derived macrophages from *Aim2* $^{-/-}$ and WT mice and infected them with various MOIs of *Lm-EGD* as described in the materials and methods section 5.4, 5.5, 5.6.

Interestingly, our results demonstrated that while infected *Aim2*- deficient macrophages do not secrete IL-1β at all, cell death is partially reduced (Figure 16 A, B). It can be interpreted that while the production of IL-1β in response to *Lm-EGD* is mainly dependent on the AIM2 inflammasome pathway, cell death seems to be partially dependent on AIM2. Hence, AIM2 seems to play a significant role in inflammasome signaling in response to *Lm-EGD* for IL-1β expression. Indeed, these results complement the results revealed in the context of infected *caspase 1/11*-deficient BMDMs (Figure 14 A, B).

It is, therefore, possible that *Lrrk2*^{G2019S} mutation modulates inflammasome signaling through modulation of AIM2.

Investigating other cytokines, we observed that the expression of TNF-α and IL-10 in *Aim2*-deficient macrophages versus WT cells in response to *Lm-EGD* were comparable. (Figure 16 C, D). This implies that AIM2 inflammasome does not have any impact on the expression of other cytokines.

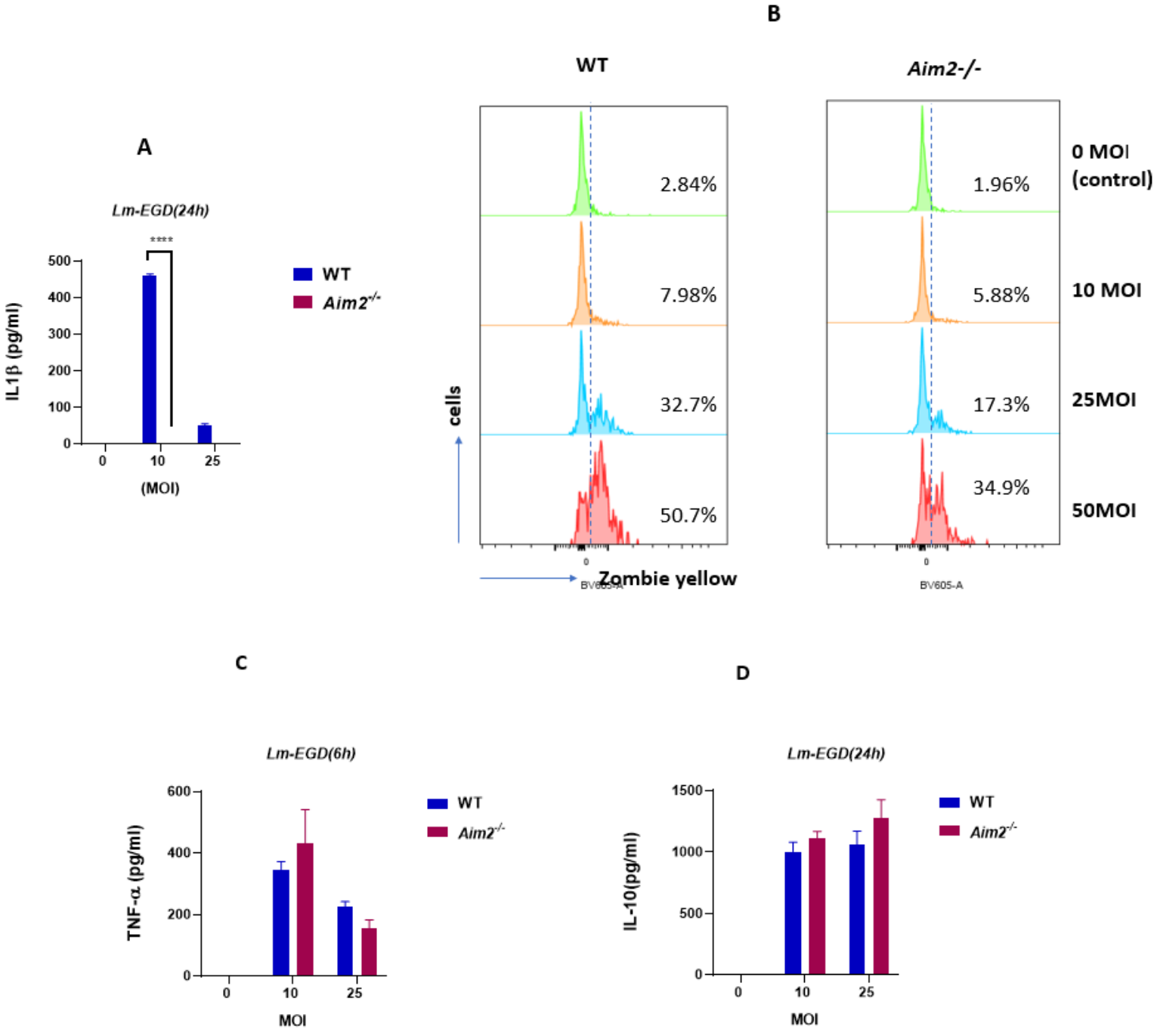
A
Lm-EGD(24h)
****
IL1β (pg/ml)
500
400
300
200
100
0
0
10
25
(MOI)
WT
Aim2-/-
B
WT
Aim2-/-
2.84%
7.98%
32.7%
50.7%
1.96%
5.88%
17.3%
34.9%
cells
Zombie yellow
BV605-A
0 MOI
(control)
10 MOI
25MOI
50MOI
C
Lm-EGD(6h)
TNF-α (pg/ml)
600
400
200
0
0
10
25
MOI
WT
Aim2-/-
D
Lm-EGD(24h)
IL-10(pg/ml)
1500
1000
500
0
0
10
25
MOI
WT
Aim2-/-

Figure 16. *Aim2* deficiency results in a striking abolishment of IL-1β and a partial reduction in cell death.

A. WT and *Aim2* knock out BMDMs were infected with *Lm-EGD* and supernatants were collected at 24 h post-infection. The expression of IL-1β was quantified in the supernatants of infected WT and *Aim2* knock out BMDMs by ELISA. Pooled data of 2 biological replicates, each performed in triplicates. Graphs depict mean ±S.E.M. Statistics were done using unpaired t-tests, where *p<0.05; **p<0.01; ***p<0.001; ****p<0.001 using GraphPad Prism 8 software.

B. WT and *Aim2* deficient BMDMs were infected with various MOIs (0,10,25 and 50) and cell death was evaluated in control and infected cells at 24 hours post-infection by Zombie Yellow staining via flow cytometric analysis. The graph displays the percentages of cell death. Data shown is the representative data of two experiments, and each experiment was performed in triplicates.

C, D: WT and *Aim2*- deficient BMDMs were generated and infected with *Lm-EGD* (0, 10 and 25 MOI) *in vitro*. The expression of various cytokines was quantified by ELISA in the supernatants of control and infected cells at different time points.

C. TNF-α expression levels at 6-h post-infection,

D. IL-10 expression levels at 24-h post-infection,

Results are the representative of 2 biological replicates with each being an average of 3 experimental replicates. Graphs depict mean ±S.E.M. Statistics were done using unpaired t-tests, where *p<0.05; **p<0.01; ***p<0.001; ****p<0.001, using GraphPad Prism 8.

6.2.4.5. *Lrrk2*^{G2019S} mutation promotes the expression of NLRP3 and the activation of caspase-1 and caspase-11.

According to the previous results regarding enhanced inflammasome activity by *Lrrk2*^{G2019S} mutant macrophages (Figure 6) and the mechanisms through which *L. monocytogenes* activates inflammasome signaling pathways (sections 6.2.4.1, 6.2.4.2, 6.2.4.3, 6.2.4.4), we designed further experiments to measure inflammasomal proteins in the context of infected *Lrrk2*^{G2019S} mutant macrophages by western blot.

In this regard, BMDMs were generated and infected with 10 MOI of *Lm-EGD*, as described in sections 5.4, 5.5 and 5.6. The cells were lysed at 0, 1, 3, and 6 hours post-infection, and the extracted cell lysates were used for detecting proteins of interest by western blot.

We observed an increased expression in the level of NLRP3 and slightly enhanced expression of active (cleaved) caspase-1 in the mutant cells compared to WT cells (Fig 17 A). It can be interpreted that the mutant macrophages activate the inflammasome signaling pathway by enhancing NLRP3 expression in response to *Lm-EGD* resulting in increased IL-1β secretion. Intriguingly, Gordon *et al.* (2018) revealed that inhibition of the NLRP3 inflammasome had a therapeutic effect when treating rodent models of Parkinson's disease (Gordon et al., 2018).

Additionally, the level of active caspase-11 was also increased in *Lrrk2*^{G2019S} macrophages (Figure 17A). The slight enhancement of active caspase-11 or active caspase-1 can be responsible for the slight increase in cell death that we observed in *Lrrk2*^{G2019S} mutant macrophages in response to *Lm-EGD* (Figure 6).

Having shown that the *Lrrk2*^{G2019S} mutation enhanced the NLRP3 inflammasome mediator in western blotting, we decided to evaluate the impact of inhibiting NLRP3 on the expression of IL-1β by WT and *Lrrk2*^{G2019S} macrophages upon infection.

To address this, we generated macrophages and infected them as described in sections 5.4, 5.5 and 5.6 and then treated the cells with an NLRP3 inhibitor (MCC 950). It should be noted that we used the same concentration of NLRP3 inhibitor (MCC950) as we used with LPS+ATP treatment (Figure 7).

Inhibition of NLRP3, reduced the expression of IL-1β by the mutant cells and WT cells similarly (Figure 17 B). This suggests that WT and *Lrrk2*^{G2019S} mutation seem to regulate the production of IL-1β via modulation of the NLRP3 inflammasome signaling pathway in response to *Lm-EGD* infection. However, the up-regulation of IL-1β production in *Lrrk2* ^{G2019S} macrophages may not be solely due to the up-regulation of NLRP3.

A

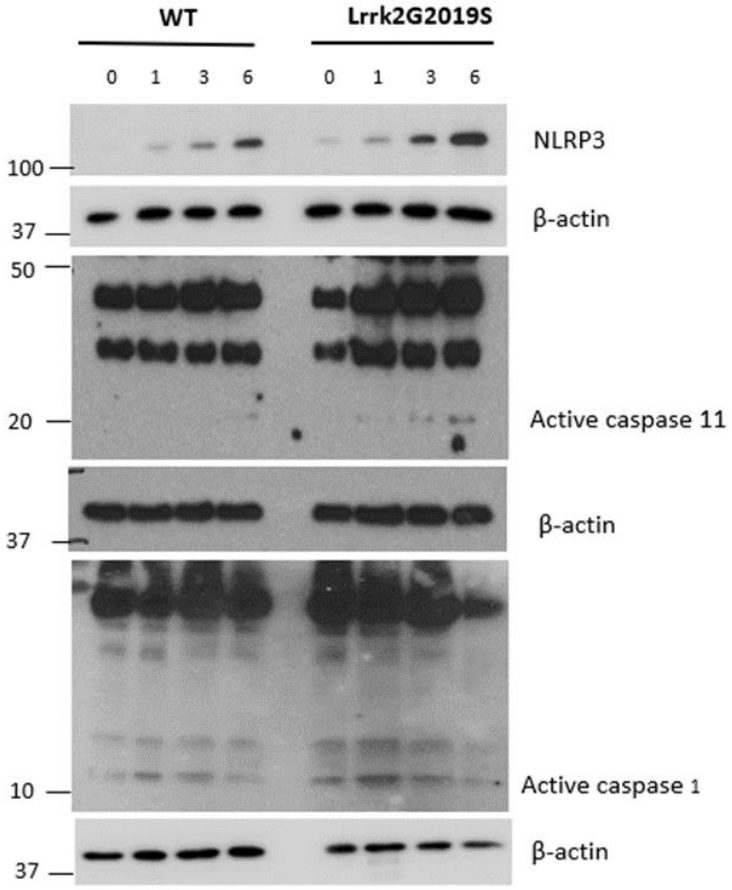
WT
Lrrk2G2019S
0 1 3 6 0 1 3 6
NLRP3
β-actin
Active caspase 11
β-actin
Active caspase 1
β-actin
100
37
50
20
37
10
37

B

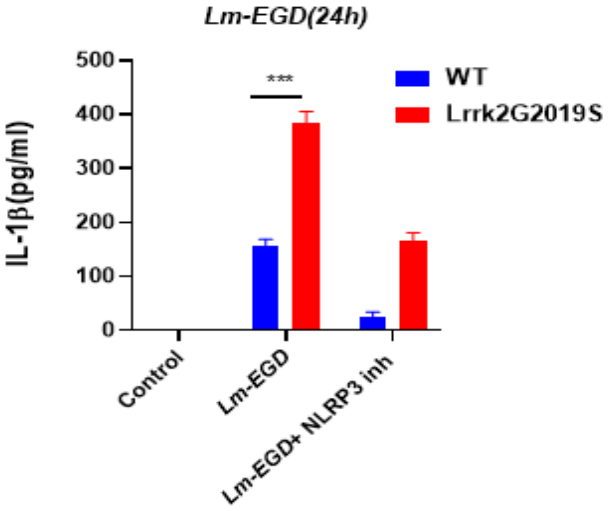
Lm-EGD(24h)
IL-1β(pg/ml)
500
400
300
200
100
0
***
WT
Lrrk2G2019S
Control
Lm-EGD
Lm-EGD+ NLRP3 inh

Figure 17. High expression of NLRP3, active caspase-11 and active caspase-1 in the *Lrrk2*^{G2019S} mutant macrophages versus WT cells in response to *Lm-EGD*.

A. Western blots of lysates extracted from WT and *Lrrk2*^{G2019S} mutant macrophages infected with 10 MOI of *Lm-EGD* at 0, 1, 3- and 6-hours post-infection for key proteins of inflammasome signaling pathways including NLRP3, active-caspase 11 and active-caspase 1. Each western blot was repeated twice to thrice.

B. BMDMs were generated from WT and *Lrrk2*^{G2019S} mice and infected with *Lm-EGD*. Cells were treated with the NLRP3 inhibitor (MCC 950, 10μM) where indicated. Expression of IL-1β cytokine in the supernatants of control, infected cells in the presence or absence of NLRP3 inhibitor (MCC 950, 10μM) was quantified by ELISA.

Statistics were done using unpaired t-tests, where *p<0.05; **p<0.01; ***p<0.001; ****p<0.001, using GraphPad Prism 8.

6.2.5. *Lrrk2*^{G2019S} mutation does not modulate NF-κB pathway in response to *Lm-EGD* infection.

The transcription factor NF-κB is a key mediator of the inflammatory response which regulates multiple aspects of innate immunity. NF-κB is normally sequestered in the cytoplasm as an inactive complex with IKKα/β (Solt and May, 2008). It becomes activated in response to immune and stress stimuli, including ligands of various cytokine receptors and interactions between pattern-recognition receptors (PRRs) and pathogen-associated molecular patterns (PAMPs) (Liu et al., 2017a).

Among the NF-κB family members, P65: P50 complex is the best characterized form, which is activated by pathogenic stimuli via the IKKα/β complex (Oeckinghaus and Ghosh, 2009). Typically, the IKKα/β is bound to the P65: P50 complex, which is present in a resting state in the cytoplasm (Solt and May, 2008). Activation (phosphorylation) of IKKα/β, causes degradation of this complex resulting in the release of p65 dimers from this inhibitory complex (Giridharan and Srinivasan, 2018). P65 then translocases to the nucleus and binds to the nucleotide sequence of the target genes and mediates tightly controlled transcriptional programs that regulate the expression of a wide variety of cytokines (Giridharan and Srinivasan, 2018). LLO secreted from *L. monocytogenes* activates the NF-κB signaling pathway in endothelial cells via the phosphorylation of IKK β in IKKα/β complex (Kaya et al., 2002). It has also been shown that *L. monocytogenes* can induce the phosphorylation of IKKα/β complex, which subsequently promotes the translocation of p65 to the nucleus which might be involved in the subsequent transcriptional induction of TNF-α and IL-1 genes (Hauf et al., 1994).

Our previous results revealed that *Lrrk2*^{G2019S} mutation increases the expression of some cytokines in response to *Lm-EGD* (Figure 8). In this regard, we performed western blotting to

measure the activation of IKKα/β and p65, which are two key proteins belonging to the NF-κB signaling pathway.

We generated WT and *Lrrk2*^{G2019S} BMDMs and infected them with *Lm-EGD* (10 MOI) as described in sections 5.4, 5.5, 5.6. Cell lysates were collected at different time points (0,1,3 and 6 hours) for performing western blotting as described in the materials and methods, section 5.8.

Our western blotting analysis appears to indicate that there is increased phosphorylation of IKKα/β in *Lrrk2*^{G2019S} BMDMs; however, the expression of total IKKα/β was also higher (Figure 18). A similar result was obtained with the phosphorylation of p65 (Figure 18). Thus, *Lrrk2*^{G2019S} mutation does not amplify the NF-κB signaling pathway in response to *Lm-EGD*.

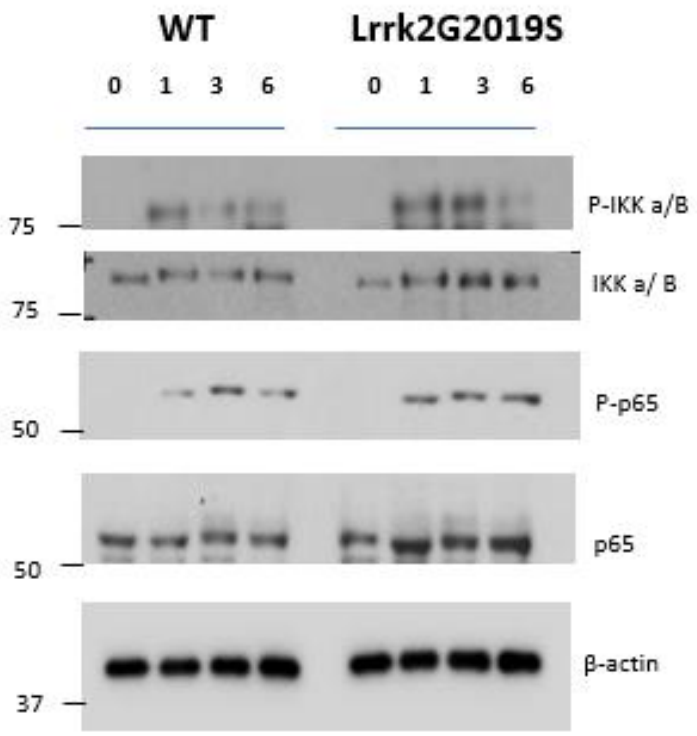
WT
Lrrk2G2019S
0 1 3 6
0 1 3 6
75
P-IKK a/B
75
IKK a/ B
50
P-p65
50
p65
37
β-actin

Figure 18. Activated IKKα/β and activated p65 expression were similar in *Lrrk2*^{G2019S} mutant and WT BMDMs in response to *Lm-EGD* infection.

Western blots of lysates extracted from WT and *Lrrk2*^{G2019S} mutant macrophages infected with 10 MOI of *Lm-EGD* at 0, 1, 3 and 6- hours post-infection for key proteins of NF-kB pathway including IKKα/β and p65. Each western blot was repeated twice to thrice.

6.2.6. *Lrrk2*^{G2019S} mutation enhances the activation of the MAPK pathway in macrophages in response to *Lm-EGD* infection.

PRR-PAMP interaction and cytokine-receptor signaling can promote sequential activation of kinases within different MAPK cascades. These cascades transmit various extracellular signals and thus control a large number of distinct and even opposing cellular processes, such as inflammation, proliferation, survival and apoptosis (Keshet and Seger, 2010). Three main MAPK sub-families have been identified including p38 (stress-activated protein kinases), JNK (Jun amino-terminal kinases) and ERK (extracellular-signal-regulated kinases), which contribute to the regulation of pro-inflammatory and anti-inflammatory cytokines (Lucas et al., 2005; Morrison, 2012; Sabio and Davis, 2014). Of note, there has been evidence suggesting that all these MAPK modules can be activated by infection with *L. monocytogenes* in Hela epithelial cells (Tang et al., 1998).

Since our results have so far indicated that *Lrrk2*^{G2019S} mutation affects the production of pro-inflammatory cytokines, IL-1β and TNF-α (Figure 8 A, B), and anti-inflammatory cytokine IL-10 (Figure 8 C), we aimed to figure out whether MAPK pathways are modulated by *Lrrk2*^{G2019S} mutation in response to *Lm-EGD.* To address this, we decided to evaluate the expression/ activation of p38, ERK and JNK proteins by western blotting.

We generated WT and *Lrrk2*^{G2019S} BMDMs, infected them with *Lm-EGD* (10 MOI) as described in the materials and methods sections 5.4, 5.5, 5.6. and collected cell lysates at various time points (0, 1, 3 and 6 hours) post-infection. These lysates were then used for performing western blots as described in the materials and methods, section 5.8.

While we did not observe any difference in the levels of phosphorylated and total forms of JNK between WT and *Lrrk2*^{G2019S} mutant macrophages, *Lrrk2*^{G2019S} mutation enhanced the phosphorylation of p38 (the active form of p38) in response to *Lm-EGD* infection (Figure19). Moreover, the levels of both phosphorylated and total ERK1/2 were significantly enhanced in response to *Lm-EGD* infection (Figure 19).

P38MAPK is strongly activated by environmental stresses, infections and inflammatory cytokines, that contribute to inflammation, apoptosis, cell differentiation and cell cycle regulation (Raingeaud et al., 1995). It has been shown that microglia (resident macrophages in the CNS) regulate the production of IL-1β and TNF-α via the p38 MAPK signaling pathway (Bachstetter and Van Eldik, 2010). Additionally, LPS stimulation induces the activation of p38α (an isoform of p38) in macrophages, which subsequently activates a downstream signaling cascade of proinflammatory cytokines, including TNF-α, IL-1, and IL-6 (Kang et al., 2008; Ono and Han, 2000).

Sequestered in the cytoplasm of un-stimulated cells, p42/p44 ERK1/2 is phosphorylated and subsequently activated in response to cytokines, infections and growth factors (Lu and Malemud, 2019). Consequently, active (phosphorylated) ERK1/2 is translocated to the nucleus, where it activates transcription factors (Lu and Malemud, 2019). The ERK1/2 signaling pathway has been implicated in diverse cellular events, including proliferation, growth, differentiation, cell migration, cell survival, metabolism and transcription of cytokines (Carter et al., 1999; Lu and Malemud, 2019). Joseph *et.al*. (2016) also displayed that the level of IL-10 was reduced by inhibiting ERK MAPK mediator, suggesting that ERK1/2 mediates IL-10 expression (Joseph et al., 2016).

Collectively, ERK and p38 seem important in the regulation of pro-inflammatory and anti-inflammatory cytokine expression in response to infections.

Having shown that the *Lrrk2*^{G2019S} mutation enhanced the activation of p38 and ERK as well as the production of cytokines in response to *Lm-EGD* infection, we decided to evaluate the impact of inhibiting p38 and ERK on the production of cytokines by WT and *Lrrk2*^{G2019S} macrophages upon infection.

To address this, we generated macrophages as described in sections 5.4, 5.5. We pre-treated the cells with various doses of the p38 MAPK inhibitor (LY2228820,100 nM) or ERK inhibitor (U-0126, 1uM), and infected them as described in section 5.6.

Inhibition of p38, reduced the production of TNF-α and IL-1β by the mutant cells to the levels observed in WT cells (Figure 20 A, B). This suggests that *Lrrk2*^{G2019S} mutation may be regulating the production of cytokines via augmentation of the p38 MAPK pathway in response to *Lm-EGD* infection.

Inhibition of ERK signaling with the commonly used inhibitor (U-0126) reduced the expression of IL-10 in *Lrrk2*^{G2019S} macrophages to the levels similar to WT macrophages in response to *Lm-EGD* (Figure 21 C). These results indicate that *Lrrk2*^{G2019S} mutation drives the over-expression of ERK and its subsequent activation to up-regulate IL-10 expression upon *Lm- EGD* infection.

Interestingly, Kim *et al.* (2019) has recently demonstrated that LRRK2 kinase activity plays a critical role in manganese-induced inflammation via p38 and ERK MAPK signaling in macrophages and microglia (Kim et al., 2019).

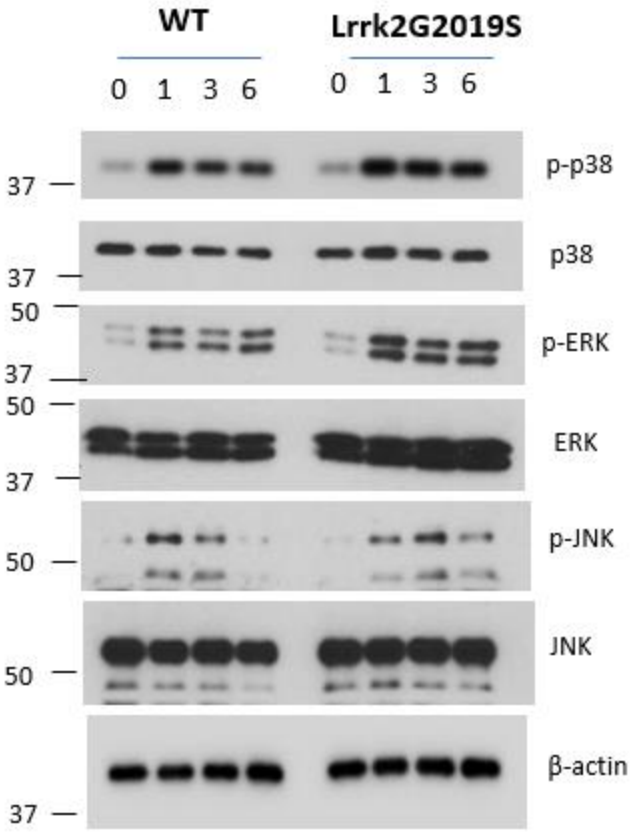
WT
Lrrk2G2019S
0 1 3 6
0 1 3 6
37
p-p38
37
p38
50
37
p-ERK
50
37
ERK
50
p-JNK
50
JNK
37
β-actin

Figure 19. Enhanced expression of activated p38 and ERK 1/2 in the *Lrrk2*^{G2019S} mutant macrophages versus WT cells in response to *Lm-EGD* infection.

Western blots of lysates extracted from WT and *Lrrk2*^{G2019S} mutant macrophages infected with 10 MOI of *Lm-EGD* at 0, 1, 3 and 6- hours post-infection for the activated and total forms of key proteins of MAPK pathways including p38, ERK, and JNK. Each western blot was repeated twice to thrice.

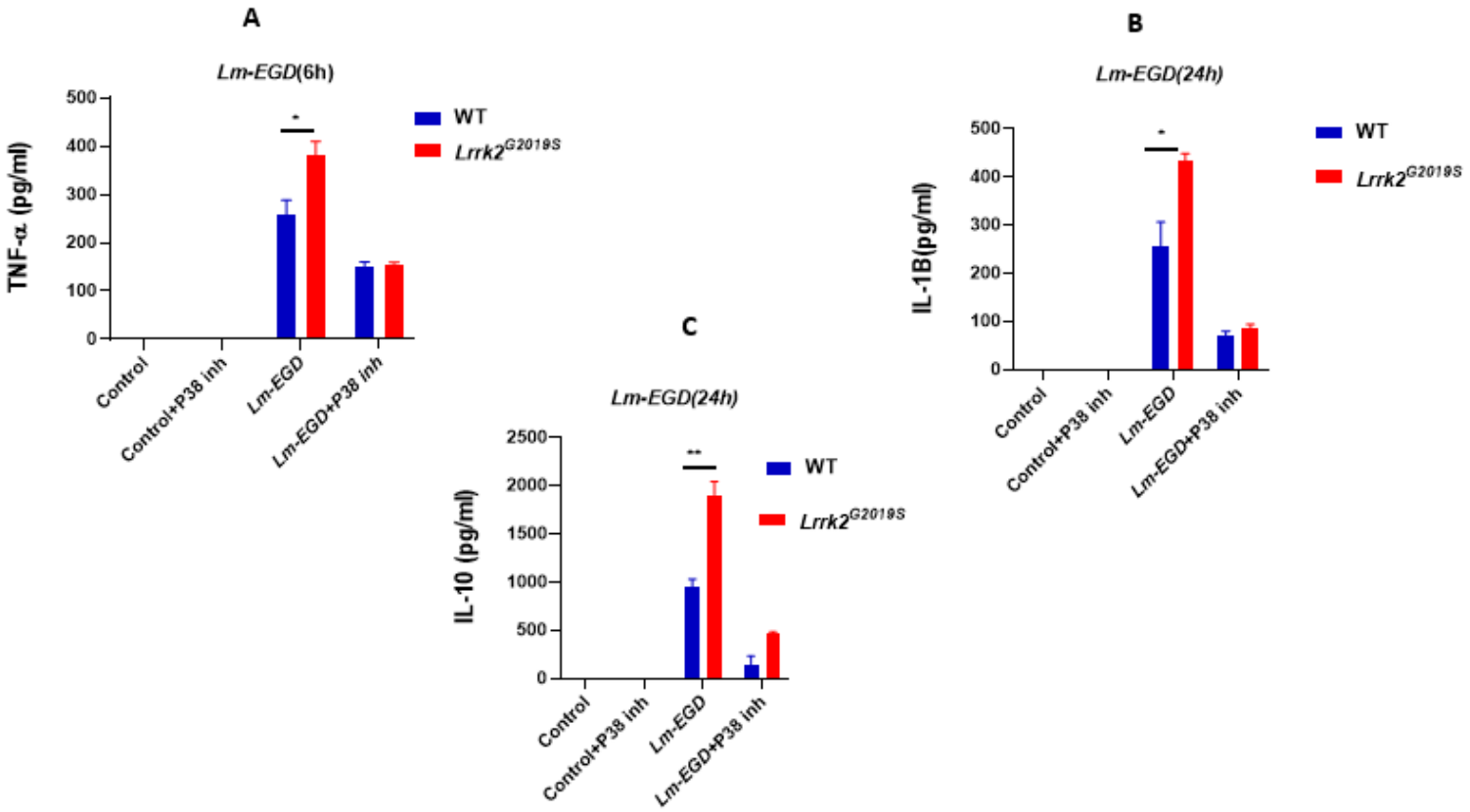
A
Lm-EGD(6h)
TNF-α (pg/ml)
500
400
300
200
100
0
*
WT
Lrrk2G2019S
Control
Control+P38 inh
Lm-EGD
Lm-EGD+P38 inh
B
Lm-EGD(24h)
IL-1B(pg/ml)
500
400
300
200
100
0
*
WT
Lrrk2G2019S
Control
Control+P38 inh
Lm-EGD
Lm-EGD+P38 inh
C
Lm-EGD(24h)
IL-10 (pg/ml)
2500
2000
1500
1000
500
0
**
WT
Lrrk2G2019S
Control
Control+P38 inh
Lm-EGD
Lm-EGD+P38 inh

Figure 20. Inhibition of p38 reduced the levels of TNF-α and IL-1β in *Lrrk2*^{G2019S} macrophages to WT levels.

BMDMs were generated from WT and *Lrrk2*^{G2019S} mice. Cells were pre-treated with the p38MAPK inhibitor (LY2228820,100 nM) for 30 minutes followed by infection with *Lm-EGD (*10 MOI for IL-1β and 25 MOI for TNF-α and IL-10) for 6 and 24 hours. The expression of various cytokines in the supernatants of infected macrophages was quantified by ELISA.

A. Expression of TNF-α levels measured at 6 hours after infection.

B. Expression of IL-1β levels measured at 24 hours after infection.

C. Expression of IL-10 levels at 24 hours after infection.

Data shown is representative of three experiments, each performed in triplicates and presented as mean ± SEM. Statistical analysis was done by unpaired student's t-test, where *p<0.05; **p<0.01; ***p<0.001; ****p<0.001 using GraphPad Prism 8 software.

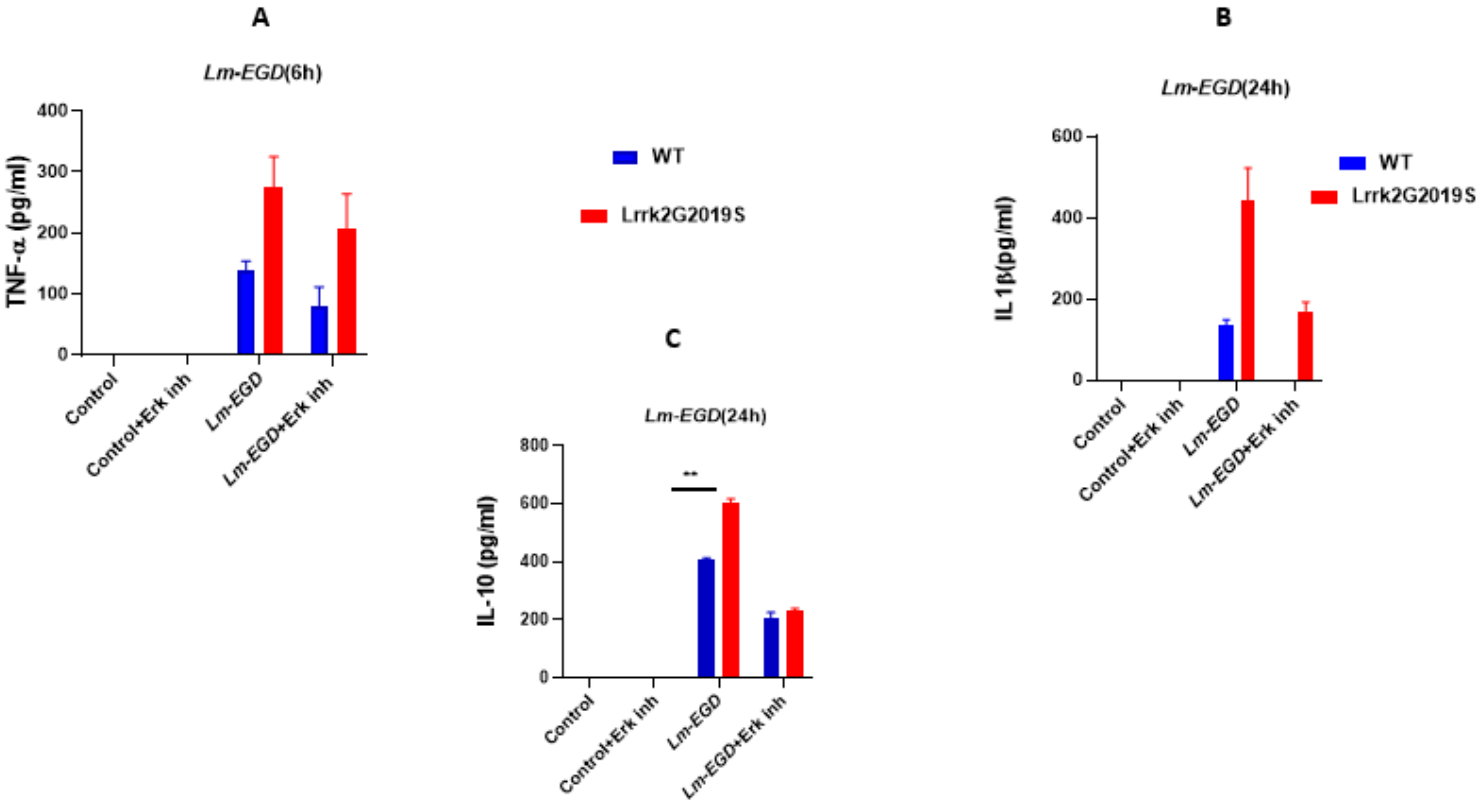
A
Lm-EGD(6h)
TNF-α (pg/ml)
400
300
200
100
0
Control
Control+Erk inh
Lm-EGD
Lm-EGD+Erk inh
WT
Lrrk2G2019S
C
Lm-EGD(24h)
IL-10 (pg/ml)
800
600
400
200
0
**
Control
Control+Erk inh
Lm-EGD
Lm-EGD+Erk inh
B
Lm-EGD(24h)
IL 1β(pg/ml)
600
400
200
0
WT
Lrrk2G2019S
Control
Control+Erk inh
Lm-EGD
Lm-EGD+Erk inh

Figure 21. Inhibition of ERK1/2 reduced the levels of IL-10 in *Lrrk2*^{G2019S} macrophages to WT levels.

BMDMs were generated from WT and *Lrrk2*^{G2019S} mice. Cells were pre-treated with ERK inhibitor (U-0126, 1uM) for 30 minutes followed by infection with *Lm-EGD* (10 MOI for IL-1 β and 25 MOI for TNF-α and IL-10) for 6 and 24 hours. The expression of various cytokines in the supernatants of infected macrophages was quantified by ELISA.

A. Expression of TNF-α levels measured at 6 hours after infection.

B. Expression of IL-1β levels measured at 24 hours after infection.

C. Expression of IL-10 levels measured at 24 hours after infection.

Data shown is representative of 2-3 experiments, each performed in triplicates and presented as mean ± SEM. Statistical analysis was done by unpaired student's t-test, *p<0.05; **p<0.01; ***p<0.001; ****p<0.001 using GraphPad Prism 8 software.

6.2.7. *Lrrk2*^{G2019S} mutation enhances the activation of TAK1 in macrophages in response to *Lm-EGD* infection.

Since our results have so far revealed that p38 MAPK may be regulating the production of the pro-inflammatory cytokines (TNF-α and IL-1β) in infected *Lrrk2*^{G2019S} mutant macrophages, we conducted experiments to evaluate the role of MK2 as one of the essential substrates in this pathway.

Morrison (2012) shows that important substrates in the p38 module include the downstream kinases MK2, MK3, PRAK, MSK1 and MSK2, as well as various transcription factors. It has been shown that MK2 is an essential component of the inflammatory response as it regulates the biosynthesis of TNF-α at the post-transcriptional level (Kotlyarov et al., 1999).

Alternatively, the upstream cascade for p38 pathway includes MLK2, MLK3, MEKKs, ASKs, TAK1, TAO1 and TAO2 (Morrison, 2012; Raman et al., 2007). TAK1 (TGFβ-activating kinase1) is activated by numerous exogenous and endogenous ligands, such as LPS, IL-1, TNF-α and TNF-related apoptosis-inducing ligand (TRAIL) and initiates cell signaling leading to the activation of NF-κB and MAPK (Mihaly et al., 2014). Therefore, since TAK1 directly phosphorylates MAPK mediators, we reasoned that TAK1 may also be modulated by *Lrrk2*^{G2019S}.

We generated WT and *Lrrk2*^{G2019S} BMDMs, infected them with *Lm-EGD* (10 MOI) and collected cell lysates at various time points (0, 1, 3 and 6 hours) post-infection as described in the materials and methods, sections 5.4, 5.5, 5.6. These lysates were then used for performing western blots to detect MK2 and TAK1.

While the expressions of total and phosphorylated forms of MK2 in *Lrrk2* ^{G2019S} mutant and WT cells were similar, *Lrrk2*^{G2019S} mutant macrophages expressed more activated TAK1 (Figure 22). Hence, while MK2 may not be significantly modulated, *Lrrk2* ^{G2019S} seems to increase TAK1 activity over time in response to *Lm-EGD*. Presumably, the enhanced IL-1 β secretion by the *Lrrk2*^{G2019S} cells may be augmenting the activation of TAK1, which in turn may be contributing to the increase p38 MAPK signaling pathway (Figure 19). And while MK2 may not be modulated by *Lrrk2* ^{G2019S} (Figure 22), it requires further investigations to find how *Lrrk2*^{G2019S} is modulating other substrates of P38 MAPK signaling pathway as well.

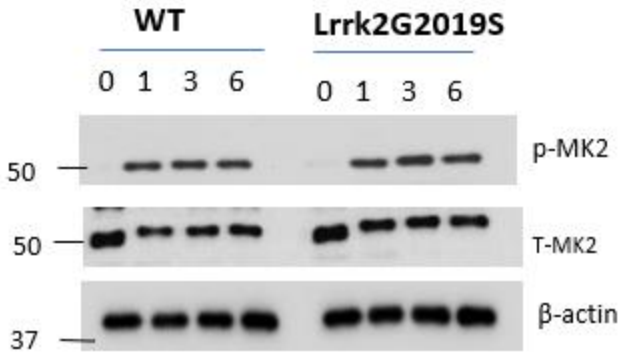
WT
Lrrk2G2019S
0 1 3 6
0 1 3 6
50
p-MK2
50
T-MK2
37
β-actin

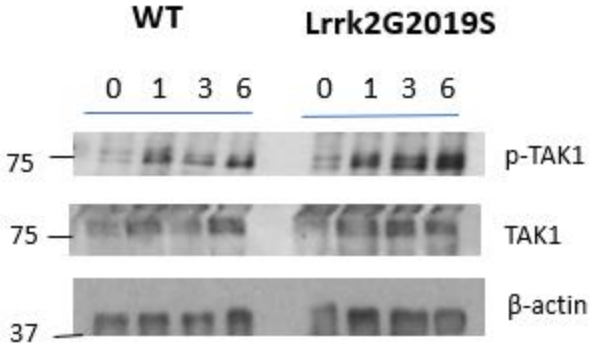
WT
Lrrk2G2019S
0 1 3 6
0 1 3 6
75
p-TAK1
75
TAK1
37
β-actin

Figure 22. Increased activation of TAK1 and similar expression of MK2 in the *Lrrk2*^{G2019S} mutant macrophages versus WT cells in response to *Lm-EGD* infection.

Western blots of lysates extracted from WT and *Lrrk2*^{G2019S} mutant macrophages infected with 10 MOI of *Lm-EGD* at 0, 1, 3 and 6- hours post-infection for the activated and total forms of key proteins of MAPK pathways including MK2 and TAK1. Each western blot was repeated twice to thrice.

6.2.8. *Lrrk2*^{G2019S} mutation enhances the activation of RIPK1 in macrophages in response to *Lm-EGD* infection.

RIPK1 is a member of the receptor-interacting protein (RIP) family of serine/threonine protein kinases that has emerged as a key regulator of multiple downstream inflammatory signaling pathways. It regulates cell death including apoptosis and necroptosis as well as inflammatory responses downstream of TNF-α receptor 1 (TNFR1) (Degterev et al., 2019). In particular, activation of RIPK1 in the cells of myeloid lineage (e.g., microglia and macrophages) promotes the expression of proinflammatory cytokines (e.g., TNF-α) independently from cell death (Christofferson et al., 2012).

Laurien *et al*. (2020) have shown that RIPK1 phosphorylation at serine 166 (S166) is required for the activation of RIPK1 kinase-dependent apoptosis and inflammatory activities *in vitro* and *in vivo*. They also provided evidence that S166 phosphorylation enhances the kinase activity of RIPK1 suggesting that S166 phosphorylation can serve as a reliable biomarker for RIPK1 kinase-dependent pathologies (Laurien et al., 2020). Jaco *et al.* (2017) also demonstrated that activation of TNFR1 leads to phosphorylation of RIPK1(S166) which activates TAK1 and subsequently P38 MAPK inflammatory signaling pathway (Jaco et al., 2017). Furthermore, TAK1 seems to play a key role in regulating cell death mediated by RIPK1 (Amin et al., 2018).

On the other hand, LRRK2 is alternately classified as RIPK7 which shows several interactions with RIPK1. Amin *et al.* (2018) demonstrated that LRRK2 stabilizes activated RIPK1 and therefore promotes ubiquitination of RIPK1, which specifically promoted RIPK1-dependent apoptosis. Indeed, RIPK1 has been recently considered as a potential therapeutic target for PD patients (Yuan et al., 2019).

Since our results have so far indicated that *Lrrk2* ^{G2019S} enhances the activation of P38 MAPK, TAK1 and expression of TNF-α, we decided to evaluate the impact on the phosphorylation of RIPK1 in *Lrrk2* ^{G2019S} and WT BMDMs.

We generated WT and *Lrrk2*^{G2019S} BMDMs, infected them with *Lm-EGD* (10 MOI) and collected cell lysates at various time points (0, 1, 3 and 6 hours) post-infection as described in the materials and methods, sections 5.4, 5.5, 5.6. These lysates were then used for performing western blots to detect activated and total RIPK1. Results indicate that the *G2019S* mutation of *Lrrk2* enhances the S166 phosphorylation of RipK1 (Figure 23A). Thus, these results highlight the increased phosphorylation of RIPK1 as the most upstream event that is enhanced by *G2019S* mutation, which results in increased expression of TNF-α.

It should be noted that *K45A* mutation of *Ripk1* inactivates the kinase activity of RIPK1, and this has been shown to attenuate the inflammatory response and consequently exacerbate the bacterial burden following challenge with *Salmonella Typhimurium* (Shutinoski et al., 2016).

Since we observed increased activation of RIPK1 in *LRRK2* ^{G2019S} mutant macrophages (Figure 23A), we generated *Lrrk2* ^{G2019S} mice with a *K45A* mutation of *Ripk1* to evaluate whether the enhanced control of *Lm-EGD* in *LRRK2* ^{G2019S} mice is indeed due to the enhanced activation of *Ripk1* in these mice.

We observed that the bacterial burden in *Ripk1* ^{K45A} mutant and WT mice following challenge with 10e4 CFU of *Lm-EGD* was similar in the spleens of infected mice at day 3 post-infection (Figure 23B). We also observed that the bacterial burden did not increase in the *Lrrk2*^{G2019S} - *Ripk1*^{k45A} double mutant mice in comparison to the *Lrrk2*^{G2019S} mice (Figure 23 C). Rather, there was a slight reduction in the bacterial burden in the double knock-in mice. These results indicate

that the enhanced control of *L. monocytogenes* in *Lrrk2*^{G2019S} mice is not due to the enhanced activation of RIPK1.

A

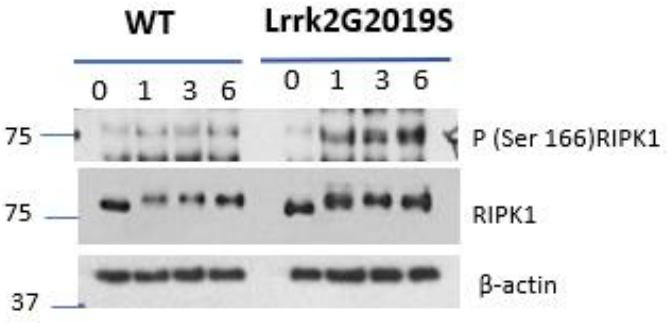
WT
Lrrk2G2019S
0 1 3 6
0 1 3 6
75
75
37
P (Ser 166)RIPK1
RIPK1
β-actin

B

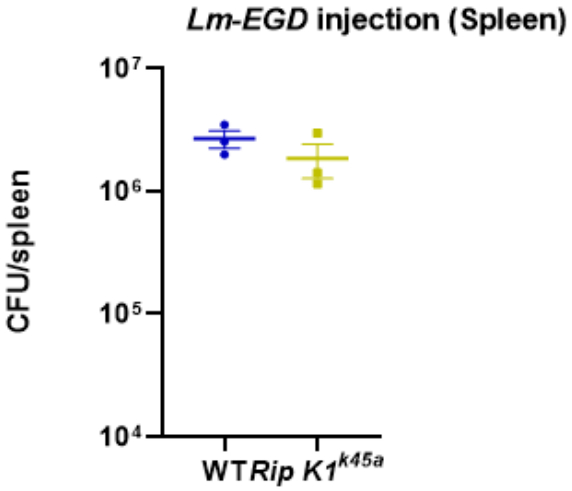
Lm-EGD injection (Spleen)
CFU/spleen
10^7
10^6
10^5
10^4
WT
Rip K1^k45a

C

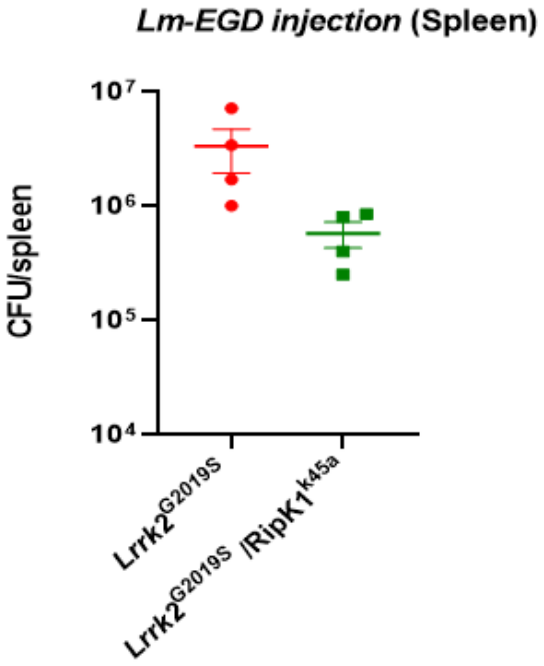
Lm-EGD injection (Spleen)
CFU/spleen
10^7
10^6
10^5
10^4
Lrrk2^G2019S
Lrrk2^G2019S /RipK1^k45a

Figure 23. Increased activation of RIPK1 in the *Lrrk2*^{G2019S} mutant macrophages versus WT cells in response to *Lm-EGD* infection.

A. Western blots of lysates extracted from WT and *Lrrk2*^{G2019S} mutant macrophages infected with 10 MOI of *Lm-EGD* at 0, 1, 3 and 6- hours post-infection for the activated RIPK1 (Ser166) and total form of RIPK1. Western blot was repeated twice.

B. Spleens were collected from WT and *Ripk1* ^{k45A} mutant mice infected with 10e4 CFU *Lm-EGD* via tail vein injection *in vivo*. At day 3 post-infection, the bacterial burden was evaluated in the collected spleens upon plating serial dilutions on BHI agar plates. Graphs display bacterial colony forming unit (CFU) of *Lm-EGD* in spleens. Every dot corresponds to a single mouse.

C. Spleens were collected from *Lrrk2*^{G2019S} and *Lrrk2*^{G2019S} /*Ripk1*^{k45A} double knock-in mutant mice infected with 10e4 CFU *Lm-EGD* via tail vein injection *in vivo*. At day 3 post-infection, the bacterial burden was evaluated in the collected spleens upon plating serial dilutions on BHI agar plates. Graphs display bacterial colony forming unit (CFU) of *Lm-EGD* in spleens. Every dot corresponds to a single mouse.

6.2.9. *G2019S* mutation of *Lrrk2* modulates reactive oxygen species (ROS) production in response to *L. monocytogenes* infection.

Reactive oxygen species (ROS) are oxygen-containing radicals, such as hydrogen peroxide and superoxide, which are deadly weapons used by phagocytes and other cell types against pathogens (Paiva and Bozza, 2014). Phagocytes recognize microbes through many molecular patterns and try to engulf them. Respiratory burst is a process by which NADPH oxidase (NADPH oxidase 2 [NOX2]) generates ROS in response to microbe recognition and helps to get rid of many microbes (Paiva and Bozza, 2014). ROS effectively combat certain microbes such as *L. monocytogenes*, and it has been shown that ROS inhibit *L. monocytogenes* invasion into epithelial cells (Chen *et al*., 2018).

Indeed, ROS can kill pathogens directly by causing oxidative damage to bio-compounds or indirectly by various nonoxidative mechanisms through pattern recognition receptors to stimulate cell signaling cascades (Paiva and Bozza, 2014; Zhang et al., 2016). More importantly, both NF-κB and MAPK signaling pathways, including P38, ERK and JNK pathways, have been shown to be activated either directly or indirectly by ROS (Zhang *et al*., 2016). Since *Lrrk2*^{G2019S} mutation is associated with the increased activation of the inflammatory signaling pathways and confers a better protection against bacterial infections in mice, we were interested in evaluating the ROS levels produced by *Lrrk2*^{G2019S} and WT mice in response to *Lm-EGD.*

To evaluate whether *Lrrk2*^{G2019S} mutation triggers a greater respiratory burst to eliminate *Lm-EGD*, we measured ROS levels in naïve and infected *Lrrk2*^{G2019S} mutant and WT mice through bioluminescence imaging (Figure 24 A, B). While there was no significant difference in the production of ROS by naïve *Lrrk2*^{G2019S} mice compared to naïve WT mice (Figure 24 A), *Lrrk2*^{G2019S} mice produced significantly higher levels of ROS in response to infection compared

with WT mice (Figure 24 B). This supports the role of ROS in controlling the *Lm-EGD* infection in *Lrrk2*^{G2019S} mutant mice *in vivo*.

It was also previously reported that the LRRK2 kinase domain increases the generation of ROS and causes enhanced neurotoxicity under H_2O_2 treatment (Heo *et al*., 2010). Additionally, Shutinoski *et al*. (2019) detected a significant increase in H_2O_2 production in *Lrrk2*^{G2019S} mutant bone marrow derived macrophages (BMDMs) after exposure to *Salmonella* (Shutinoski *et al*., 2019).

Taken together, ROS may be acting as a mediator in *Lrrk2*^{G2019S} host cells to prevent *Listeria monocytogenes*' invasion along with activating the immune response via stimulating various signaling pathways. Evaluating whether inflammatory signaling pathways in BMDMs activated by ROS *in vitro* requires further investigation.

Furthermore, we measured reactive oxygen species in various ages of naïve mice (4 months, 8 months and 10 months) to evaluate whether *Lrrk2* ^{G2019S} mutation enhances the production of ROS in older mice compared to the young (Figure 25). The results indicate that various aged- *Lrrk2*^{G2019S} mutant and WT mice produced ROS similarly. Accordingly, it can be implicated that age does not seem to be an important contributing factor in inducing oxidative stress in mutant mice compared to WT mice.

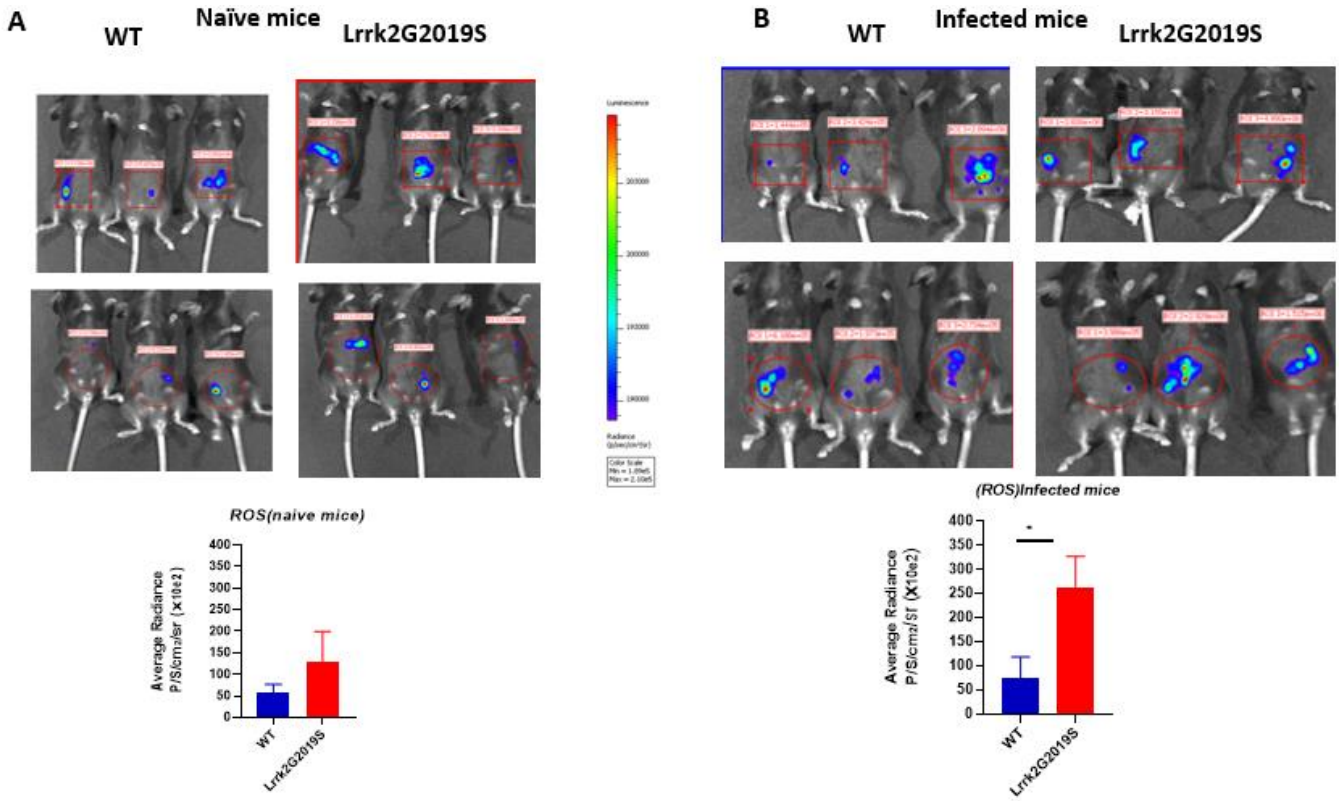
A
WT
Naïve mice
Lrrk2G2019S
ROS(naive mice)
Average Radiance P/S/cm2/sr (x10e2)
400
350
300
250
200
150
100
50
0
WT
Lrrk2G2019S
B
WT
Infected mice
Lrrk2G2019S
(ROS)Infected mice
Average Radiance P/S/cm2/Sr (X10e2)
*
400
350
300
250
200
150
100
50
0
WT
Lrrk2G2019S

Figure 24. Infected *Lrrk2*^{G2019S} mutant mice expressed more reactive oxygen species (ROS) in response to *L. monocytogenes* infection.

A, B. *Lrrk2*^{G2019S} mutant and WT mice (8-12 weeks) were injected with 10e4 CFU *Lm-EGD* via tail vein and the levels of reactive oxygen species (ROS) were measured *in vivo*

A. before infection **B**. at day 3 post-infection.

Mice were anesthetized with isoflurane and injected intraperitoneally (20 μg/ g of body weight) with L-012 dissolved in PBS. Bioluminescence signaling was measured at 5 min post-injection using an IVIS Spectrum imaging system. Bar graphs quantifying the data are shown in each panel.

Data are two independent experiments. Pooled data was analyzed using Student's unpaired t-test $*P \leq 0.05$, $**P < 0.01$, and $***P < 0.001$ using GraphPad Prism 8 software.

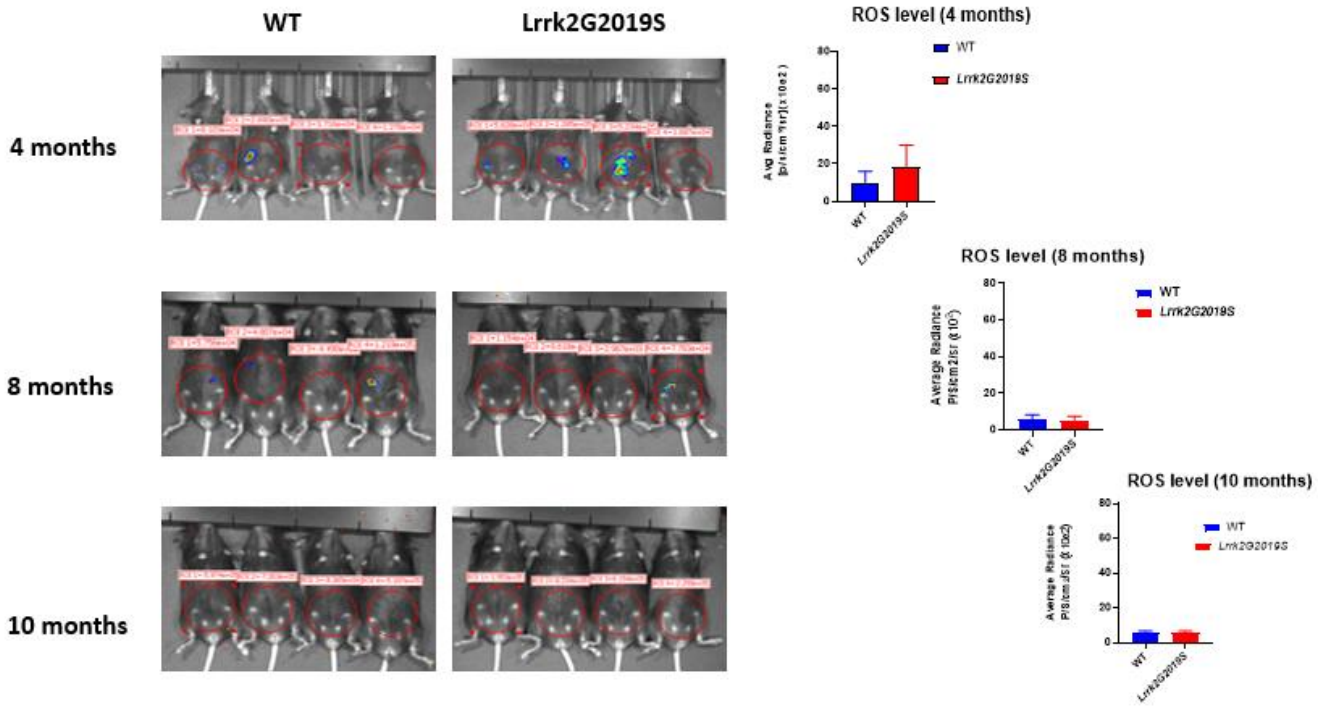
WT
Lrrk2G2019S
4 months
8 months
10 months
ROS level (4 months)
WT
Lrrk2G2019S
Avg Radiance (p/s/cm^2/sr) (x 10e2)
ROS level (8 months)
WT
Lrrk2G2019S
Average Radiance P/s/cm2/sr (x 10^2)
ROS level (10 months)
WT
Lrrk2G2019S
Average Radiance P/s/cm2/sr (x 10e2)

Figure 25. *Lrrk2*^{G2019S} mutant and WT mice of various ages produced reactive oxygen species (ROS) similarly.

The level of reactive oxygen species (ROS) was measured in naïve mutant and WT mice of various ages. Mice were anesthetized with isoflurane and injected intraperitoneally (20 μg/ g of body weight) with L-012 dissolved in PBS. Bioluminescence signaling was measured at 5 min post-injection using an IVIS Spectrum imaging system. Bar graphs quantify the data which are shown in each panel of mice with different ages (4 months, 8 months and 10 months old naïve mice)

7.Discussion

7.1. The role of *Lrrk2* mutations in controlling microbial infections.

Our *in vivo* results emphasize the protective role that *Lrrk2*^{G2019S} expression plays in mice infected with *L. monocytogenes.* The hyperactive *G2019S* mutation of *Lrrk2* conferred a gain-of-function effect resulting in a reduced bacterial burden in the spleens of mice infected with *Lm-EGD* (Figure 5). Our findings are consistent with other recent studies reporting the protective role of *Lrrk2* in various other infection models in mice.

According to Liu *et al.* (2017), *Lrrk2*-deficient mice are more susceptible to *Salmonella Typhimurium*- induced peritoneal inflammation, as they exhibited enhanced bacterial burden in the spleens compared to WT mice (Liu et al., 2017b). Moreover, *Lrrk2* harbors a protective effect in controlling the infections with *S. Typhimurium* and *reovirus* (Shutinoski *et al*., 2019). Shutinoski *et al.* (2019) demonstrated that *Lrrk2*-deficient mice displayed higher bacterial burden and viral load in the spleens and the brains respectively. In addition, they observed that the *G2019S* mutation in *Lrrk2* has a protective effect, and mice carrying this mutation displayed less bacterial burden in the spleens. These findings strongly support our data that *Lrrk2*^{G2019S} mutation controls the infection with *L. monocytogenes* better and significantly reduces the splenic bacterial burden with a similar trend in the brain (Figure 5).

Another report in 2015 identified a Nod2-type role (NOD2 encodes a cytosolic bacterial sensor that induces the expression of cytokines and antimicrobial peptide genes) for *Lrrk2* in protecting the murine intestinal tract against *L. monocytogenes* infection (Zhang et al., 2015). Zhang *et al.*

(2015) infected WT and *Lrrk*2 knock out mice orally with *L. monocytogenes* to determine the bacterial burden in various organs. Bacterial loads were significantly increased in fecal samples and livers from infected *Lrrk2* knock out mice compared with those from WT mice. A similar trend towards a higher bacterial burden in the *Lrrk2*- deficient spleens was also observed indicating that LRRK2 deficiency leads to a specific defect in controlling intestinal infection (Zhang et al., 2015). These results can partly support our *in vivo* results, which show that *Lrrk2*^{G2019S} mutation has a protective effect in controlling *L. monocytogenes* infection. However, we were not able to show this effect with oral infection (Figure 3).

Conversely, Hartlova *et al*. in 2018 showed that LRRK2 has a negative impact on the control of *Mycobacterium Tuberculosis* (*M. tuberculosis)*. They showed that LRRK2 deficiency in mice resulted in a significant decrease in *M. tuberculosis* burden early during an *in vivo* infection (Härtlova et al., 2018). However, Weindel *et al.* (2020) recently showed that there was not any significant difference in *M. tuberculosis* burdens in the spleens or the lungs of infected *Lrrk2*-deficient and WT mice. In contrast, there was a significant increase in CFU recovered from BMDMs following infection with *M. tuberculosis in vitro,* suggesting that *Lrrk2*- deficient macrophages can control *M. tuberculosis* replication early after infection compared to heterozygote macrophages (Weindel *et al*., 2020). Indeed, these two recent studies display controversial data regarding the protective effect of *Lrrk2* in controlling *M. tuberculosis* infections.

Collectively, these data uphold the implication of *Lrrk2* mutations in differentially controlling microbial infections, and this may be dependent on the genotype of the host as well as the type of pathogen.

7.2. *Lrrk2* increases IL-1β expression in macrophages in response to *Lm-EGD*.

Although genetic polymorphisms in the *Lrrk2* gene are associated with a variety of inflammatory diseases, and the protective effect of LRRK2 in controlling infections has been shown in several studies (Liu et al., 2017b; Shutinoski et al., 2019; Zhang et al., 2015), the physiological function of LRRK2 protein remains poorly understood.

Hakimi *et al.* (2011) demonstrated a predominance of higher molecular weight of LRRK2 in murine BMDMs and a significant up-regulation of the protein upon exposure to microbial structures. Therefore, in order to investigate the mechanism by which LRRK2 operates, we decided to perform *in vitro* experiments on BMDMs, representative cells of the innate immune system.

Liu *et al.* (2017) also found that the *G2019S* mutation of *Lrrk2*, the most common pathogenic mutation associated with PD, enhanced caspase-1 activation and IL-1β production in peritoneal macrophages in response to *Salmonella Typhimurium*.

In agreement with these notions, we also observed that *Lrrk2*^{G2019S} significantly increased IL-1β expression in BMDMs in response to *Lm-EGD* (Figure 6). Since inflammasome signaling pathways are very important in the processing of the IL-1β cytokine, we conducted experiments to determine which inflammasomal pathway is affected by the *Lrrk2*^{G2019S} mutation.

7.2.1. The role of the inflammasome signaling pathways through which BMDMs respond to *Lm-EGD*.

To explore the inflammasome pathways that are modulated by LRRK2 during infection with *Lm-EGD*, we evaluated the expression of IL-1β and the cell death in BMDMs deficient in various signaling pathways.

Lm-EGD has been shown to induce the activation of caspase-1 which results in cell death by pyroptosis and activation of caspase-1 results in the secretion of IL-1β and IL-18 production (Cervantes et al., 2008; Tsuchiya et al., 2010). Consistently, our results showed that the rate of cell death in *caspase 1/11*-deficient BMDMs was reduced compared to that in WT cells in response to *Lm-EGD* (Figure 14). We observed that cell death was reduced, but not abolished in caspase1/11-deficient macrophages (Figure 14). This indicates that there are other inflammasomes independent cell death pathways that induce cell death in macrophages infected with *L. monocytogenes* (McDougal and Sauer, 2018). In contrast to cell death, we observed that caspase-1 activation was critical in triggering the production of IL-1β in *Lm-EGD* infected macrophages. This was expected because several other research groups observed that IL-1β production was dependent on caspase-1 in the context of *L. monocytogenes* infection (Eitel, Suttorp, & Opitz, 2011; Hara *et al*., 2008; Tsuchiya *et al.*, 2010).

Caspase-11, which was first characterized in the late 1990s (Wang et al., 1998) has recently received much attention especially in case of infection with *Salmonella Typhimurium* (Broz *et al*., 2012.). It is believed that caspase-11 is mainly activated by LPS, present on the surface of the Gram-negative bacteria, which gains access to the cytosol, and induces inflammasome signaling and pyroptosis (Huang *et al*., 2019; Kayagaki *et al.*, 2013; Kayagaki *et al*., 2011). It also has been shown that caspase-11 can be induced by interferon gamma, and interferon beta in addition to LPS (Lee *et al*., 2001). In fact, Hara *et al*. (2018) recently demonstrated that LTA (Lipoteichoic acid), a molecule present in the cell wall of Gram-positive bacteria including *L. monocytogenes*, binds

to and activates NLRP6 inflammasome, leading to the recruitment and processing of caspase-11 and caspase-1 via the adaptor protein ASC. However, Man *et al*. (2017) found no role for caspase-11 in the activation of the inflammasome induced by *L. monocytogenes,* consistent with the notion that caspase-11 specifically mediates recognition of LPS from Gram-negative bacteria. Thus, there is controversy regarding the role of caspase-11 in inflammasome signaling by Gram-positive bacteria, such as *L. monocytogenes*. In our studies, we have shown that *caspase-11*-deficient BMDMs displayed significantly reduced cell death in response to *Lm-EGD,* confirming that caspase-11 constitutes an important mediator of cell death in *Lm-EGD* infected BMDMs (Figure 14). Hara *et al*. (2018) also demonstrated that the release of IL-1β was impaired in *Listeria*-infected *Casp11*$^{-/-}$ BMDMs compared with WT cells. Conversely, we observed high expression of IL-1β by *caspase-11* deficient BMDMs in the context of *L. monocytogenes* (Figure 14). We assumed that caspase-1, which is the main IL-1β converting enzyme (ICE), might be hyper-activated in the *caspase-11* knock out mice, resulting in high IL-1β expression. All in all, further investigations need to be carried out to further delineate the role of caspase-11 during infection with *Lm-EGD*.

Regarding inflammasome signaling mediators, we found that NLRP3 and AIM2 inflammasome compartments are activated by *Lm-EGD* (Figure 10, Figure 16)

Whether NLRC4 inflammasome senses *L. monocytogenes* is controversial. In contrast to *Salmonella Typhimurium*, which mainly activates NLRC4 (Mariathasan et al., 2004; Zhang et al., 2005), *L. monocytogenes* does not seem to have a significant impact. It has been reported that *L. monocytogenes* can slightly activate the NLRC4 inflammasome (Tsuchiya et al., 2010; Wu et al., 2010). Other reports, however, found no evidence for a critical role of NLRC4 in *Listeria*-mediated caspase-1 activation, and this was consistent with our results (Kim et al., 2010; Meixenberger et

al., 2010). Due to alterations in the expression of flagellin in some *L. monocytogenes* strains (Gründling et al., 2004), we speculate that these differences in flagellin expression among bacterial strains may be responsible for the differential involvement of NLRC4 during *L. monocytogenes* infection.

Many studies reported that *L. monocytogenes* induces the NLRP3 inflammasome (Mariathasan et al., 2006; Meixenberger et al., 2010; Warren et al., 2008). We also observed that NLRP3-deficient cells exhibited reduced IL-1β and cell death; therefore, we can conclude that *L. monocytogenes* can be predominantly sensed by NLRP3 compared to NLRC4 (Figure 10, 12).

Interestingly, we found that the AIM2 inflammasome mediates an important role in inducing the secretion of IL-1β and partly in causing cell death in response to infection with *Lm-EGD* (Figure 16). Tsuchiya *et al.* (2010) also emphasized that AIM2 plays an important role in inducing the activation of caspase-1 in macrophages infected with *L. monocytogenes.* They demonstrated that the genomic DNA of *Listeria* is detected by AIM2, thereby inducing the secretion of the caspase1–dependent cytokines (IL-1β and IL-18). Other findings implicated the role of AIM2, activated by the DNA of *Listeria*, in triggering caspase-1 activation, cell death and secretion of the IL-1 family of cytokines, which are consistent with our findings (Kim et al., 2010; Sauer et al., 2010).

Taken together, the inflammasome-mediated immune response of BMDMs to *L. monocytogenes* is mediated primarily with the involvement of NLRP3 and AIM2 inflammasome signaling pathways leading to the activation of caspase-1 and/or -11.

7.2.2. The role of the inflammasome mediators in the context of *Lrrk2^{G2019S}* macrophages in response to *Lm-EGD*.

Since we observed that the NLRC4 inflammasome did not have any impact on the production of IL-1β, other cytokines, and cell death induced in BMDMs in response to *L. monocytogenes*, we did not evaluate the expression of NLRC4 in the context of *Lrrk2* ^{G2019S}.

While enhanced NLRP3 expression was observed in western blotting performed on infected WT and *Lrrk2*^{G2019S} mutant macrophages, inhibiting NLRP3 reduced IL-1β expression in *Lrrk2*^{G2019S} and WT macrophages similarly (Figure 17). Additionally, we did not find any difference in the production of IL-1β by *Lrrk2* ^{G2019S} and WT macrophages treated with LPS +ATP which is considered as a potent trigger of NLRP3 inflammasome signaling pathway (Figure 7). Thus, the up-regulation of IL-1β production in *Lrrk2* ^{G2019S} macrophages may not solely due to the up-regulation of NLRP3, and this is consistent with the previously published data with *Salmonella Typhimurium* (Liu et al., 2017b).

We observed that the activation of caspase-1 was increased in *Lrrk2*^{G2019S} macrophages (Figure 17). In this regard, we speculate that the slight increase in caspase-1 activation may contribute to the increased production of IL-1β, as shown also by *Liu et al*. (2017) in the context of *Salmonella*.

We also found slightly increased activation of caspase-11 in *Lrrk2* ^{G2019S} mutant BMDMs in response to *Lm-EGD* (Figure 17). While previous findings showed the impact of caspase-11 on inflammatory dopaminergic cell death in the brain of a 1-Methyl-4-Phenyl-1,2,3,6-Tetrahydropyridine mouse model of Parkinson's Disease (Furuya *et al*., 2004), no other studies demonstrated the mechanistic association of *Lrrk2* mutation and caspase-11 activation in immune cells, such as macrophages. Further investigations must be done to evaluate the role of caspase-11 in association with *Lrrk2* mutations in response to *Lm-EGD* in immune cells.

7.3. The profile of inflammatory cytokines in the context of *Lrrk2* mutations.

Abundant evidence in humans has demonstrated a role for chronic inflammation and innate immune activation in PD. Clinical data suggest that a key causative factor could be the inflammation caused by bacterial or viral infections in PD (Brugger *et al.*, 2015), such that peripheral infections may enhance neurodegeneration either through direct toxicity of circulating bacterial toxins or through circulating cytokines that have been produced at the site of the inflammation (Gelders et al., 2018).

Kozina *et al*. (2018) found that following administration of LPS, significant differences were detected in the induction of pro-inflammatory cytokines such as IL-1α, IFN-γ and chemokines, such as CXCL-1 and CXCL-10, in the substantia nigra of $Lrrk2^{R1441G}$ mutant mice. In addition, *Lrrk2* knockdown or kinase inhibition in primary microglia has been shown to reduce the production of pro-inflammatory cytokines such as TNF-α and IL-1β *(*Moehle *et al*., 2012). However, the absence of LRRK2 resulted in enhanced secretion of pro-inflammatory cytokines with high levels of IFN-γ but an almost complete absence of the type I IFN-α (Härtlova *et al.*, 2018). Our results indicate that there is an augmentation of IL-1β and TNF-*α* levels in macrophages that is caused by the *G2019S* mutation of *Lrrk2* (Figure 8)

However, some reports observed no differences in cytokines released by *Lrrk2*-knockout BMDMs (Dzamko et al., 2012; Hakimi et al., 2011). For instance, Dzamko *et al*. (2012) found that *Lrrk2*-deficient macrophages do not have an altered pattern of pro-inflammatory cytokine secretion after Toll-like receptor 2 or 4 (TLR2 or TLR4) stimulation, indicating that LRRK2 function might be regulated by PAMP signaling without affecting downstream cytokine responses. Hakimi *et al.* (2011) also demonstrated that LRRK2 protein expression does not control IL-6 and KC cytokine signaling in BMDMs.

There is also evidence that LRRK2 regulates the secretion of the anti-inflammatory cytokine IL-10 in mouse macrophages after infection with *M. tuberculosis* but had very little effect on the production of pro-inflammatory cytokines such as TNF-α or IL-6 (Härtlova *et al.*, 2018). Our results also indicate that the *G2019S* mutation of *Lrrk2* results in significant amplification of IL-10 expression by macrophages (Figure 8).

Thus, it seems that the context is important for LRRK2 in immunological responses and perhaps unsurprisingly, responses may differ between mutations, species and nature of the stimuli.

We observed that while the expression of pro-inflammatory (IL-1β and TNF-α) cytokines, in response to *Lm-EGD* infection, increased in *Lrrk2*^{G2019S} mutant BMDMs, there were no differences in their expression by infected *Lrrk2*-deficient BMDMs. In our studies, *Lrrk2*^{G2019S} mutant macrophages also increased IL-10 expression, while *Lrrk*2- deficient BMDMs reduced its secretion in response to *Lm-EGD*.

However, we found that *Lrrk2*-deficient BMDMs highly expressed IL-12 compared to WT cells, possibly due to the reduced expression of the anti-inflammatory effect of IL-10.

All in all, our data implicate the role of *Lrrk2* mutations in increasing the expression of pro- and anti-inflammatory cytokines.

7.3.1. The role of LRRK2 in NF-κB and MAPK inflammatory signaling pathways in response to *Lm-EGD*.

Previous studies have indicated the role of LRRK2 in numerous pathways, including transcription, mitochondrial function and neurotransmitter release (Cirnaru et al., 2014; Singh et al., 2019). In the context of immune cells; however, immune signaling pathways are still elusive.

In the present study, we explored the role of LRRK2 in mediating two important cellular pathways: NF-κB and MAPK signaling pathway.

NF-κB signaling pathway is considered as one of the key mechanisms of innate immune signaling, in which LRRK2 has been implicated. A recent study revealed that microglia from *Lrrk2*- deficient mice exhibited a reduction in IL-1β and cyclooxygenase-2 expression resulting in a dampened inflammatory response upon LPS treatment (Russo *et al.*, 2015). It was also demonstrated that loss of LRRK2 or inhibition of its kinase activity resulted in the increased expression of the NF-κB inhibitory subunit p50, leading to an attenuated inflammatory response in microglia (Russo et al., 2015). Takagawa *et al*. (2018) conducted studies in transgenic mice over-expressing LRRK2 and showed that these mice exhibited more severe colitis induced by dextran sodium sulfate (DSS) than did littermate control animals. They also showed that colitis severity was driven by LRRK2 activation of NF-κB pathway components including TAK1 complex and tumor necrosis factor receptor-associated factor (TRAF6) in bone marrow-derived dendritic cells (BMDCs) (Takagawa et al., 2018). In addition, LRRK2 mutations including $Lrrk2^{G2019S}$ and $Lrrk2^{R1441C}$, have been recently shown to stimulate IL-1β-mediated inflammatory signaling through phosphorylation of RCAN1, which is a protein inhibitor of calcineurin, the main activator of nuclear factor of activated T-cells (NFAT), leading to the increased transcriptional activity of NF-κB and IL-8 production (Han et al., 2017). There is also evidence that *Lrrk2* deficiency attenuates LPS-induced mRNA and/or protein expression of inducible TNF-a, IL-1β and IL-6 in brain microglia (Kim et al., 2012a). They also demonstrated that the reduced transcriptional activity of NF-kB resulted from the increased binding of the inhibitory NF-kB homodimer p50/p50 to DNA in murine microglia (Kim et al., 2012b).

In our case, we observed that *Lrrk2*^{G2019S} had a marginal impact on the expression of total NF-κB, p65 and subsequent activated forms (Figure 18). We, therefore, assume that *Lrrk2*^{G2019S} mutation might be enhancing the inflammatory cytokines through the other inflammatory signaling pathways.

The MAPK signaling pathway is another important signaling pathway which was the first to be investigated as potentially relating to LRRK2.

MAPK pathway comprises of three proteins situated in a cascade, with different subtypes leading to the activation of different effectors involved in a range of functions, such as apoptosis and inflammation.

We observed that *Lrrk2*^{G2019S} mutation enhanced the phosphorylation of p38 (activated p38) in response to *Lm-EGD* infection (Figure 19). Inhibition of p38, reduced the production of TNF-α and IL-1β by the mutant cells to the levels observed in WT cells (Figure 20). This suggests that *Lrrk2*^{G2019S} might be regulating the production of pro-inflammatory cytokines via increased activation of p38 MAPK.

Moreover, the levels of both phosphorylated and total ERK1/2 were significantly enhanced in response to *Lm-EGD* infection (Figure 19). Inhibition of ERK1/2 regulated IL-10 secretion suggesting that *Lrrk2*^{G2019S} might be controlling IL-10 production through ERK1/2 (Figure 21).

However, we did not observe any difference in the levels of phosphorylated and total forms of JNK in WT and *Lrrk2*^{G2019S} mutant macrophages (Figure 19).

Hsu. *et al*. (2010) found that LRRK2 binds and phosphorylates MAPK kinases including MKK3, 6, and 7. It has been shown that LRRK2 interacts with and phosphorylates MAPK kinases MKK3/6 and MKK4/7 and consequently activates the ERK and p38 MAPK pathways (Yoon *et al*., 2017).

They also found that the PD-linked *Lrrk2* mutations including *G2019S* and *R1441C* enhance the binding of LRRK2 to MKK6 (Hsu *et al*., 2010). Chen *et al*. (2012) also suggested that mutant $Lrrk2^{G2019S}$ activates MKK4-JNK-c-Jun pathway in the substantia nigra and causes the resulting degeneration of dopaminergic neurons in PD transgenic mice (Chen et al., 2012). While these results showed the association between *Lrrk2* and MAPK pathway activation in neurons, their interplay in immune cells requires further investigation.

It has been recently demonstrated that *Lrrk2* deletion also attenuated Manganese (Mn)- induced production of reactive oxygen species (ROS) and the pro-inflammatory cytokine TNF-α (Kim et al., 2019). Mn-induced phosphorylation of p38MAPK and ERK signaling proteins were significantly attenuated in *Lrrk2*- deficient macrophages. These results indicate that the LRRK2-mediated- p38 MAPK and ERK signaling pathways play an important role in regulating Mn-induced toxicity in immune cells, while affecting their functions, such as oxidative stress, inflammation and apoptosis (Kim et al., 2019). Because $Lrrk2^{G2019S}$ enhances the kinase activity, and LRRK2 kinase is involved in Mn-activated p38, it can be interpreted that $Lrrk2^{G2019S}$ functions through p38 MAPK for controlling the inflammation (Kim et al., 2019).

Other studies also reported that the activation of p38 is involved in $Lrrk2^{G2019S}$-induced inflammation, potentially implicating that *G2019S* mutation induced LRRK2 kinase activity through p38 MAPK (Kim et al., 2012b). For instance, *G2019S* mutation in *Lrrk2* increased basal and LPS-induced levels of phosphorylated p38 and JNK, whereas other pathologic mutations did not show any changes (Kim et al., 2012b). Similarly, the levels of phosphorylated p38 (P-p38) were specifically attenuated in *Lrrk2* knock down microglia cells after LPS treatment compared to control cells, while the levels of p-ERK and p-JNK were not different (Kim et al., 2012b). These results are supportive of our data which displayed that p38 MAPK can be considered as one of the

main pathways that is enhanced by *Lrrk2*^{G2019S} in response to *Lm-EGD* infection. Nonetheless, these data demonstrate that the MAPK signaling pathway and LRRK2 function in similar biological pathways and support a role for LRRK2 in modulating the cellular stress response via this inflammatory signaling pathway.

Since p38 MAPK seems to be one of the important pathways modulated by *Lrrk2* ^{G2019S}, we decided to evaluate one of its important mediators in downstream and upstream cascades. It has been shown that (MAPKAPK2 or MK2), a downstream substrate of the p38 MAPK influences crucial signaling events, regulates inflammatory cytokines, transcript stability and critical cellular processes in response to diverse extracellular stimuli (Soni et al., 2019). MK2 is an essential component of the inflammatory response as it regulates the biosynthesis of TNF-α at the post-transcriptional level (Kotlyarov *et al*., 1999). However; we were not able to find any difference in the expression of MK2 in *Lrrk2* ^{G2019S} and WT BMDMs in response to *Lm-EGD* by western blotting (Figure 22). It should be noted that we have not found any study regarding LRRK2-MK2 association so far.

However, *Lrrk2*^{G2019S} mutant macrophages expressed more activated TAK1, an upstream mediator of p38 MAPK, in response to *Lm-EGD* (Figure 22). In agreement with this observation, it has been shown that TAK1 activity was significantly enhanced by LRRK2 after IL-1β stimulation (Han *et al.*, 2017). TAK1 is considered to be a central component of NF-κB and MAPK signaling pathways (Wang et al., 2001). Its activation is triggered by diverse stimuli including proinflammatory cytokines such as IL-1,TNF, and toll like receptor (TLR) or node like receptors (NLR) ligands and culminates in the downstream activation of NF-κB and MAPK signaling pathways including p38, JNK, and ERK (Ajibade et al., 2013).

8. Conclusion

Research over the last decade has increased the understanding of the pathophysiological role of LRRK2 in diseases and supports its role in inflammation and immune cell function. We present some novel insights into the impact of *Lrrk2*^{G2019S} mutation on the innate immune response to *Listeria monocytogenes (L. monocytogenes)*. We found that *Lrrk2*^{G2019S} mutant mice controlled *L. monocytogenes* better than WT mice. A similar trend was observed in the brain.

The mechanism behind the better control of *L. monocytogenes* by the *G2019S* mutation of LRRK2 was investigated in BMDMs following *in vitro* infection with *L. monocytogenes*. Interestingly, we found that *Lrrk2*^{G2019S} mutation enhances the production of TNF-α, IL-1β and IL-10 in infected BMDMs. The impact on TNF-α and IL-1β was specifically due to the *G2019S* mutation of *Lrrk2* since there was no impact on the expression of these cytokines in *Lrrk2* knockout macrophages. I observed that the *G2019S* mutation of *Lrrk2* enhances MAPK signaling (TAK1, P38 and ERK). Modulation of the expression of the pro-inflammatory cytokines, TNF-α and IL-1β by *G2019S* mutation of *Lrrk2* occurred via P38 MAPK activation. The impact on IL-10 expression occurred through increased ERK activation by the *G2019S* mutation of *Lrrk2*.

I did not observe any impact of *G2019S* mutation of *Lrrk2* on the activation of NF-κB and JNK MAPK and MK2 pathway. I found that *Lrrk2*^{G2019S} mutant BMDMs enhanced inflammasome activation in response to *L. monocytogenes*. I observed that inflammasome signaling in response to *L. monocytogenes* is mainly mediated by AIM2 and partly by NLRP3, and is dependent on activation of caspase-1. I found that *Lrrk2*^{G2019S} mutation enhanced the expression of NLRP3 and caspase-1.

Finally, I found that the expression of reactive oxygen species (ROS) following infection with *L. monocytogenes* was significantly augmented by *G2019S* mutation of *Lrrk2*, and this can be an important mechanism that promotes the enhanced clearance of the bacterium *in vivo*.

Overall, these results present new insights into the signaling mechanisms through which the *G2019S* mutation of *Lrrk2* augments innate immune response which leads to better control of infection. Since the *G2019S* mutation has been observed in a cohort of Parkinson's disease patients, it is conceivable that this mutation can function as a susceptible gene to augment the inflammatory response in PD.

REFERENCES

1. Ajibade, A.A., Wang, H.Y., and Wang, R.-F. (2013). Cell type-specific function of TAK1 in innate immune signaling. Trends Immunol. *34*.
2. Amin, P., Florez, M., Najafov, A., Pan, H., Geng, J., Ofengeim, D., Dziedzic, S.A., Wang, H., Barrett, V.J., Ito, Y., et al. (2018). Regulation of a distinct activated RIPK1 intermediate bridging complex I and complex II in TNFα-mediated apoptosis. Proc. Natl. Acad. Sci. U. S. A. *115*, E5944–E5953.
3. Angeles, D.C., Gan, B.-H., Onstead, L., Zhao, Y., Lim, K.-L., Dachsel, J., Melrose, H., Farrer, M., Wszolek, Z.K., Dickson, D.W., et al. (2011). Mutations in *LRRK2* increase phosphorylation of peroxiredoxin 3 exacerbating oxidative stress-induced neuronal death. Hum. Mutat. *32*, 1390–1397.
4. Bachstetter, A.D., and Van Eldik, L.J. (2010). The p38 map kinase family as regulators of proinflammatory cytokine production in degenerative diseases of the CNS. Aging Dis. *1*, 199–211.
5. Bauernfeind, F.G., Horvath, G., Stutz, A., Alnemri, E.S., MacDonald, K., Speert, D., Fernandes-Alnemri, T., Wu, J., Monks, B.G., Fitzgerald, K.A., et al. (2009). Cutting Edge: NF-κB Activating Pattern Recognition and Cytokine Receptors License NLRP3 Inflammasome Activation by Regulating NLRP3 Expression. J. Immunol. *183*, 787–791.
6. Bécavin, C., Bouchier, C., Lechat, P., Archambaud, C., Creno, S., Gouin, E., Wu, Z., Kühbacher, A., Brisse, S., Graciela Pucciarelli, M., et al. (2014). Comparison of widely used Listeria monocytogenes strains EGD, 10403S, and EGD-e highlights genomic differences underlying variations in pathogenicity. MBio *5*.
7. Bergsbaken, T., Fink, S.L., and Cookson, B.T. (2009). Pyroptosis: Host cell death and inflammation. Nat. Rev. Microbiol. *7*, 99–109.
8. Biskup, S., Moore, D.J., Rea, A., Lorenz-Deperieux, B., Coombes, C.E., Dawson, V.L., Dawson, T.M., and West, A.B. (2007). Dynamic and redundant regulation of LRRK2 and LRRK1 expression. BMC Neurosci. *8*, 102.
9. Brodacki, B., Staszewski, J., Toczyłowska, B., Kozłowska, E., Drela, N., Chalimoniuk, M., and Stepien, A. (2008). Serum interleukin (IL-2, IL-10, IL-6, IL-4), TNFα, and INFγ concentrations are elevated in patients with atypical and idiopathic parkinsonism. Neurosci. Lett. *441*, 158–162.
10. Broz, P., and Dixit, V.M. (2016). Inflammasomes: Mechanism of assembly, regulation and signalling. Nat. Rev. Immunol. *16*, 407–420.
11. Broz, P., Ruby, T., Belhocine, K., Bouley, D.M., Kayagaki, N., Dixit, V.M., and Monack, D.M. Caspase-11 increases susceptibility to Salmonella infection in the absence of caspase-1.
12. Brugger, F., Erro, R., Balint, B., Kägi, G., Barone, P., and Bhatia, K.P. (2015). Why is there motor deterioration in Parkinson's disease during systemic infections-a hypothetical view. Npj Park. Dis. *1*, 1–5.
13. Carter, A.B., Monick, M.M., and Hunninghake, G.W. (1999). Both Erk and p38 kinases are necessary for cytokine gene transcription. Am. J. Respir. Cell Mol. Biol. *20*, 751–758.
14. Casson, C.N., and Shin, S. (2013). Inflammasome-mediated cell death in response to bacterial pathogens that access the host cell cytosol: Lessons from Legionella pneumophila. Front. Cell. Infect. Microbiol. *3*, 111.
15. Cervantes, J., Nagata, T., Uchijima, M., Shibata, K., and Koide, Y. (2008). Intracytosolic

Listeria monocytogenes induces cell death through caspase-1 activation in murine macrophages. Cell. Microbiol. *10*, 41–52.
16. Chen, C.Y., Weng, Y.H., Chien, K.Y., Lin, K.J., Yeh, T.H., Cheng, Y.P., Lu, C.S., and Wang, H.L. (2012). (G2019S) LRRK2 activates MKK4-JNK pathway and causes degeneration of SN dopaminergic neurons in a transgenic mouse model of PD. Cell Death Differ. *19*, 1623–1633.
17. Chen, G. wei, Wu, M., Liu, W. kang, Xie, M. man, Zhang, W. sheng, Fan, E. guo, and Liu, Q. (2018). Reactive oxygen species inhibits Listeria monocytogenes invasion into HepG2 epithelial cells. Food Sci. Nutr. *6*, 1501–1507.
18. Choubey, D., Walter, S., Geng, Y., and Xin, H. (2000). Cytoplasmic localization of the interferon-inducible protein that is encoded by the AIM2 (absent in melanoma) gene from the 200-gene family. FEBS Lett. *474*, 38–42.
19. Christofferson, D.E., Li, Y., Hitomi, J., Zhou, W., Upperman, C., Zhu, H., Gerber, S.A., Gygi, S., and Yuan, J. (2012). A novel role for RIP1 kinase in mediating TNFα production. Cell Death Dis. *3*, 320.
20. Cintia Ferrari, C., Clara Pott Godoy, M., Tarelli, R., Chertoff, M., Mara Depino, A., and Juan Pitossi, F. (2006). Progressive neurodegeneration and motor disabilities induced by chronic expression of IL-1β in the substantia nigra.
21. Cirnaru, M.D., Marte, A., Belluzzi, E., Russo, I., Gabrielli, M., Longo, F., Arcuri, L., Murru, L., Bubacco, L., Matteoli, M., et al. (2014). LRRK2 kinase activity regulates synaptic vesicle trafficking and neurotransmitter release through modulation of LRRK2 macro-molecular complex. Front. Mol. Neurosci. *7*.
22. Coll, R.C., Robertson, A.A.B., Chae, J.J., Higgins, S.C., Muñoz-Planillo, R., Inserra, M.C., Vetter, I., Dungan, L.S., Monks, B.G., Stutz, A., et al. (2015). A small-molecule inhibitor of the NLRP3 inflammasome for the treatment of inflammatory diseases. Nat. Med. *21*, 248–257.
23. Cuenda, A., and Rousseau, S. (2007). p38 MAP-Kinases pathway regulation, function and role in human diseases. Biochim. Biophys. Acta - Mol. Cell Res. *1773*, 1358–1375.
24. David, T., Ling, S.F., and Barton, A. (2018). Genetics of immune-mediated inflammatory diseases. Clin. Exp. Immunol. *193*, 3–12.
25. Degterev, A., Ofengeim, D., and Yuan, J. (2019). Targeting RIPK1 for the treatment of human diseases. Proc. Natl. Acad. Sci. U. S. A. *116*, 9714–9722.
26. Deng, H., Wang, P., and Jankovic, J. (2018). The genetics of Parkinson disease.
27. DeYoung, K.L., Ray, M.E., Su, Y.A., Anzick, S.L., Johnstone, R.W., Trapani, J.A., Meltzer, P.S., and Trent, J.M. (1997). Cloning a novel member of the human interferon-inducible gene family associated with control of tumorigenicity in a model of human melanoma. Oncogene *15*, 453–457.
28. Dinner, S., Kaltschmidt, J., Stump-Guthier, C., Hetjens, S., Ishikawa, H., Tenenbaum, T., Schroten, H., and Schwerk, C. (2017). Mitogen-activated protein kinases are required for effective infection of human choroid plexus epithelial cells by Listeria monocytogenes. Microbes Infect. *19*, 18–33.
29. Dramsi, S., and Cossart, P. (2002). Listeriolysin O: A genuine cytolysin optimized for an intracellular parasite. J. Cell Biol. *156*, 943–946.
30. Drevets, D.A., and Bronze, M.S. (2008). Listeria monocytogenes: Epidemiology, human disease, and mechanisms of brain invasion. FEMS Immunol. Med. Microbiol. *53*, 151–165.

31. Duncan, J.A., and Canna, S.W. (2018). The NLRC4 Inflammasome ORIGINS NLRC4 was originally described by Poyet and colleagues as a pro-apoptotic protein. Searching for structural homologues of APAF1: a protein known to activate apoptotic caspases in response to cytosolic cytochrome c, and containing a Caspase-Activation and Recruitment Domain (CARD) and ATP-binding site 2 , they identified a protein capable of HHS Public Access. Immunol Rev *281*, 115–123.
32. Duque, G.A., and Descoteaux, A. (2014). Macrophage cytokines: Involvement in immunity and infectious diseases. Front. Immunol. *5*.
33. Dzamko, N.L. (2017). LRRK2 and the immune system. In Advances in Neurobiology, (Springer New York LLC), pp. 123–143.
34. Dzamko, N., Inesta-Vaquera, F., Zhang, J., Xie, C., Cai, H., Arthur, S., Tan, L., Choi, H., Gray, N., Cohen, P., et al. (2012). The IkappaB kinase family phosphorylates the Parkinson's disease kinase LRRK2 at Ser935 and Ser910 during Toll-Like Receptor signaling. PLoS One *7*.
35. Dzamko, N., Rowe, D.B., and Halliday, G.M. (2016). Increased peripheral inflammation in asymptomatic leucine-rich repeat kinase 2 mutation carriers. Mov. Disord. *31*, 889–897.
36. Eitel, J., Suttorp, N., and Opitz, B. (2011). Innate Immune Recognition and Inflammasome Activation in Listeria Monocytogenes Infection. Front. Microbiol. *1*, 149.
37. Fava, V., Orlova, M., Cobat, A., Alcaïs, A., Mira, M., and Schurr, E. (2012). Genetics of leprosy reactions: An overview. Mem. Inst. Oswaldo Cruz *107*, 132–142.
38. Fernandes-Alnemri, T., Yu, J.-W., Wu, J., Datta, P., and Alnemri, E.S. (2009). AIM2 activates the inflammasome and cell death in response to cytoplasmic DNA HHS Public Access. Nature *458*, 509–513.
39. Franchi, L., Eigenbrod, T., Muñoz-Planillo, R., and Nuñez, G. (2009). The inflammasome: A caspase-1-activation platform that regulates immune responses and disease pathogenesis. Nat. Immunol. *10*, 241–247.
40. Funayama, M., Hasegawa, K., Kowa, H., Saito, M., Tsuji, S., and Obata, F. (2002). A new locus for Parkinson's Disease (PARK8) maps to chromosome 12p11.2-q13.1. Ann. Neurol. *51*, 296–301.
41. Furuya, T., Hayakawa, H., Yamada, M., Yoshimi, K., Hisahara, S., Miura, M., Mizuno, Y., and Mochizuki, H. (2004). Neurobiology of Disease Caspase-11 Mediates Inflammatory Dopaminergic Cell Death in the 1-Methyl-4-Phenyl-1,2,3,6-Tetrahydropyridine Mouse Model of Parkinson's Disease.
42. Gage, G.J., Kipke, D.R., and Shain, W. (2012). Whole Animal Perfusion Fixation for Rodents. J. Vis. Exp 3564.
43. Gelders, G., Baekelandt, V., and Perren, A. Van der (2018). Linking Neuroinflammation and Neurodegeneration in Parkinson's Disease. J. Immunol. Res. *2018*.
44. Ghosh, R., Gilda, J.E., and Gomes, A. V. (2014). The necessity of and strategies for improving confidence in the accuracy of western blots. Expert Rev. Proteomics *11*, 549–560.
45. Giridharan, S., and Srinivasan, M. (2018). Mechanisms of NF-κB p65 and strategies for therapeutic manipulation. J. Inflamm. Res. *11*, 407–419.
46. Goetz, C.G. (2011). The history of Parkinson's disease: Early clinical descriptions and neurological therapies. Cold Spring Harb. Perspect. Med. *1*.
47. Gordon, R., Albornoz, E.A., Christie, D.C., Langley, M.R., Kumar, V., Manotovani, S.,

Robertson, A.A.B., Butler, M.S., Rowe, D.B., O'neill, L.A., et al. (2018). Inflammasome inhibition prevents α-synuclein pathology and dopaminergic neurodegeneration in mice HHS Public Access. Sci Transl Med *10*.
48. Greggio, E. (2012). Role of LRRK2 kinase activity in the pathogenesis of Parkinson's disease. Biochem. Soc. Trans. *40*, 1058–1062.
49. Gründling, A., Burrack, L.S., Bouwer, H.G.A., and Higgins, D.E. (2004). Listeria monocytogenes regulates flagellar motility gene expression through MogR, a transcriptional repressor required for virulence. Proc. Natl. Acad. Sci. U. S. A. *101*, 12318–12323.
50. Hakimi, M., Selvanantham, T., Swinton, E., Padmore, R.F., Tong, Y., Kabbach, G., Venderova, K., Girardin, S.E., Bulman, D.E., Scherzer, C.R., et al. (2011). Parkinson's disease-linked LRRK2 is expressed in circulating and tissue immune cells and upregulated following recognition of microbial structures. J. Neural Transm. *118*, 795–808.
51. Hamon, M.A., and Cossart, P. (2011). K Efflux Is Required for Histone H3 Dephosphorylation by Listeria monocytogenes Listeriolysin O and Other Pore-Forming Toxins. Infect. Immun. *79*, 2839–2846.
52. Han, K.A., Yoo, L., Sung, J.Y., Chung, S.A., Um, J.W., Kim, H., Seol, W., and Chung, K.C. (2017). Leucine-rich repeat kinase 2 (LRRK2) stimulates IL-1β-mediated inflammatory signaling through phosphorylation of RCAN1. Front. Cell. Neurosci. *11*.
53. Hara, H., Tsuchiya, K., Nomura, T., Kawamura, I., Shoma, S., and Mitsuyama, M. (2008). Dependency of Caspase-1 Activation Induced in Macrophages by Listeria monocytogenes on Cytolysin, Listeriolysin O, after Evasion from Phagosome into the Cytoplasm . J. Immunol. *180*, 7859–7868.
54. Hara, H., Seregin, S.S., Yang, D., Fukase, K., Chamaillard, M., Alnemri, E.S., Inohara, N., Chen, G.Y., and Núñez, G. (2018). The NLRP6 inflammasome recognizes lipoteichoic acid and regulates Gram-positive pathogen infection HHS Public Access. Cell *175*, 1651–1664.
55. Härtlova, A., Herbst, S., Peltier, J., Rodgers, A., Bilkei-Gorzo, O., Fearns, A., Dill, B.D., Lee, H., Flynn, R., Cowley, S.A., et al. (2018). LRRK2 is a negative regulator of Mycobacterium tuberculosis phagosome maturation in macrophages . EMBO J. *37*.
56. Hartmann, A. (2004). Postmortem studies in Parkinson's disease. Dialogues Clin. Neurosci. *6*, 281–293.
57. Harvey, K., and Outeiro, T.F. (2019). The role of LRRK2 in cell signalling.
58. Hauf, N., Goebel,', W., Serfling, E., and Kuhn', M. (1994). Listeria monocytogenes Infection Enhances Transcription Factor NF-KB in P388D1 Macrophage-Like Cells.
59. Hauf, N., Goebel, W., Fiedler, F., Sokolovic, Z., and Kuhn, M. (1997). Listeria monocytogenes infection of P388D1 macrophages results in a biphasic NF-κB (RelA/p50) activation induced by lipoteichoic acid and bacterial phospholipases and mediated by IκBα and IκBβ degradation. Proc. Natl. Acad. Sci. U. S. A. *94*, 9394–9399.
60. Healy, D.G., Falchi, M., O'Sullivan, S.S., Bonifati, V., Durr, A., Bressman, S., Brice, A., Aasly, J., Zabetian, C.P., Goldwurm, S., et al. (2008). Phenotype, genotype, and worldwide genetic penetrance of LRRK2-associated Parkinson's disease: a case-control study. Lancet Neurol. *7*, 583–590.
61. Heo, H.Y., Park, J.M., Kim, C.H., Han, B.S., Kim, K.S., and Seol, W. (2010). LRRK2 enhances oxidative stress-induced neurotoxicity via its kinase activity. Exp. Cell Res.

316, 649–656.
62. Herzig, M.C., Kolly, C., Persohn, E., Theil, D., Schweizer, T., Hafner, T., Stemmelen, C., Troxler, T.J., Schmid, P., Danner, S., et al. (2011). LRRK2 protein levels are determined by kinase function and are crucial for kidney and lung homeostasis in mice. Hum. Mol. Genet. *20*, 4209–4223.
63. Horton, A.A., Wang, B., Camp, L., Price, M.S., Arshi, A., Nagy, M., Nadler, S.A., Faeder, J.R., and Luckhart, S. (2011). The mitogen-activated protein kinome from Anopheles gambiae: Identification, phylogeny and functional characterization of the ERK, JNK and p38 MAP kinases. BMC Genomics *12*, 574–574.
64. Hsu, C.H., Chan, D., Greggio, E., Saha, S., Guillily, M.D., Ferree, A., Raghavan, K., Shen, G.C., Segal, L., Ryu, H., et al. (2010). MKK6 binds and regulates expression of Parkinson's disease-related protein LRRK2. J. Neurochem. *112*, 1593–1604.
65. Huang, G., Shi, L.Z., and Chi, H. (2009). Regulation of JNK and p38 MAPK in the immune system: Signal integration, propagation and termination. Cytokine *48*, 161–169.
66. Huang, X., Feng, Y., Xiong, G., Whyte, S., Duan, J., Yang, Y., Wang, K., Yang, S., Geng, Y., Ou, Y., et al. (2019). Caspase-11, a specific sensor for intracellular lipopolysaccharide recognition, mediates the non-canonical inflammatory pathway of pyroptosis. Cell Biosci. *9*, 1–11.
67. Hui, K.Y., Fernandez-Hernandez, H., Hu, J., Schaffner, A., Pankratz, N., Hsu, N.-Y., Chuang, L.-S., Carmi, S., Villaverde, N., Li, X., et al. (2018). Functional variants in the LRRK2 gene confer shared effects on risk for Crohn's disease and Parkinson's disease. Sci. Transl. Med. *10*.
68. Jaco, I., Annibaldi, A., Lalaoui, N., Wilson, R., Tenev, T., Laurien, L., Kim, C., Jamal, K., Wicky John, S., Liccardi, G., et al. (2017). MK2 Phosphorylates RIPK1 to Prevent TNF-Induced Cell Death. Mol. Cell *66*, 698-710.e5.
69. Joseph, J., Ametepe, E.S., Haribabu, N., Agbayani, G., Krishnan, L., Blais, A., and Sad, S. (2016). Inhibition of ROS and upregulation of inflammatory cytokines by FoxO3a promotes survival against Salmonella typhimurium. Nat. Commun. *7*, 12748.
70. Kalia, L. V., and Lang, A.E. (2015). Parkinson's disease. Lancet *386*, 896–912.
71. Kang, U.-B., and Marto, J.A. (2017). Leucine-rich repeat kinase 2 and Parkinson's disease. Proteomics *17*, 1600092.
72. Kang, Y.J., Chen, J., Otsuka, M., Mols, J., Ren, S., Wang, Y., and Han, J. (2008). Macrophage Deletion of p38α Partially Impairs Lipopolysaccharide-Induced Cellular Activation. J. Immunol. *180*, 5075–5082.
73. Kaya, S., Lilienbaum, A., Join-Lambert, O., Li, X., Israël, A., and Berche, P. (2002). Listeriolysin O secreted by Listeria monocytogenes induces NF-κB signalling by activating the IκB kinase complex. Mol. Microbiol. *44*, 1407–1419.
74. Kayagaki, N., Warming, S., Lamkanfi, M., Walle, L. Vande, Louie, S., Dong, J., Newton, K., Qu, Y., Liu, J., Heldens, S., et al. (2011). Non-canonical inflammasome activation targets caspase-11. Nature *479*, 117–121.
75. Kayagaki, N., Wong, M.T., Stowe, I.B., Ramani, S.R., Gonzalez, L.C., Akashi-Takamura, S., Miyake, K., Zhang, J., Lee, W.P., Muszyński, A., et al. (2013). Noncanonical inflammasome activation by intracellular LPS independent of TLR4. Science (80-.). *341*, 1246–1249.
76. Keshet, Y., and Seger, R. (2010). The MAP kinase signaling cascades: a system of hundreds of components regulates a diverse array of physiological functions. Methods

Mol. Biol. *661*, 3–38.
77. Kim, B., Yang, M.-S., Choi, D., Kim, J.-H., Kim, H.-S., Seol, W., Choi, S., Jou, I., Kim, E.-Y., and Joe, E. (2012a). Impaired Inflammatory Responses in Murine Lrrk2-Knockdown Brain Microglia. PLoS One *7*, e34693.
78. Kim, B., Yang, M.-S., Choi, D., Kim, J.-H., and Kim, H.-S. (2012b). Impaired Inflammatory Responses in Murine Lrrk2-Knockdown Brain Microglia. PLoS One *7*, 34693.
79. Kim, J., Pajarillo, E., Rizor, A., Son, D.S., Lee, J., Aschner, M., and Lee, E. (2019). LRRK2 kinase plays a critical role in manganese-induced inflammation and apoptosis in microglia. PLoS One *14*.
80. Kim, S., Bauernfeind, F., Ablasser, A., Hartmann, G., Fitzgerald, K.A., Latz, E., and Hornung, V. (2010). Listeria monocytogenes is sensed by the NLRP3 and AIM2 inflammasome. Eur. J. Immunol. *40*, 1545–1551.
81. Klein, C., and Schlossmacher, M.G. (2006). The genetics of Parkinson disease: Implications for neurological care. Nat. Clin. Pract. Neurol. *2*, 136–146.
82. Kluss, J.H., Mamais, A., and Cookson, M.R. (2019). LRRK2 links genetic and sporadic Parkinson's disease. Biochem. Soc. Trans. *47*, 651–661.
83. Kotlyarov, A., Neininger, A., Schubert, C., Eckert, R., Birchmeier, C., Volk, H.D., and Gaestel, M. (1999). MAPKAP kinase 2 is essential for LPS-induced TNF-α biosynthesis. Nat. Cell Biol. *1*, 94–97.
84. Kouli, A., Torsney, K.M., and Kuan, W.-L. (2018). Parkinson's Disease: Etiology, Neuropathology, and Pathogenesis. In Parkinson's Disease: Pathogenesis and Clinical Aspects, (Codon Publications), pp. 3–26.
85. Kreutzberg, G.W. (1996). Microglia: A sensor for pathological events in the CNS. Trends Neurosci. *19*, 312–318.
86. Lacy, P., and Stow, J.L. (2011). Cytokine release from innate immune cells: Association with diverse membrane trafficking pathways. Blood *118*, 9–18.
87. Lage, S.L., Longo, C., Branco, L.M., da Costa, T.B., Buzzo, C. de L., and Bortoluci, K.R. (2014). Emerging concepts about NAIP/NLRC4 inflammasomes. Front. Immunol. *5*.
88. Lamkanfi, M., and Dixit, V.M. (2014). Leading Edge Review Mechanisms and Functions of Inflammasomes. Cell *157*, 1013–1022.
89. Laurien, L., Nagata, M., Schünke, H., Delanghe, T., Wiederstein, J.L., Kumari, S., Schwarzer, R., Corona, T., Krüger, M., Bertrand, M.J.M., et al. (2020). Autophosphorylation at serine 166 regulates RIP kinase 1-mediated cell death and inflammation. Nat. Commun. *11*, 1–16.
90. Lee, J., Hur, J., Lee, P., Kim, J.Y., Cho, N., Kim, S.Y., Kim, H., Lee, M.-S., and Suk, K. (2001). Dual Role of Inflammatory Stimuli in Activation-induced Cell Death of Mouse Microglial Cells INITIATION OF TWO SEPARATE APOPTOTIC PATHWAYS VIA INDUCTION OF INTERFERON REGULATORY FACTOR-1 AND CASPASE-11*.
91. Li, P., Allen, H., Banerjee, S., Franklin, S., Herzog, L., Johnston, C., Mcdowell, J., Paskind, M., Rodman, L., Salfeld, J., et al. (1995). Mice Deficient in IL-lp-Converting Enzyme Are Defective in Production of Mature IL-lp and Resistant to Endotoxic Shock.
92. Liu, T., Zhang, L., Joo, D., and Sun, S.C. (2017a). NF-κB signaling in inflammation. Signal Transduct. Target. Ther. *2*, 1–9.
93. Liu, W., Liu, X., Li, Y., Zhao, J., Liu, Z., Hu, Z., Wang, Y., Yao, Y., Miller, A.W., Su, B., et al. (2017b). LRRK2 promotes the activation of NLRC4 inflammasome during

Salmonella Typhimurium infection. J. Exp. Med. *214*, 3051–3066.
94. Liu, Z., Lee, J., Krummey, S., Lu, W., Cai, H., and Lenardo, M.J. (2011). The kinase LRRK2 is a regulator of the transcription factor NFAT that modulates the severity of inflammatory bowel disease. Nat. Immunol. *12*, 1063–1070.
95. Lu, N., and Malemud, C.J. (2019). Extracellular signal-regulated kinase: A regulator of cell growth, inflammation, chondrocyte and bone cell receptor-mediated gene expression. Int. J. Mol. Sci. *20*.
96. Lu, Y.C., Yeh, W.C., and Ohashi, P.S. (2008). LPS/TLR4 signal transduction pathway. Cytokine *42*, 145–151.
97. Lucas, M., Zhang, X., Prasanna, V., and Mosser, D.M. (2005). ERK Activation Following Macrophage FcγR Ligation Leads to Chromatin Modifications at the IL-10 Locus. J. Immunol. *175*, 469–477.
98. Lugrin, J., and Martinon, F. (2018). The AIM2 inflammasome: Sensor of pathogens and cellular perturbations. Immunol. Rev. *281*, 99–114.
99. Mahmood, T., and Yang, P.C. (2012). Western blot: Technique, theory, and trouble shooting. N. Am. J. Med. Sci. *4*, 429–434.
100. Maini, R.N., Elliott, M.J., Brennan, F.M., and Feldmann, M. (1995). Beneficial effects of tumour necrosis factor-alpha (TNF-α) blockade in rheumatoid arthritis (RA). Clin. Exp. Immunol. *101*, 207–212.
101. Malik, A., and Kanneganti, T.-D. (2017). Inflammasome activation and assembly at a glance. J. Cell Sci. *130*, 3955–3963.
102. Manzoni, C., Denny, P., Lovering, R.C., and Lewis, P.A. (2015). Computational analysis of the LRRK2 interactome. PeerJ *2015*.
103. Mariathasan, S., Newton, K., Monack, D.M., Vucic, D., French, D.M., Lee, W.P., Roose-Girma, M., Erickson, S., and Dixit, V.M. (2004). Differential activation of the inflammasome by caspase-1 adaptors ASC and Ipaf.
104. Mariathasan, S., Weiss, D.S., Newton, K., McBride, J., O'Rourke, K., Roose-Girma, M., Lee, W.P., Weinrauch, Y., Monack, D.M., and Dixit, V.M. (2006). Cryopyrin activates the inflammasome in response to toxins and ATP. Nature *440*, 228–232.
105. Martin, I., Kim, J.W., Dawson, V.L., and Dawson, T.M. (2014). LRRK2 pathobiology in Parkinson's disease. J. Neurochem. *131*, 554–565.
106. Mcdougal, C.E., and Sauer, J.-D. (2018). Listeria monocytogenes: The Impact of Cell Death on Infection and Immunity.
107. McDougal, C.E., and Sauer, J.D. (2018). Listeria monocytogenes: The impact of cell death on infection and immunity. Pathogens *7*, 8.
108. Meixenberger, K., Pache, F., Eitel, J., Schmeck, B., Hippenstiel, S., Slevogt, H., N'Guessan, P., Witzenrath, M., Netea, M.G., Chakraborty, T., et al. (2010). Listeria monocytogenes -Infected Human Peripheral Blood Mononuclear Cells Produce IL-1β, Depending on Listeriolysin O and NLRP3 . J. Immunol. *184*, 922–930.
109. Mihaly, S.R., Ninomiya-Tsuji, J., and Morioka, S. (2014). TAK1 control of cell death. Cell Death Differ. *21*, 1667–1676.
110. Mills, R.D., Mulhern, T.D., Liu, F., Culvenor, J.G., and Cheng, H.C. (2014). Prediction of the Repeat Domain Structures and Impact of Parkinsonism-Associated Variations on Structure and Function of all Functional Domains of Leucine-Rich Repeat Kinase 2 (LRRK2). Hum. Mutat. *35*, 395–412.
111. Ming Man, S., and Kanneganti, T.-D. (2015). Converging roles of caspases in

inflammasome activation, cell death and innate immunity. Nat. Publ. Gr.
112. Ming Man, S., Karki, R., Briard, B., Burton, A., Gingras, S., Pelletier, S., and Kanneganti, T.D. (2017). Differential roles of caspase-1 and caspase-11 in infection and inflammation. Sci. Rep. *7*, 1–11.
113. Moehle, M.S., Webber, P.J., Tse, T., Sukar, N., Standaert, D.G., Desilva, T.M., Cowell, R.M., and West, A.B. (2012). LRRK2 inhibition attenuates microglial inflammatory responses. J. Neurosci. *32*, 1602–1611.
114. Mogensen, T.H. (2009). Pathogen recognition and inflammatory signaling in innate immune defenses. Clin. Microbiol. Rev. *22*, 240–273.
115. Mogi, M., Harada, M., Kondo, T., Riederer, P., Inagaki, H., Minami, M., and Nagatsu E', T. (1994). Interleukin-lfl, interleukin-6, epidermal growth factor and transforming growth factor-are elevated in the brain from parkinsonian patients.
116. Morrison, D.K. (2012). MAP kinase pathways. Cold Spring Harb. Perspect. Biol. *4*.
117. Mosser, D.M., and Zhang, X. (2008). Interleukin-10: New perspectives on an old cytokine. Immunol. Rev. *226*, 205–218.
118. Muhammad, M. (2019). Tumor Necrosis Factor Alpha: A Major Cytokine of Brain Neuroinflammation. In Cytokines [Working Title], (IntechOpen), p.
119. Newman, M.A., Sundelin, T., Nielsen, J.T., and Erbs, G. (2013). MAMP (microbe-associated molecular pattern) triggered immunity in plants. Front. Plant Sci. *4*, 139.
120. Nguyen, B.N., Peterson, B.N., and Portnoy, D.A. (2019). Listeriolysin O: A phagosome-specific cytolysin revisited. Cell. Microbiol. *21*, e12988.
121. Oeckinghaus, A., and Ghosh, S. (2009). The NF-kappaB family of transcription factors and its regulation. Cold Spring Harb. Perspect. Biol. *1*.
122. Ono, K., and Han, J. (2000). The p38 signal transduction pathway Activation and function. Cell. Signal. *12*, 1–13.
123. Paiva, C.N., and Bozza, M.T. (2014). Are reactive oxygen species always detrimental to pathogens? Antioxidants Redox Signal. *20*, 1000–1034.
124. Pamer, E.G. (2004a). Immune responses to Listeria monocytogenes. Nat. Rev. Immunol. *4*, 812–823.
125. Pamer, E.G. (2004b). R E V I E W S IMMUNE RESPONSES TO LISTERIA MONOCYTOGENES.
126. Peter, I., Dubinsky, M., Bressman, S., Park, A., Lu, C., Chen, N., and Wang, A. (2018). Anti-tumor necrosis factor therapy and incidence of Parkinson disease among patients with inflammatory bowel disease. JAMA Neurol. *75*, 939–946.
127. Pitts, M.G., and D'Orazio, S.E.F. (2018). A comparison of oral and intravenous mouse models of listeriosis. Pathogens *7*.
128. Poewe, W., Seppi, K., Tanner, C.M., Halliday, G.M., Brundin, P., Volkmann, J., Schrag, A.E., and Lang, A.E. (2017). Parkinson disease. Nat. Rev. Dis. Prim. *3*, 1–21.
129. Qi, M., and Elion, E.A. (2005). MAP kinase pathways. J. Cell Sci. *118*, 3569–3572.
130. Rahim, S.S., Khan, N., Boddupalli, C.S., Hasnain, S.E., and Mukhopadhyay, S. (2005a). Interleukin-10 (IL-10) mediated suppression of IL-12 production in RAW 264.7 cells involves c-rel transcription factor. Immunology *114*, 313–321.
131. Rahim, S.S., Khan, N., Boddupalli, C.S., Hasnain, S.E., and Mukhopadhyay, S.

(2005b). Interleukin-10 (IL-10) mediated suppression of IL-12 production in RAW 264.7 cells involves c-rel transcription factor. Immunology *114*, 313–321.
132. Raingeaud, J., Gupta, S., Rogers, J.S., Dickens, M., Han, J., Ulevitch, R.J., and Davis, R.J. (1995). Pro-inflammatory cytokines and environmental stress cause p38 mitogen- activated protein kinase activation by dual phosphorylation on tyrosine and threonine. J. Biol. Chem. *270*, 7420–7426.
133. Raman, M., Chen, W., and Cobb, M.H. (2007). Differential regulation and properties of MAPKs. Oncogene *26*, 3100–3112.
134. Ramos-Junior, E.S., and Morandini, A.C. (2017). Gasdermin: A new player to the inflammasome game. Biomed. J. *40*, 313–316.
135. Ray Dorsey, E., Elbaz, A., Nichols, E., Abd-Allah, F., Abdelalim, A., Adsuar, J.C., Ansha, M.G., Brayne, C., Choi, J.Y.J., Collado-Mateo, D., et al. (2018). Global, regional, and national burden of Parkinson's disease, 1990–2016: a systematic analysis for the Global Burden of Disease Study 2016. Lancet Neurol. *17*, 939–953.
136. Rivas, M.A., Avila, B.E., Koskela, J., Huang, H., Stevens, C., Pirinen, M., Haritunians, T., Neale, B.M., Kurki, M., Ganna, A., et al. (2018). Insights into the genetic epidemiology of Crohn's and rare diseases in the Ashkenazi Jewish population. PLoS Genet. *14*, e1007329.
137. Rudenko, I.N., and Cookson, M.R. (2014). Heterogeneity of Leucine-Rich Repeat Kinase 2 Mutations: Genetics, Mechanisms and Therapeutic Implications. Neurotherapeutics *11*, 738–750.
138. Rudenko, I.N., Chia, R., and Cookson, M.R. (2012). Is inhibition of kinase activity the only therapeutic strategy for LRRK2-associated Parkinson's disease? BMC Med. *10*, 20.
139. Russo, I., Berti, G., Plotegher, N., Bernardo, G., Filograna, R., Bubacco, L., and Greggio, E. (2015). Leucine-rich repeat kinase 2 positively regulates inflammation and down-regulates NF-κB p50 signaling in cultured microglia cells. J. Neuroinflammation *12*, 230.
140. Sabio, G., and Davis, R.J. (2014). TNF and MAP kinase signaling pathways.
141. Sakamoto, S., Putalun, W., Vimolmangkang, S., Phoolcharoen, W., Shoyama, Y., Tanaka, H., and Morimoto, S. (2018). Enzyme-linked immunosorbent assay for the quantitative/qualitative analysis of plant secondary metabolites. J. Nat. Med. *72*, 32–42.
142. Sauer, J.D., Witte, C.E., Zemansky, J., Hanson, B., Lauer, P., and Portnoy, D.A. (2010). Listeria monocytogenes triggers AIM2-mediated pyroptosis upon infrequent bacteriolysis in the macrophage cytosol. Cell Host Microbe *7*, 412–419.
143. Sauer, J.D., Pereyre, S., Archer, K.A., Burke, T.P., Hanson, B., Lauer, P., and Portnoy, D.A. (2011). Listeria monocytogenes engineered to activate the Nlrc4 inflammasome are severely attenuated and are poor inducers of protective immunity. Proc. Natl. Acad. Sci. U. S. A. *108*, 12419–12424.
144. Scholarlycommons, S., and Reyes Ruiz, V.M. (2019). Investigating The Role Of The Human Naip/nlrc4 Inflammasome In Host Defense Against Gram-Negative Bacterial Infection.
145. Schroder, K., and Tschopp, J. (2010). The Inflammasomes. Cell *140*, 821–832.
146. Shi, J., Zhao, Y., Wang, Y., Gao, W., Ding, J., Li, P., Hu, L., and Shao, F. (2014). Inflammatory caspases are innate immune receptors for intracellular LPS. Nature *514*, 187–192.

147. Shi, J., Zhao, Y., Wang, K., Shi, X., Wang, Y., Huang, H., Zhuang, Y., Cai, T., Wang, F., and Shao, F. (2015). Cleavage of GSDMD by inflammatory caspases determines pyroptotic cell death. Nature *526*, 660–665.
148. Shin, .-I, Banning, U., Kim, Y.-M., Verheyen, J., Hannen, M., and Bönig & D Körholz, H. (1999). Interleukin 10 Inhibits TNF-Alpha Production in Human Monocytes Independently of Interleukin 12 and Interleukin 1 Beta. Immunol. Invest. *28*, 165–175.
149. Shutinoski, B., Alturki, N.A., Rijal, D., Bertin, J., Gough, P.J., Schlossmacher, M.G., and Sad, S. (2016). K45A mutation of RIPK1 results in poor necroptosis and cytokine signaling in macrophages, which impacts inflammatory responses in vivo. Cell Death Differ. *23*, 1628–1637.
150. Shutinoski, B., Hakimi, M., Harmsen, I.E., Lunn, M., Rocha, J., Lengacher, N., Zhou, Y.Y., Khan, J., Nguyen, A., Hake-Volling, Q., et al. (2019). Lrrk2 alleles modulate inflammation during microbial infection of mice in a sex-dependent manner. Sci. Transl. Med. *11*.
151. Silva, M.T. (2010). When two is better than one: macrophages and neutrophils work in concert in innate immunity as complementary and cooperative partners of a myeloid phagocyte system. J. Leukoc. Biol. *87*, 93–106.
152. Singh, A., Zhi, L., and Zhang, H. (2019). LRRK2 and mitochondria: Recent advances and current views. Brain Res. *1702*, 96–104.
153. Singleton, A.B., Farrer, M.J., and Bonifati, V. (2013). The genetics of Parkinson's disease: Progress and therapeutic implications. Mov. Disord. *28*, 14–23.
154. Solt, L.A., and May, M.J. (2008). The IκB kinase complex: Master regulator of NF-κB signaling. Immunol. Res. *42*, 3–18.
155. Soni, S., Anand, P., and Padwad, Y.S. (2019). MAPKAPK2: The master regulator of RNA-binding proteins modulates transcript stability and tumor progression. J. Exp. Clin. Cancer Res. *38*, 1–18.
156. Stojakovic, A., Paz-Filho, G., Arcos-Burgos, M., Licinio, J., Wong, M.L., and Mastronardi, C.A. (2017). Role of the IL-1 Pathway in Dopaminergic Neurodegeneration and Decreased Voluntary Movement. Mol. Neurobiol. *54*, 4486–4495.
157. Swaminathan, B., and Gerner-Smidt, P. (2007). The epidemiology of human listeriosis. Microbes Infect. *9*, 1236–1243.
158. Takagawa, T., Kitani, A., Fuss, I., Levine, B., Brant, S.R., Peter, I., Tajima, M., Nakamura, S., Strober, W., Transl, S., et al. (2018). An increase in LRRK2 suppresses autophagy and enhances Dectin-1-induced immunity in a mouse model of colitis HHS Public Access Author manuscript. Sci Transl Med *10*.
159. Takeuchi, O., and Akira, S. (2010). Pattern Recognition Receptors and Inflammation. Cell *140*, 805–820.
160. Tang, P., Sutherland, C.L., Gold, M.R., and Finlay, B.B. (1998). Listeria monocytogenes invasion of epithelial cells requires the MEK-1/ERK-2 mitogen-activated protein kinase pathway. Infect. Immun. *66*, 1106–1112.
161. Thaler, A., Ash, E., Gan-Or, Z., Orr-Urtreger, A., and Giladi, N. (2009). The LRRK2 G2019S mutation as the cause of Parkinson's disease in Ashkenazi Jews. J. Neural Transm. *116*, 1473–1482.
162. Theisen, E., and Sauer, J.D. (2016). Listeria monocytogenes and the inflammasome: From cytosolic bacteriolysis to tumor immunotherapy. Curr. Top. Microbiol. Immunol. *397*, 133–160.

163. Thornberry, N.A., Bull, H.G., Calaycay, J.R., Chapman, K.T., Howard, A.D., Kostura, M.J., Miller, D.K., Molineaux, S.M., Weidner, J.R., Aunins, J., et al. (1992). A novel heterodimeric cysteine protease is required for interleukin-1βprocessing in monocytes. Nature *356*, 768–774.
164. Tong, Y., Pisani, A., Martella, G., Karouani, M., Yamaguchi, H., Pothos, E.N., and Shen, J. (2009). R1441C mutation in LRRK2 impairs dopaminergic neurotransmission in mice. Proc. Natl. Acad. Sci. U. S. A. *106*, 14622–14627.
165. Torres, D., Barrier, M., Bihl, F., Quesniaux, V.J.F., Maillet, I., Akira, S., Ryffel, B., and Erard, F. (2004). Toll-Like Receptor 2 Is Required for Optimal Control of Listeria monocytogenes Infection. Infect. Immun. *72*, 2131–2139.
166. Través, P.G., de Atauri, P., Marín, S., Pimentel-Santillana, M., Rodríguez-Prados, J.-C., Marín de Mas, I., Selivanov, V.A., Martín-Sanz, P., Boscá, L., and Cascante, M. (2012). Relevance of the MEK/ERK Signaling Pathway in the Metabolism of Activated Macrophages: A Metabolomic Approach. J. Immunol. *188*, 1402–1410.
167. Tsuchiya, K., Hara, H., Kawamura, I., Nomura, T., Yamamoto, T., Daim, S., Dewamitta, S.R., Shen, Y., Fang, R., and Mitsuyama, M. (2010). Involvement of Absent in Melanoma 2 in Inflammasome Activation in Macrophages Infected with Listeria monocytogenes . J. Immunol. *185*, 1186–1195.
168. Valeria, M.R.R., Ramirez, J., Naseer, N., Palacio, N.M., Siddarthan, I.J., Yan, B.M., Boyer, M.A., Pensinger, D.A., Sauer, J.D., and Shin, S. (2017). Broad detection of bacterial type III secretion system and flagellin proteins by the human NAIP/NLRC4 inflammasome. Proc. Natl. Acad. Sci. U. S. A. *114*, 13242–13247.
169. Vignali, D.A.A., and Kuchroo, V.K. (2012). iL-12 family cytokines: immunological playmakers. Nat. Immunol. *13*.
170. Villumsen, M., Aznar, S., Pakkenberg, B., Jess, T., and Brudek, T. (2019). Inflammatory bowel disease Inflammatory bowel disease increases the risk of Parkinson's disease: a Danish nationwide cohort study 1977-2014. Gut *68*, 18–24.
171. Wahner, A.D., Sinsheimer, J.S., Bronstein, J.M., and Ritz, B. (2007). Inflammatory cytokine gene polymorphisms and increased risk of Parkinson disease. Arch. Neurol. *64*, 836–840.
172. Wallings, R.L., and Tansey, M.G. (2019). LRRK2 regulation of immune-pathways and inflammatory disease. Biochem. Soc. Trans. *47*, 1581–1595.
173. Wang, C., Deng, L., Hong, M., Akkaraju, G.R., Inoue, J.I., and Chen, Z.J. (2001). TAK1 is a ubiquitin-dependent kinase of MKK and IKK. Nature *412*, 346–351.
174. Wang, D., Xu, L., Lv, L., Su, L.Y., Fan, Y., Zhang, D.F., Bi, R., Yu, D., Zhang, W., Li, X.A., et al. (2015). Association of the LRRK2 genetic polymorphisms with leprosy in Han Chinese from Southwest China. Genes Immun. *16*, 112–119.
175. Wang, S., Miura, M., Jung, Y.K., Zhu, H., Li, E., and Yuan, J. (1998). Murine caspase-11, an ICE-interacting protease, is essential for the activation of ICE. Cell *92*, 501–509.
176. Warren, S.E., Mao, D.P., Rodriguez, A.E., Miao, E.A., and Aderem, A. (2008). Multiple Nod-Like Receptors Activate Caspase 1 during Listeria monocytogenes Infection . J. Immunol. *180*, 7558–7564.
177. Warren, S.E., Armstrong, A., Hamilton, M.K., Mao, D.P., Leaf, I.A., Miao, E.A., and Aderem, A. (2010). Cutting Edge: Cytosolic Bacterial DNA Activates the Inflammasome via Aim2. J. Immunol. *185*, 818–821.

178. Way, S.S., Thompson, L.J., Lopes, J.E., Hajjar, A.M., Kollmann, T.R., Freitag, N.E., and Wilson, C.B. (2004). Characterization of flagellin expression and its role in Listeria monocytogenes infection and immunity. Cell. Microbiol. *6*, 1013.
179. Webber, P.J., Smith, A.D., Renfrow C, M.B., Mobley B,C, J.A., and West, A.B. (2011). Autophosphorylation in the Leucine-Rich Repeat Kinase 2 (LRRK2) GTPase Domain Modifies Kinase and GTP-Binding Activities. J Mol Biol *412*, 94–110.
180. Weindel, C.G., Bell, S.L., Vail, K.J., West, K.O., Patrick, K.L., and Watson, R.O. (2020). LRRK2 maintains mitochondrial homeostasis and regulates innate immune responses to Mycobacterium tuberculosis. Elife *9*.
181. Wu, J., Fernandes-Alnemri, T., and Alnemri, E.S. (2010). Involvement of the AIM2, NLRC4, and NLRP3 inflammasomes in caspase-1 activation by Listeria monocytogenes. J. Clin. Immunol. *30*, 693–702.
182. Yang, Y., Wang, H., Kouadir, M., Song, H., and Shi, F. (2019). Recent advances in the mechanisms of NLRP3 inflammasome activation and its inhibitors. Cell Death Dis. *10*, 1–11.
183. Yi, Y.S. (2018). Regulatory roles of the caspase-11 non-canonical inflammasome in inflammatory diseases. Immune Netw. *18*.
184. Yoon, J.H., Mo, J.S., Kim, M.Y., Ann, E.J., Ahn, J.S., Jo, E.H., Lee, H.J., Lee, Y.C., Seol, W., Yarmoluk, S.M., et al. (2017). LRRK2 functions as a scaffolding kinase of ASK1-mediated neuronal cell death. Biochim. Biophys. Acta - Mol. Cell Res. *1864*, 2356–2368.
185. Yuan, J., Amin, P., and Ofengeim, D. (2019). Necroptosis and RIPK1-mediated neuroinflammation in CNS diseases. Nat. Rev. Neurosci. *20*, 19–33.
186. Zarubin, T., and Han, J. (2005). Activation and signaling of the p38 MAP kinase pathway. Cell Res. *15*, 11–18.
187. Zha, Q.B., Wei, H.X., Li, C.G., Liang, Y.D., Xu, L.H., Bai, W.J., Pan, H., He, X.H., and Ouyang, D.Y. (2016). ATP-induced inflammasome activation and pyroptosis is regulated by AMP-activated protein kinase in macrophages. Front. Immunol. *7*.
188. Zhang, Y., and Dong, C. (2007). Regulatory mechanisms of mitogen-activated kinase signaling. Cell. Mol. Life Sci. *64*, 2771–2789.
189. Zhang, J., Wang, X., Vikash, V., Ye, Q., Wu, D., Liu, Y., and Dong, W. (2016). Review Article ROS and ROS-Mediated Cellular Signaling.
190. Zhang, M., Yao, C., Cai, J., Liu, S., Liu, X.N., Chen, Y., Wang, S., Ji, P., Pan, M., Kang, Z., et al. (2019). LRRK2 is involved in the pathogenesis of system lupus erythematosus through promoting pathogenic antibody production. J. Transl. Med. *17*.
191. Zhang, P., Martin, M., Michalek, S.M., and Katz, J. (2005). Role of Mitogen-Activated Protein Kinases and NF-B in the Regulation of Proinflammatory and Anti-Inflammatory Cytokines by Porphyromonas gingivalis Hemagglutinin B. Infect. Immun. *73*, 3990–3998.
192. Zhang, Q., Pan, Y., Yan, R., Zeng, B., Wang, H., Zhang, X., Li, W., Wei, H., and Liu, Z. (2015). Commensal bacteria direct selective cargo sorting to promote symbiosis. Nat. Immunol. *16*, 918–926.
193. Zhao, Y., Yang, J., Shi, J., Gong, Y.N., Lu, Q., Xu, H., Liu, L., and Shao, F. (2011). The NLRC4 inflammasome receptors for bacterial flagellin and type III secretion apparatus. Nature *477*, 596–602.
194. Zhou, Y., Lu, M., Du, R.H., Qiao, C., Jiang, C.Y., Zhang, K.Z., Ding, J.H., and

Hu, G. (2016). MicroRNA-7 targets Nod-like receptor protein 3 inflammasome to modulate neuroinflammation in the pathogenesis of Parkinson's disease. Mol. Neurodegener. *11*.

LEILA SAM

CANADIAN EDUCATION and MEDICAL LICENSING EXAMS

-Master of Immunology, Microbiology, Pathology and Experimental Medicine — January 2018-Present

University of Ottawa, faculty of medicine, Ottawa, ON, Canada,

Under the supervision of professor Subash Sad

Canadian Medical Equivalency

-Proficiency of Language, TOEFL Exam — 2019

-Proficiency of Language, IELTS Exam — 2017

-National Assessment Collaboration OSCE (NAC OSCE) — 2016

-Medical Council of Canada Qualifying Exam Part 1 (MCCQE1) — 2016

-Medical Council of Canada Evaluating Exam (MCCEE**)** — 2015

CLINICAL EXPERIENCE

-Clinical observership/elective — 2017

Pathology department of Sunnybrook Hospital,

University of Toronto,Toronto, ON, Canada

Breast and Gynecopathology,

Under the supervision of Dr. Lu Fang

-Founder and associate member, anatomical and clinical pathologist,

Hadaf Pathobiology Lab, Karaj, Alborz, Iran — 2011-2017

-Anatomical Pathologist (Full time staff) 2006-2013

Department of pathology and laboratory medicine,

Alborz General Hospital,

Karaj, Alborz, Iran

- Clinical Pathologist

Mehrshahr Day Clinic, Karaj, Alborz, Iran 2004-2006

-Residency in General Pathology Program 2000-2004

Tehran university of medical sciences, Tehran, Iran

-Hospitalist , 1998-2000

NEDAJA General Hospital, Tehran, Iran

-Doctor of Medicine-MD

Tehran University of Medical Sciences, 1998

Tehran, Iran.

Research, Publications and Certificates

-Impact of *G2019S* mutation of *Lrrk2* on innate immune response to *Listeria monocytogenes*.
University of Ottawa, Faculty of medicine, BMI Department,
Under the supervision of Dr. Subash Sad 2018-present

- FoxO3a rescues gut inflammation caused by impaired IL10 signaling. (I have worked on pathologic features of inflammatory bowel disease (IBD) in this research, University of Ottawa, Faculty of medicine, Under the supervision of Dr. Subash Sad. 2017

- Dermatopathology Published Cases, Digital Laboratory Medicine Library,
University of Toronto, Under the supervision of Dr. Sachar Sade 2017

- Incidence of abnormal pap-smears, in patients referred to the gynecology clinic of Alborz General Hospital using the Bethesda System..
Alborz General Hospital, Karaj, Alborz, Iran. 2012-2013

-Liquid based cytopathology (Thin prep) certificate, Hologic Company, 2008

London, The United Kingdom (UK)

- Asymptomatic bacteriuria in type 2 Iranian diabetic women: A cross sectional study. BMC Women's Health. Boroumand, M. A., Sam, L., Abbasi, S. H., Salarifar, M., Kassaian, E., & Forghani, S. (2006). https://doi.org/10.1186/1472-6874-6-4 2006

- Asymptomatic bacteriuria in type 2 diabetic women in Iran. Iranian Journal of Diabetes and Lipid Disorders, 4(2). Boroumand, M. A., Sam, L., Abbasi, S. H., Salarifar, M., Kassaian, E., & Forghani, S. (2005). 2005

PROFESSIONAL AFFILIATIONS

-Iran Medical Council Organization #68798	1998-present
-Iran Pathology Society	2004-present
-Iran Medical Laboratory Organization	2004-present
-Medical Council of Canada #15642-93320	2011-present

PROFESSIONAL ACTIVITY

- Worked at various pathology and medical laboratory departments (clinic and research) with the following assignments and responsibilities:
    - Gross pathology (Macroscopic description), Preparing sections, Microscopic Diagnosis, Sign out anatomical and clinical pathology reports, Immunohistochemistry.
    - Cancer Registries based on the international classification of diseases for oncology, WHO coding (ICD-O Codes).
    - Monitored pathobiology laboratory standards for ISO 15189 pathobiology laboratories and quality control (QC).

- Interests and skills as an anatomical pathologist:
    - Cytopathology, Neuropathology, Dermatopathology, Breast and Gynecopathology, GI pathology, Soft tissue.

- Interests and skills as a clinical pathologist:
    - Medical microbiology, Immunology, Hematopathology and Clinical Biochemistry.